

Acknowledgements

There are so many people who I would like to thank that helped me get to this moment in time, but of course it's hard to remember everybody, so I hope I don't forget the most important.

Firstly, special thanks to my parents whom without their guidance and belief I would not be where I am and going to where I'm going. Thanks to my sister as well, who has grown so much and become a better person in order to better the family.

Special thanks to my MSc advisor, Prof. António Albuquerque, who has shown me the joys of investigation work and who has help be define what I'll be in the future. You're good disposition is contagious and thus you have my deepest gratitude and respect.

Special thanks to my MSc co-advisor, Prof. António Espírito Santo, who was ever so helpful when concerning the electronic part of the project and all the great ideas proposed which unfortunately did not make it into this thesis, but I'm sure in future projects they will. Without your expertise, none of this would have been possible.

To all my friends from Faro to Covilhã, thank you for being there when I needed and for listening.

Resumo

Os sistemas de tratamento por filtração (e.g. leitos percoladores, leitos filtrantes ou leitos de macrófitas) são muito utilizados para o tratamento de águas residuais, em especial em pequenos aglomerados populacionais. Normalmente, a medição de caudal está instalada à entrada do tratamento preliminar ou à entrada do sistema de filtração, não havendo registo de caudal noutras pontas, o que é especialmente útil para o controlo da carga hidráulica, da evolução da colmatagem e da estimativa da evapotranspiração em leitos filtrantes. Os medidores de nível existentes, ou são pesados, ou difíceis de implementar em vários pontos de leitos filtrantes além de serem tecnologias caras.

Com este trabalho pretendeu-se desenvolver um sensor de nível leve, de instalação fácil, robusto e com leituras fiáveis, que pudesse ser instalados em vários pontos de um sistema de tratamento por filtração. O sistema inclui uma sonda capacitiva, um data-logger e uma interface com o computador. A sonda baseia-se num princípio de variação da capacidade que se modifica em função do nível de água, e que é medida por um método adequado à funcionalidade desejada. O data-logger permite guardar vários registos de capacidade no tempo, enquanto que a interface permite enviar os dados para um computador. Foram realizados ensaios em laboratório para determinar as curvas de calibração que permitem passar os dados de capacidade para alturas de água (ou nível de água). Estas curvas foram validadas com medições em laboratório.

O leito de macrófitas da ETAR de Vila Fernando (Guarda) foi utilizado para medições experimentais de nível em 35 pontos de medição. Dado que., à escala real, existem condições adversas que podem interferir, quer com a sonda, quer com o data-logger, foram realizados ensaios experimentais para avaliar o efeito das características da água residual na qualidade da medição, tendo sido concluído que o medidor de nível (sonda e data-logger) responderam satisfatoriamente a estas variações. No entanto, serão necessário testes adicionais para avaliar o efeito destes parâmetros e outros, como a humidade ou/e a temperatura, na qualidade da medição a longo termo. A duração da bateria para alimenta o data-logger é outro aspecto que terá de ser melhorado.

Os resultados de 2 meses de medição permitiram concluir que a sonda fez medições de nível adequadas, que seguiram o padrão de bombagens do influente, tendo, ainda, sido possível verificar que o leito já se encontra colmatado em três regiões junto à entrada. Ou seja, além de medição de nível, este equipamento permitiu, indiretamente, detectar um problema de operação que não seria possível de identificar com a medição convencional.

Palavras-chave: medidor capacitivo, meio filtrante, medição de nível, tratamento de águas residuais.

Abstract

Wastewater treatment processes by filtration (e.g. trickling filters, filter beds or constructed wetlands) are widely used for treating several types of wastewater, being a suitable solution for small urban agglomerates. Typically, the flow measurement is installed at the entrance of the plant (in the preliminary treatment) or at the entry of the filtration system, and there is no registration of flow rate in other points, which could be especially useful for the control of hydraulic loads and bed clogging and for evapotranspiration estimates. The existing water level meters are heavy to transport or difficult to setup in various points of filter beds and in addition may be an expensive technology for replication throughout the bed area.

This work aimed to develop a light water level sensor, easy to transport and install, robust and with reliable readings, which could be installed at various points of a filtration treatment system. The developed sensor includes a capacitive probe, a data-logger and a computer interface. The system has a capacitive probe that changes depending on the water level. The capacitive value is measured with an appropriated method. The data-logger allows saving multiple records of capacity in time, while the interface can send data to a computer. Laboratory tests were conducted to determine the calibration curves that allow data to be converted from capacity to water height (or water level). These curves have been validated with laboratory measurements.

The horizontal subsurface flow constructed wetland of Vila Fernando (Guarda) was used for experimental measurements of water level in 35 measuring points. Since at real scale there are adverse conditions that can interfere with either the probe or with the data-logger readings, laboratory experimental assays were conducted to evaluate the effects of salinity, temperature and wastewater characteristics on the quality of measurement. It was concluded that the water level meter (probe and data-logger) responded satisfactorily to these variations. However, additional tests are needed to evaluate the effect of these and other parameters such as humidity, in long-term measurements. The battery lifetime for feeding the data-logger is another aspect that has to be improved.

The results of two months measurements show that the probe measurements were correct, following the pattern of the flow pumped from upstream and has also been possible to verify that the bed is already clogged in three regions near the entrance. Therefore, in addition to water level measurements, this technology allowed an indirect detection of a problem (bed clogging), which would not be possible to identify with the conventional water level measurement

Keywords: capacitive probe, filtration beds, wastewater treatment, water level measurement

Contents

1	Introduction	11
1.1	Purpose and justification	11
1.2	Objectives.....	12
1.3	Outline of the thesis.....	13
2	Fixed-film Wastewater Treatment process.....	14
2.1	Type of processes for wastewater treatment	14
2.2	Fixed-film wastewater treatment processes.....	16
2.3	Bed media in filtration systems.....	17
2.4	Operational parameters	19
2.5	Constructed wetlands.....	21
3	Flow Measurement	25
3.1	Introduction.....	25
3.2	Types of flow measurement devices.....	25
3.3.	Capacitive sensor level measurement	46
4	Material and Methods.....	62
4.1	Development of the capacitive sensor.....	62
4.1.1	Architecture of the system.....	62
4.1.2	Capacitive probe theoretical model	62
4.1.3	Probe construction	66
4.1.4	Data-logger development	70
4.1.5	Computer interface.....	72
4.1.6	Sensor calibration.....	72
4.2	Effect of water characteristics.....	75
4.2.1	Introduction	75
4.2.2	Effect of salinity	77
4.2.3	Effect of temperature.....	78
4.3	Field work measurements	79
4.3.1	Wastewater treatment plant.....	79
4.3.2	Installation of measuring points.....	80
4.3.3	Installation of the sensors.....	84
4.3.4	Water level measurements.....	84
5	Results and Discussion	85
5.1	Effect of water characteristics.....	85
5.1.1	Protocol for evaluating the effect of temperature	86
5.2	Water level measurements	87
6	Conclusions	93
6.1	Main Conclusions.....	93
6.2	Further Work	93
7	References	95
	Annexes	102
	Annex I - Calibration curves for water level and number of cycles	103
	Annex II - Calibration curves for water level and capacitance	112
	Annex III - Results of field work measurement.....	113

List of Tables

Table 2.1 - Removal efficiencies of parameters characterizing wastewater in some operations and treatment processes (adapted from Albuquerque, 2008)	17
Table 2.2 - Characteristics of some types of filling material used in biofilters.	19
Table 3.1 - Capacitive sensors.....	57
Table 3.2 - Capacitive sensors (continues).....	58
Table 4.1 - Physical dimensions.....	64
Table 4.2 - Capacitive probe theoretical model parameters.	76
Table 4.3 - Experimental and theoretical results.	77
Table 5.1 - Sensor capacitance for different salinities solutions.....	85
Table 5.2 - Theoretical and experimental probe capacity for a solution with 214 pF.	86
Table 5.3 - Sensor capacitance for different mediums with probe totally submerged.....	86

List of Figures

Figure 2.1- Typical stages in the conventional treatment of sewage (adapted from Parr et al., 2000).	14
Figure 2.2 - Biofilm on different bed medias; a) Gravel/Crushed rock; b) LECA; (adapted from Silva, 2010).	18
Figure 2.3 - Classification of constructed wetlands (adapted from Wallace and Knight, 2006).	22
Figure 2.4 - Different types of macrophytes plants: emerging (I), floating (II) and submerged (III). The species present in this illustration are (a) <i>Scirpus lacustris</i> , (b) <i>Phragmites australis</i> , (c), <i>Typha latifolia</i> (d) <i>Nymphaea alba</i> , (e) <i>Eichhornia gramineus</i> , (f) <i>Hydrocotyle vulgaris</i> , (g) <i>Eichhornia crassipes</i> , (h) <i>Lemna minor</i> (i) <i>Potamogeton crispus</i> and (j) <i>Littorella uniflora</i> . (adapted from Brix and Schierup, 1989).....	23
Figure 2.5 - Flow Orientation.....	24
Figure 3.1 - Oscillation Piston Meter (adapted from OMEGA, 1995).	26
Figure 3.2 - Nutating disc (adapted from OMEGA, 1995).	27
Figure 3.3 - Oval Gear Meter (adapted from OMEGA, 1995).	27
Figure 3.4 - Turbine flow meter: A) with reluctance pickup coil. B) with Inductance pickup coil (adapted from OMEGA, 1995).	28
Figure 3.5 - Woltmann turbine meter (adapted from OMEGA, 1995).....	28
Figure 3.6 - Multijet flow meter.	28
Figure 3.7 - Vena Contracta (A) and Venturi meter (B) (adapted from Falkovich, 2011).	29
Figure 3.8 - Rotometer (adapted from Falkovich, 2011).	30
Figure 3.9 - Orifice plate meter (A), Different types of orifice plates (B) (adapted from Falkovich, 2011).....	31
Figure 3.10 - Pitot tube (adapted from Falkovich, 2011).	31
Figure 3.11 - Optical flow meter (adapted from OMEGA, 1995).....	32
Figure 3.12 - Weir in a natural stream (A) and different shape weirs (B) (adapted from Smajstrla et al., 2002).	33
Figure 3.13 - Doppler calculating velocity.	35
Figure 3.14 - Constant temperature differential probe (adapted from http://www.foxthermalinstruments.com/flowmeter-technology.php).	36
Figure 3.15 - Vortex flow meter (bluff body and sensors) (Adapted from http://www.efunda.com/designstandards/sensors/flowmeters/flowmeter_vtx.cfm).	37
Figure 3.16 - Magnetic Glow Meter (Adapted from http://www.efunda.com/designstandards/sensors/flowmeters/flowmeter_mag.cfm).	38
Figure 3.17 - Ultrasonic Flow Meters (Adapted from http://www.alicatscientific.com/types_of_devices.php).	40

Figure 3.18 - Proposed liquid level and volume measurement system (Adapted from A New Non-Intrusive Optical Technique to Measure Transparent Liquid Level and Volume (Hidam Kumarjit Singh et al., 2010)).	43
Figure 3.19 - Sensor structure. (a) view of the top of the sensor (1, 2, 3, 4: electrodes; 5: plastic pipe); (b) profile view of the sensor (mm); (adapted from Guirong and Shuyue, 2010).	47
Figure 3.20 - Two electrodes mode and four electrodes mode (adapted from Guirong and Shuyue, 2010).	47
Figure 3.21 - Schematics and principal of measuring (adapted from Blander et al., 2010).	48
Figure 3.22 - Experimental results (dielectric air) (adapted from Blander et al., 2010).	49
Figure 3.23 - Sensor setup (adapted from Canbolat, 2009).	51
Figure 3.24 - Setup for level measurement of conducting liquids (adapted from Canbolat, 2009).	52
Figure 3.25 - Structure of sensor: (a) plan form of sensor; (b) sensor's structure; (c) prototype sensor; (adapted from Wang and Shida, 2006).	53
Figure 3.26 - Sensor setup (adapted from Bera et al., 2006).	54
Figure 3.27 - Schematics of the sensor with the conductive liquid connected to the ground (adapted from Toth et al. (1996)).	56
Figure 3.28 - Capacity measurement with a RC circuit.	60
Figure 3.29 - Capacity measurement with an oscillator.	61
Figure 4.1 - Capacitive probe structure.	63
Figure 4.2 - Theoretical model of the capacitive probe.	64
Figure 4.3 - Heat retracting sleeve over solid aluminium rod; a) heat applied to sleeve; b) sleeve inserted over rod; c) sleeve inserted over rod top view; d) sleeve inserted over rod after applying heat source to retract the sleeve.	67
Figure 4.4 - Heat shrinkable sleeve; a) sealed tightly around the bottom end of the solid aluminium rod; b) plastic cap placed on the bottom of solid aluminium rod after sealed tightly.	67
Figure 4.5 - Solid aluminium rod being inserted into hollow aluminium rod.	68
Figure 4.6 - Plastic cap placed on the top part of the sensor.	68
Figure 4.7 - Slits; a) slit incision at the top of the sensor and hole for attaching vessel that houses data logger and power source; b) slit incision at the bottom of the sensor.	68
Figure 4.8 - Details on sensor construction. a) vessel connected to sensor; b) terminal with electrical wire to connect to data logger; c) O-ring terminals with wire to connect to sensor.	69
Figure 4.9 - Capacitive water level sensors.	70
Figure 4.10 - Data-logger.	70
Figure 4.11 - Expected measurement process.	71
Figure 4.12 - Interface for data data-logger.	72

Figure 4.13 - a) Measuring tube used for sensor calibration; b) Sensor inside the tube and connected to the data-logger; c) Data-logger and interface for computer.	73
Figure 4.14 - Calibration curves for water depth and number of cycles.	74
Figure 4.15 - Capacitance calibration curve.	74
Figure 4.16 - Mini-sensors.	75
Figure 4.17 - Capacitive probe finite element method.	76
Figure 4.18 - Capacitance measurement with samples from HSSF-CW.....	77
Figure 4.19 - WWTP location.	79
Figure 4.20 - Wastewater Plant Setup	80
Figure 4.21 - General view of the unvegetated filtration bed of Vila Fernando (A); HSSF-CW bed of Vila Fernando with <i>Phragmites australis</i> (B).	80
Figure 4.22 - Measuring point's layout at the CW of Vila Fernando.	81
Figure 4.23 - General view of the HSSF-CW bed with measuring points installed.....	81
Figure 4.24 - Schematic representation of the HSSF-CW bed of Vila Fernando.	82
Figure 4.25 - Longitudinal section of the HSSF-CW of Vila Fernando.....	83
Figure 4.26 - A) Network of measuring tubes with sensors. B) Sensors inserted into a tube... 84	
Figure 5.1 - Reference sensors for temperature; a) Sensor inserted into tap water at 20°C; b) c) Data logger inserted into a vessel to measure the temperature of the wastewater;	87
Figure 5.2 - Sensor placement.....	88
Figure 5.3 - Water level measuring in the first transversal row (11th of February 2012 from 17h30 to 00h00).	89
Figure 5.4 - Water level measuring in the first transversal row (12th February).	90
Figure 5.5 - Second 12 hours from February the 12th from 12h05. Perspective view and aerial view. Seventh Row.	92

List of Acronyms

BOD₅ - Biochemical Oxygen Demand

CDC1 - Capacitance to Digital Converter

CDC2- Clock Distribution Circuit

CO₂ - Carbon Dioxide

COD - Chemical Oxygen Demand

CW - Constructed Wetland/s

DECA-UBI - Departamento de Engenharia Civil e Arquitectura da Universidade da Beira Interior

DO - Dissolved Oxygen

HDPE - High-density polyethylene

HLR - Hydraulic Loading Rate

HRT - Hydraulic Retention Time

HSSF - CW - Horizontal Subsurface Flow - Constructed Wetlands

LECA - Light Expanded Clay Aggregate

LDR - Light Dependent Resistor

MHz - Mega Hertz

Mohm - Mega Ohms

NH₄ - Ammonia

NLR - Nitrogen Loading Rate

NO_x - Nitrogen Oxide

NO₂ - Nitrite

NO₃ - Nitrate

NT - Total Nitrogen

OLR - Organic Loading Rate

PD - Photodetector

PVC - Polyvinyl Chloride

RE - Removal Efficiency

RC - Resistor Capacitor

SLR - Solids Loading Rate

SOx - Sodium Oxide

TP - Total Phosphorous

TSS - Total Suspended Solids

WWTP - Wastewater Treatment Plant

ϵ_0 - Vacuum Electrical Permittivity

ϵ_r - Dielectric Electrical Permittivity

ϵ_{r_air} - Air Dielectric Constant

ϵ_{r_sh} - Sheath Dielectric Constant

ϵ_{r_water} - Water Dielectric Constant

l_{air} - Air Height

l_{water} - Water Height

1 Introduction

1.1 Purpose and justification

Wastewater treatment plants (WWTP) have increased significantly in the last 20 years due to high investments made in our country under the development plans PEAASAR I (2000-2006) and PEAASAR II (2006-2013). These strong investments have pushed up the percentage of population served with drainage systems and wastewater treatment to approximately 80%.

For agglomerates with less than 2000 population equivalents, especially the ones located on the country side and in areas with a low population density, the solution was based on filtration systems (constructed wetlands and percolating filters). However, most of the water companies in these regions do not have many specialised human resources, financial support and equipment's for the properly management of the WWTP, some of which are located at long distances from the headquarters.

Several studies developed by the DECA-UBI in constructed wetlands with horizontal subsurface flow (HSSF-CW) have pointed out performance failure due to clogging (Albuquerque *et al.*, 2009; Simões, 2009), which is referred by several authors (Kadlec and Wallace, 2008; Vymazal and Kropfelova, 2008) as one of the main factors that affects treatment performance. However, it was not possible to locate the extension of clogging.

In another study (Amado *et al.*, 2012) it was detected a drop in treatment performance due to high variation of the hydraulic loading rate (HLR), which was forecasted based on the influent average monthly flow rate and the effective surface area. However, HSSF-CW have high evapotranspiration rates that reduce its water volume (Galvão, 2009; Białowiec *et al.*, 2011), which can only be properly forecasted if the temperature and the water table can be monitored in several points of the bed. Most of the WWTP only have flow rate measurement at the entrance (normally located at the preliminary stage), since the typical devices for its measurement in open channel flow (Parshall flume and ultrasonic or electromagnetic devices) are heavy or expensive to replicate in several points of the plant.

Tracer tests are the most used method to evaluate the hydrodynamic condition in filtration systems as constructed wetlands or biofilter technologies (Tchobanoglous *et al.*, 2003; Kadlec and Wallace, 2008), as well as to estimate dead volumes and the changes in the hydraulic retention time (HRT). However, it is a time consuming method, several times expensive and many times does not allow obtaining a good curve for integration as noted in several studies (Seguret, 1998; Martinez and Wise, 2003; Albuquerque, 2012).

Therefore, a smaller and easy to use water flow meter would allow the measurement of water table in several points of the bed and the flow rate in points where the use of weirs are easy to set up. Measuring the water level along the bed in different points for the same time

period would also allow, in certain conditions, estimating the evolution of the hydraulic retention time (HRT) along different bed's sections. Additionally, a smaller device for water table measurement in several points of CW beds would allow a suitable control of the clogging phenomena over time.

Water measuring depends on what is intended to quantify, some meters measure the flow velocity, others measure just the liquid level and some, especially in closed conduces, measure the flow rate. Over the years, the technology for water level measuring has evolved and novel methods using optical fibre, thermal resistance and capacitance sensors are now in study. These technologies can enable the development of sensors lighter, easier to replicate and with the ability to measure the level at various points simultaneously. However, they should also be durable and reliable and resisting to factors such as variations in temperature, humidity and characteristics of wastewater.

The capacitive technology has already been used in recent developed water and oil level measurement meters. However, there is no known application for the measurements of wastewater level in filtration wastewater treatment systems.

This work is part of a larger project that intends to develop capacitive probes for flow rate measurement in open channel and porous media system, and was developed between September of 2011 and June of 2012.

1.2 Objectives

The main objective of this work is to develop a small, easy to use and reliable water level measurement sensor (probe, meter and interface for computer), which could be used in field work for water level measurement in multiple points over time. A capacitive technology will be used to develop the probe. A constructed wetland bed and laboratory devices will be used to calibrate and validate the technology, as well to study the effect of the salinity, temperature and the characteristics of the wastewater on capacitance measurements.

1.3 Outline of the thesis

The thesis has 6 chapters and 3 annexes. Chapter 1 presents the framework and justification of the topic, as well as the objectives and the thesis's structure. The Chapter 2 shows a quickly review on wastewater treatment processes, focusing on the filtration systems and, in particular, the constructed wetland technology, since it is the system used for water level measurement tests. Chapter 3 describes several types of flow measurement devices, namely water level meters for flow rates estimates in open channel flow and an overview on capacitive meters development and application. The material and methods are described in Chapter 4. Chapter 5 presents the results and discussion and the main conclusions are presented in Chapter 6.

2 Fixed-film Wastewater Treatment process

2.1 Type of processes for wastewater treatment

The main goals of wastewater treatment is the removal of pollutants from sewage in order to produce an effluent with characteristics within the guidelines established for reuse or disposal in water and soil, reducing the risk of environmental impacts or public health problems. Biological wastewater treatment processes are those which have both technically and economically produced better results for the treatment of urban wastewater, since they are very efficient for biodegradable wastewater (Tchobanoglous *et al.*, 2003).

The removal of pollutants present in wastewater involves a combination of operations and treatment processes, which are distributed through several treatment levels of a Wastewater Treatment Plant (WWTP): preliminary, primary, secondary, tertiary and polishing treatments (Figure 2.1). Additionally, the sub-products of treatment (sludge) are also treated in the same WWTP.

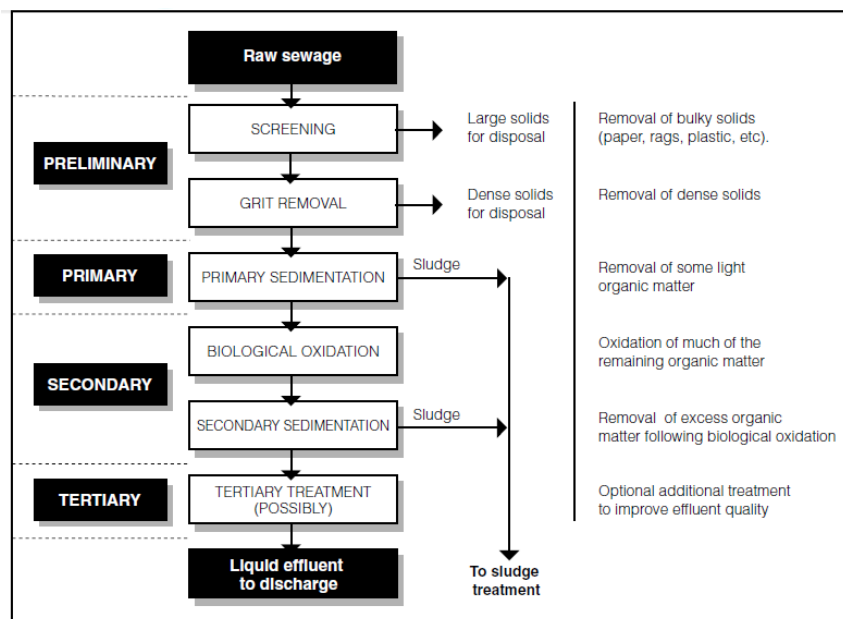


Figure 2.1- Typical stages in the conventional treatment of sewage (adapted from Parr *et al.*, 2000).

In the *preliminary stage*, the wastewater passes through screens, in order to remove large materials (such as rags and logs), which can interfere with the next treatment processes. Grit chambers are also used to remove grits (sand, broken glass, silt and pebble), which can wear and damage mechanical devices in the treatment units. Sometimes, there are also equipment to remove coarse material, oils, inert matter and fatty substances (Tchobanoglous *et al.*, 2003).

The *primary stage* includes settling tanks (also called sedimentation tanks or clarifiers) and may include flotation tanks if the influent if significant oil and grass are present. Approximately 70% of suspended solids and 30% of organic matter are removed in these tanks, by accumulating at the bottom in the form of *primary sludge*, which is then removed by mechanical scrapers and pumps. A thin foam film usually floats on top of the water (grease, oil and other floating substances) and is removed by skimming the surface with specific equipment.

Not all of the solids are removed in the primary clarifier due to light particles taking too long to settle, thus these small particles and dissolved organic matter will be removed through biological treatment in the *secondary stage*. Biological treatment may include fixed-film reactors (e.g. percolating filters, biofilters, biodiscs and constructed wetlands) or completely mixed reactors (e.g. activated sludge, stabilization ponds and digesters). The presence of oxygen will allow developing aerobic removal pathways (e.g. aerobic removal of organics and nitrification), which increase the performance of the reactors in removing organics and nutrients. The aeration may be provided naturally (e.g. percolating filters) or mechanically (e.g. activated sludge). Different biochemical conditions (aerobic, anoxic and anaerobic) may be presented in fixed-film or completely mixed reactors.

In aerobic biochemical conditions, bacteria and protozoa can use the small particles and dissolved organic matter as food, thus producing water, CO₂ and inorganic sub-products, and more microorganisms, which can then be removed in a final clarifier as *secondary sludge*. In some processes, such as activated sludge, the secondary sludge is recirculated back to the aeration tank in order to increase the treatment process (known as returned activated sludge). The excess of waste activated sludge is sent to another part of the plant for further treatment. In processes such as percolating filters, biofilters and biodiscs, the treated effluent may also be recirculated back in order to keep the filtration system irrigated and to increase the treatment performance.

In anaerobic biochemical conditions (i.e. there is no presence of molecular oxygen, but oxygen may be present as NO_x or SO_x) specialized bacteria that is able to live without oxygen use biodegradable organic matter as a food source to produce carbon dioxide, methane gas and inert organic matter (similar to peat moss), as well as new microorganisms. The most known anaerobic treatment process is anaerobic digestion, which, sometimes, recovers the biogas for energy production.

There are also hybrid processes, such as biofilters, ponds and constructed wetlands, where aerobic and anaerobic conditions coexist in the same space.

The *tertiary stage* normally includes the removal of nutrients (both through biological or chemical pathways). Fixed-film or completely mixed reactor can perform this treatment and, normally, is not needed additional treatment units. The removal of nitrogen and phosphorous may be carried out in the secondary biological reactors.

Finally the *polishing stage*, also known as advanced wastewater treatment, is applied in specific conditions when there is need of effluent disinfection (e.g. using UV radiation or chlorine) or residual pollutant removal (e.g. using filtration beds), normally when the effluent is considered hazardous for public health or when the reuse option is set-up.

2.2 Fixed-film wastewater treatment processes

Fixed-film or filtration beds (e.g. percolating filters, biofilters and constructed wetlands) are very common processes in small and medium sized WWTP, in some conditions are more cost effective than completely mixed systems (e.g. activated sludge and ponds). Basically, reactors are filled with a filling material for flow percolation (upflow or downflow). Normally, the systems are complete with a final settler for solids and biomass separation and a recirculation line to keep the bed media irrigated during low flow incoming. Most of the solid material is retained by filtration whilst the soluble material (nutrients and organics) is removed through removal pathways that occur within the biofilm (biomass developed around the media).

The effectiveness of filtration systems for wastewater treatment is usually based on the removal of organic matter, nitrogen or solid matter, using the parameters chemical oxygen demand (COD), biochemical oxygen demand (BOD_5), total nitrogen (NT), ammonia (NH_4), nitrite (NO_2), nitrate (NO_3), total phosphorous (TP) and total suspended solids (TSS). Total removal efficiency (in %) or removal rates ($g/m^2.d$ or $g/m^3.d$) are normally used. Table 2.1 presents the typical variation in removal efficiency (RE) for different filtration processes for wastewater treatment (Albuquerque, 2008). Preliminary processes and the activated sludge process are also included in order to compare the values.

Table 2.1 - Removal efficiencies of parameters characterizing wastewater in some operations and treatment processes (adapted from Albuquerque, 2008)

Types of Treatment		Removal Efficiency (%)					
		BOD ₅	COD	TSS	TP	TN	NH ₄
Preliminary and primary stages	Screening and grit chambers	0 - 0.5	0 - 0.5	0 - 1	0	0	0
	Primary settlers	20 - 40	30 - 40	50 - 60	10 - 20	10 - 20	0
Secondary and tertiary stages	Activated sludge (conventional systems)	80 - 95	80 - 90	85 - 90	10 - 30	15 - 50	10 - 15
	Trickling beds (low loading rate, gravel/crushed rock media)	60 - 90	60 - 80	60 - 90	10 - 15	15 - 20	8 - 15
	Trickling beds (high loading rate, synthetic media)	65 - 85	65 - 85	65 - 85	10 - 15	20 - 40	15 - 20
	Biofilters (submerged bed)	70 - 90	60 - 90	80 - 85	10 - 25	15 - 50	8 - 15
	Rotating biodiscs	80 - 90	80 - 85	80 - 85	10 - 25	15 - 50	8 - 15
	Constructed wetlands - horizontal flow beds	50 - 95	60 - 90	60 - 90	10 - 35	50 - 90	40 - 70
	Constructed wetlands - vertical flow beds	25 - 99	50 - 90	38 - 85	30 - 90	30 - 90	45 - 95

2.3 Bed media in filtration systems

The bed media or filling media used in fixed-film bioreactors is essential for biofilm adhesion and development, with the ability to remove pollutants (Figure 2.2), as well as for plant anchorage in vegetated beds (constructed wetlands). Defragmentation of the bed media is a major problem for system operation, since it may cause clogging due to excess of fine material, biomass retention, solid filtration and roots development.

The bed media can be constituted either by layers of natural, recycled or synthetic material with depths that ranges from 1 m (constructed wetlands) to 3 m (biofilters with natural filling) or 6 m (biofilters with plastic filling). The most used bed material are (Tchobanoglous *et al.*, 2003; Albuquerque, 2003):

- Natural material: gravel, sand, coarse gravel or pebbles;
- Recycled material: artificial aggregates (LECA and geopolymers);
- Synthetic material: polystyrene or polyethylene.

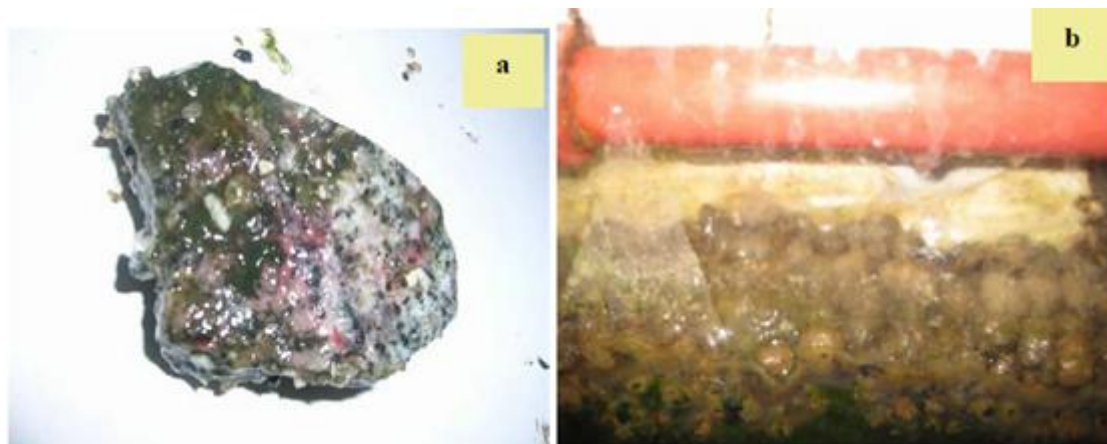


Figure 2.2 - Biofilm on different bed medias; a) Gravel/Crushed rock; b) LECA; (adapted from Silva, 2010).

Table 2.2 presents a set of bed material used in fixed-film treatment processes. The most important properties for a suitable material are: good durability, stabilization in water and good mechanical strength, high specific surface area and porosity and void ration above 0.4. The effective particle diameter should be between 2 mm and 10 mm (Tchobanoglous *et al.*, 2003; Albuquerque, 2003; Asano *et al.*, 2007).

Moreover, much attention has been given to the development of recycled materials for filling fixed-film systems. Crini (2006) tested a number of materials from the extractive industry, sludge waste and waste from agricultural activities to be reused in filters.

The particle size should be small and present a high specific surface area, in order to allow the development of the biofilm and prevent the rapid clogging of the filling medium. The bed media may include layers of increasing particle size or layers with the same particle size (homogeneous layers). For instance, if the particles sizes vary too much, the smaller particles will obstruct the media pores, consequently reducing the available volume for flow and contributing to a more rapid clogging of the bed.

For a high removal of suspended solids and pathogenic microorganisms, it is recommended to use a bed media constituted of smaller/lower particle sizes. Thinner beds allow a greater removal of microorganisms and a better absorption of nutrients, however it requires a larger implantation area and the risk of clogging increases. On the other hand, more permeable beds which are based on gravel and sand are not so effective in removing pollutants and microorganisms, but allow the application of higher hydraulic loads and are less susceptible to clogging, which is particularly important for the first two years of the bed media/systems life (Asano *et al.*, 2007).

Table 2.2 - Characteristics of some types of filling material used in biofilters.

Material	Particle Diameter (mm)	Void Index	Specific Surface Area		Source
			(m ² /m ³)	(m ² /g)	
Sand	2 - 3	0.38 - 0.50	700 - 1000	-	Tchobanoglo us <i>et al.</i> , (2003)
Filtralite (expanded clay)	2 - 10	0.4 - 0.55	1000 - 1500	5	Lekang and Kleppe (2000) Anderson <i>et al.</i> (2008)
Kaldnes rings	9	-	500	-	Lekang and Kleppe (2000)
Gravel/Crushed Rock	5 - 20	0.39 - 0.42	700 - 1000	-	Tchobanoglo us <i>et al.</i> (2003)
Biolite beads	2 - 3	0.55	494	-	Tchobanoglo us <i>et al.</i> (2003)
Pozzalan	3 - 6	0.42 - 0.52	1300 - 1640	-	Albuquerque (2003)
Fly ash	0.08 - 2	-	-	0.17 - 1	Ahmarzzama n (2009)
Absol	2 - 4	-	-	30.3	Afridi (2008)

The control of clogging is can be done by using pressure piezometers (not so practical in field scale systems) or using tracer tests (Foggler, 1999). In the last case, tracer experiments allow to identify the effective hydraulic retention time, which, in case of clogging, is much lower than the theoretical one, as well as the identification of the extension of dead volumes.

2.4 Operational parameters

Filtration systems operation involves the control of several parameters such as the hydraulic loading rate (HLR), hydraulic retention time (HRT), organic loading rate as BOD or COD (OLR), nitrogen loading rate as TN, ammonia, nitrite or nitrate (NLR), phosphorous loading rate as TP or phosphate and solids loading rate (SLR).

The variation of such parameters usually depends on several factors such as the characteristics of the influent wastewater (organics, solids and nutrient loads, temperature, pH and dissolved oxygen (DO)), the changes in influent flow-rate, the effective volume of the bed (total volume x void ratio), the bed media characteristics (*e.g.* properties of the filling media and height of the media) and the characteristics of the biofilm (*e.g.* type of colonization and thickness). These factors influence directly the distribution of pollutants in the bed, as well as their removal rates.

The HLR is normally forecasted using the average flow rate and the total surface area. However, recently studies pointed out that the effective area should be used instead of the total area, since the available area for reaction is the void area. The same is applied for the bed volume. The more suitable volume for controlling the HRT is the effective volume and not the total volume as pointed out by some studies (Albuquerque 2003; Asano et al., 2007; Albuquerque et al., 2009).

The HRT is normally forecasted based on the total volume and the average flow rate, what does not reflect the changes in the void ratios in the bed. Several studies pointed out for the changes in the void ratios over the beds due to clogging, which decrease the retention time needed for reaction and for the biofilm transform the pollutants. This occurrence was already observed in biofilters (Jimenez et al., 1988; Seguret, 1998; Albuquerque, 2003) and constructed wetlands (Martinez and Wise, 2003; Kadlec and Wallace; 2008; Albuquerque, 2012).

The growth of biomass related with the accumulation of solids and the defragmentation of the filling material may cause a progressive clogging of the medium, thus reducing the available area for percolation. During the flow through the media there is loss of energy (head loses) either to the media matrix through friction or to areas that create flow resistance (e.g. stagnated areas or dead volume). This phenomenon is expressed, in practice, by an increment of the hydrostatic pressure due to flow resistance, reproducing the development of clogging within the bed, designated generally as a pressure drop.

Constructed wetlands with horizontal subsurface flow (HSSF-CW) are biofilm reactors where clogging is very frequent and is one of the main problem related with performance failure (Kadlec and Wallace, 2008; Vymazal and Kropfelova, 2008). Several studies have been developed in order to determine the extension of clogging (Munoz et al., 2006) as well to determine methods for clogging evaluating (Chazarenc et al., 2003; Turona et al., 2009). Clogging in horizontal flow beds interfere with the effective HRT, which is lower than the theoretical one defined for the bed project and will interfere with the bed performance. Tracer tests are the most used method to evaluate the effective HRT in beds (Kadlec and Wallace, 2008). However, it is a time consuming method and, several times, is expensive and fails in getting the peak of tracer exit or a good curve for area integration.

Measuring the water level along the bed in different points for the same time period would allow, in certain conditions, estimating the evolution of the HRT along different bed's sections.

The flow rate is normally measured at the entrance, which is not useful for the control of the HLR since the evapotranspiration is important in HSSF-CW and the real water volume inside the bed changes according to evapotranspiration rates (Białowiec *et al.*, 2011). However, most of the water level measurement equipment used in CW (e.g. Parshall flume and ultrasonic or electromagnetic devices) is applied at the entrance and exit of the beds. They

are also costly or not suitable to be used inside the beds. Therefore, a more easy to use and cheaper sensor is needed in order to allow measurements in several points of the bed.

The OLR is defined by the mass of organic matter (in BOD or COD) per area or volume unit over time. The rate is normally calculated using the daily average flow rate, the average organic matter concentration (BOD or COD) and the total volume or the total surface area.

2.5 Constructed wetlands

CW are fixed-film or filtration bioreactors (also called biofilm reactors) used for the treatment of domestic, industrial, agricultural runoff and road runoff effluents. Contrary to what happens with conventional systems, CW do not need to be controlled and operated in full-time.

The main advantages of this system when compared to other conventional systems are (Kadlec and Wallace, 2008):

- a) *Low construction costs.* These costs are related mainly to the acquisition value of land and implantation, earthworks and excavations, if necessary, as well as the hydraulic control structures;
- b) *Low operating costs.* Practically no chemical reagents are used at any stage of the treatment, as well as no many electromechanical devices are applied, what makes this systems low cost in which concerns the maintenance costs (human resources, chemicals and energy);
- c) *Relatively simple maintenance.* Since it is a low-tech system it can be maintained by unqualified personnel and does not need full time supervision, on the contrary to other systems that require specialized technical monitoring personnel due to the technology used;
- d) *Good landscape integration and ecological.* The negative environmental impacts associated with CW are virtually null, where only the existence of foul odours from the preliminary and primary stages can cause discomfort, especially in warmer weather and if the influent has high organic loads. The positive impacts are a good final effluent quality, good integration in the local landscape and the creation of a habitat for numerous species of local fauna, thus generating after a short time an ecosystem of its own.

Constructed wetlands are systems that generally consist of small depressions dug in the ground or small ponds, waterproofed, partially filled with natural aggregates (sandy soil, sand, and gravel) or artificial aggregates (LECA and geopolymers), colonized with hydrophobic plant species adapted to living in flooded land, known as macrophytes.

The classification (Figure 2.3) of these systems is based on several characteristics as follows:

- a) The type of effluent to be treated:
 - i. Domestic, industrial, surface runoff, road runoff and agricultural runoff effluents;
 - ii. Sludge from wastewater treatment processes;

- b) The type of flow:
 - i. Superficial;
 - ii. Sub-superficial;

- c) The characteristics of the plant species colonizing the media (Figure 2.4):
 - i. Floating species;
 - ii. Submerged species;
 - iii. Emergent species;

- d) Flow orientation (Figure 2.5)
 - i. Horizontal flow;
 - ii. Vertical flow (upward or downward);

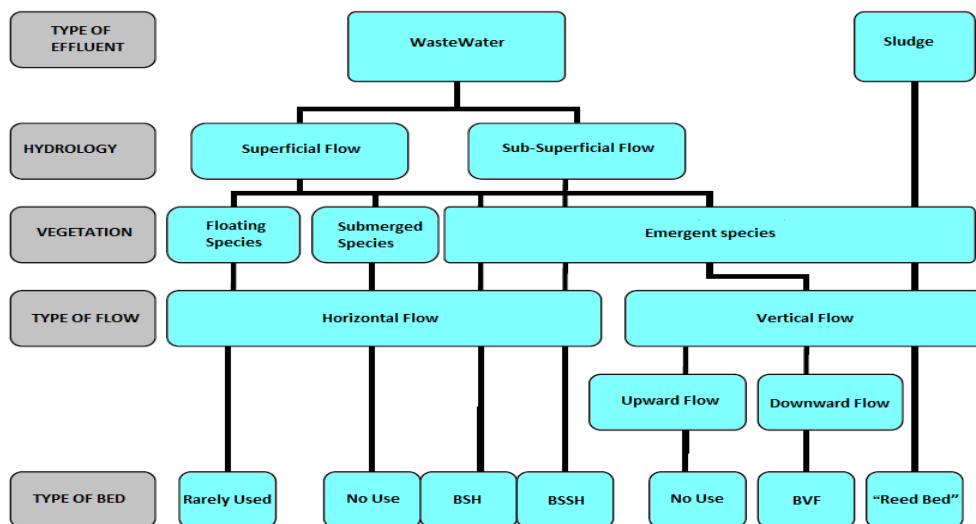


Figure 2.3 - Classification of constructed wetlands (adapted from Wallace and Knight, 2006).

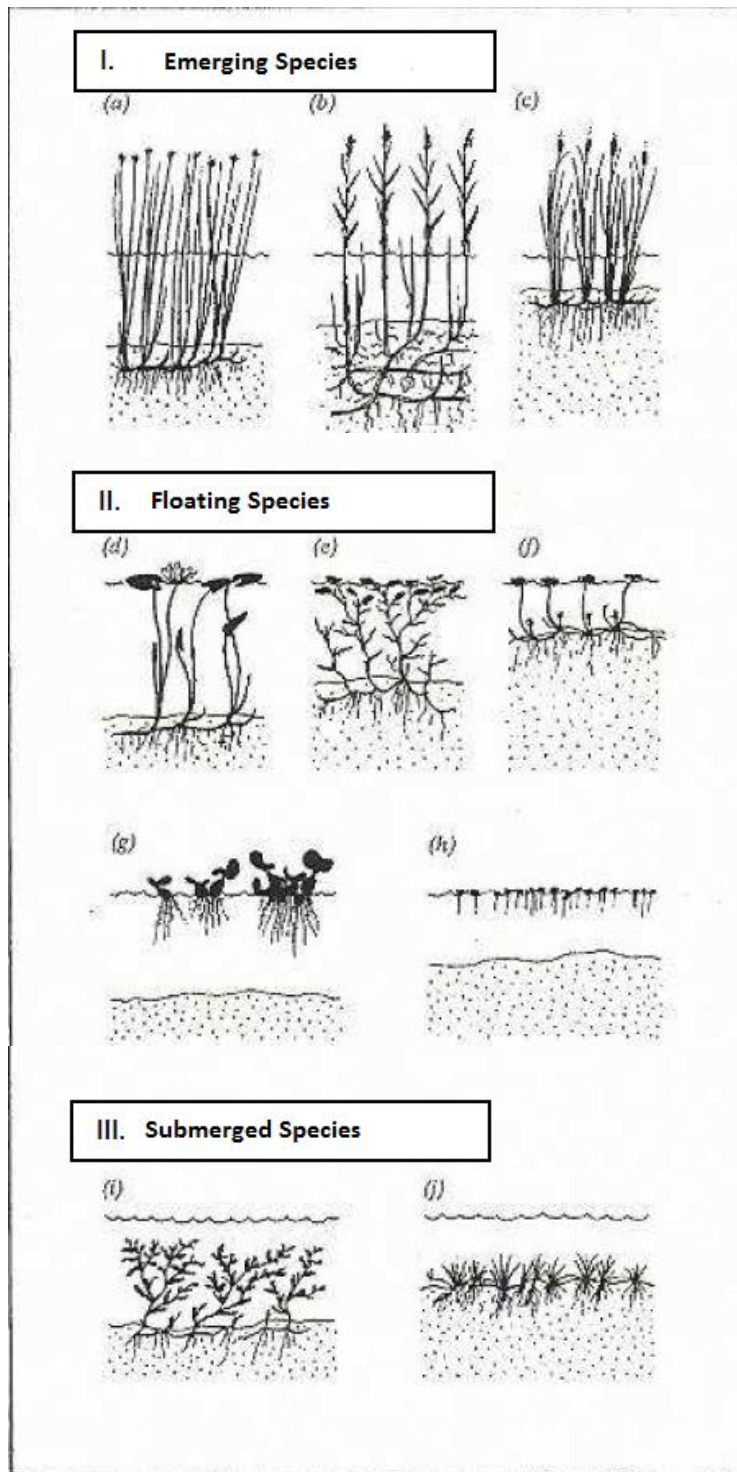


Figure 2.4 - Different types of macrophytes plants: emerging (I), floating (II) and submerged (III). The species present in this illustration are (a) *Scirpus lacustris*, (b) *Phragmites australis*, (c), *Typha latifolia* (d) *Nymphaea alba*, (e) *Eichhornia gramineus*, (f) *Hydrocotyle vulgaris*, (g) *Eichhornia crassipes*, (h) *Lemna minor* (i) *Potamogeton crispus* and (j) *Litorella uniflora*. (adapted from Brix and Schierup, 1989)

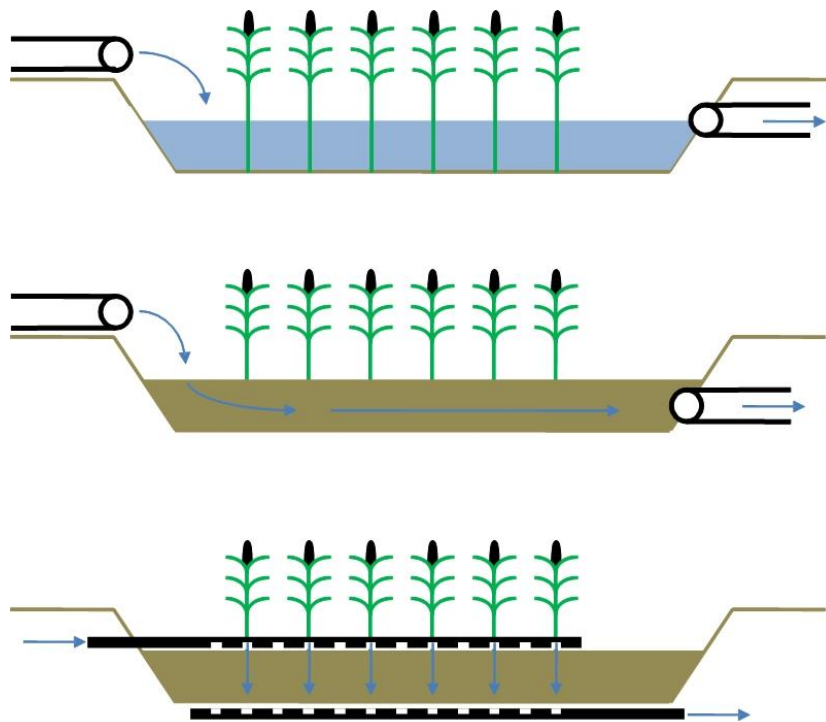


Figure 2.5 - Flow Orientation.

The plant species that are mostly used for planting in constructed wetlands are:

- Common Reed (*Phragmites Australis*);
- Club Rush, Bulrush or Tule (*Scripus Lacustris*);
- Bulrush, Common Bulrush, Broadleaf Cattail, Common Cattail, Great Reedmace, Cooper's reed or Cumbungi (*Typha Latifolia*);

In Portugal, *typha latifolia* are the most commonly used plant species because they are relatively abundant in natural wetlands.

The extensive roots and rhizomes of macrophyte plants contribute with oxygen for creating an oxidizing environment in the subsurface areas of CW, which will enhance aerobic removal pathways. In addition, the plants contribute for maintaining a suitable hydraulic conductivity of the medium by forming flow cannel as its roots and rhizomes grow. The depths of the plants are important especially in species with long, vertical roots. For example, the common reed (*Phragmites australis*) has roots that reach up to 100 cm in depth favouring the treatment processes for deeper beds.

3 Flow Measurement

3.1 Introduction

Surface flow can be described as a continuous movement of water in open channels. The volume of water that passes in a section of a channel in a period of time is called flow rate or volumetric rate of water flow (in units L^3/T). Therefore, to estimate the flow rate, is needed to measure the flow velocity (L/T) and to multiply the value by the section of the channel (L^2) or to use a water level meter over a weir with a known water level-discharge relationships (e.g. Parshall flume, rectangular, triangular or v-notch weirs).

The more accurate the water level, the more closer to reality will the data be for problem assessment, watershed project planning, calculation of treatment needs, control of HLR, design of management measures, and project evaluation.

3.2 Types of flow measurement devices

There are many types of flow measurement devices (or flow meters) used for quantifying the volume of water that flows through a channel section in a period of time, namely:

- Mechanical devices;
- Differential pressure flow meters;
- Optical flow meters;
- Open channel devices (weirs and water table measurement);
- Thermal mass flow meters;
- Vortex flow meters;
- Electromagnetic, ultrasonic and Coriolis devices;
- Laser Doppler flow measurement;

Mechanical flow meters

This type of flow meter measures flow rates from known volumes of fluid run through a series of gears or chambers', consequently causing a positive displacement. A simpler version of this measurement is done by flow/water spinning a turbine or rotor (AWWA, 2006).

The most commonly used mechanical flow meters are:

- Piston meter/Rotary meter (Figure 3.1);
- Nutating disk meter (Figure 3.2);
- Oval gear meter (Figure 3.3);

- Turbine flow meter (Figure 3.4);
- Woltmann meter (Figure 3.5);
- Single jet meter;
- Paddle wheel meter;
- Multiple jet meter (Figure 3.6);
- Pelton wheel;
- Current meter;
- Variable area meter;

The positive displacement flow meter operates by accumulating a known volume of liquid and then by counting the number of times the volume is filled to measuring flow. The measurement must be done with clean liquid, in which particles greater than 100 microns in size must be removed by a filtering system. This can be considered one of the main reasons why positive displacement meters are not recommended for measuring slurries or abrasive fluids seen that these types of fluids will wear and tear the meter and thus inaccurate results for flow measurement will be produced. This type of flow measurement meters are usually found in many homes as household water meters (Arregui *et al.*, 2007).

A turbine or rotor flow meter consists of a multi-bladed rotor with each blade angled towards the flow, being suspended in the liquid stream on a free-running bearing. The speed of the turbine spins is proportional to the volumetric flow rate. The rotation of the turbine can be detected either by mechanical sensors or solid state devices. This type of system has a high accuracy and reliability factor. The rotation of the turbine can be detected by solid state devices, as reluctance (the resistance to magnetic flux offered by a magnetic circuit, determined by the permeability and arrangement of the materials of the circuit, Figure 3.4-A) or inductance (a property of a circuit by which a change in current induces, by electromagnetic induction or electromotive force, Figure 3.4-B).

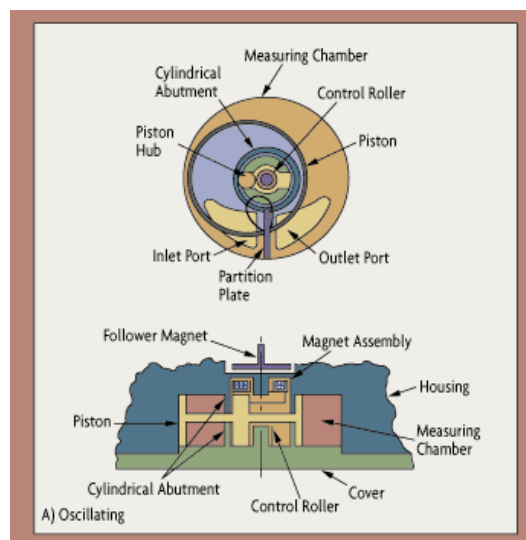


Figure 3.1 - Oscillation Piston Meter (adapted from OMEGA, 1995).

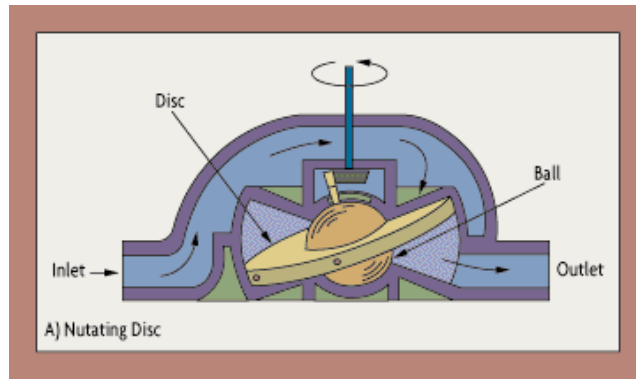


Figure 3.2 - Nutating disc (adapted from OMEGA, 1995).

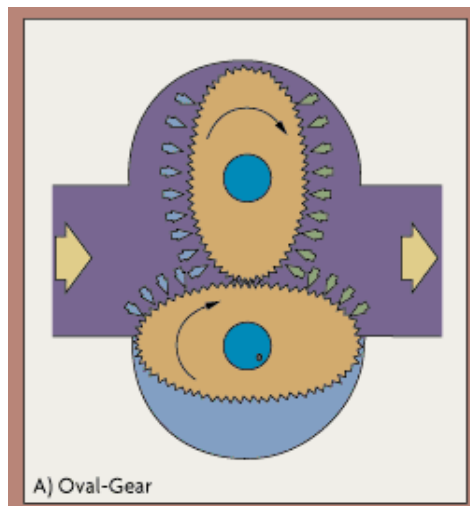


Figure 3.3 - Oval Gear Meter (adapted from OMEGA, 1995).

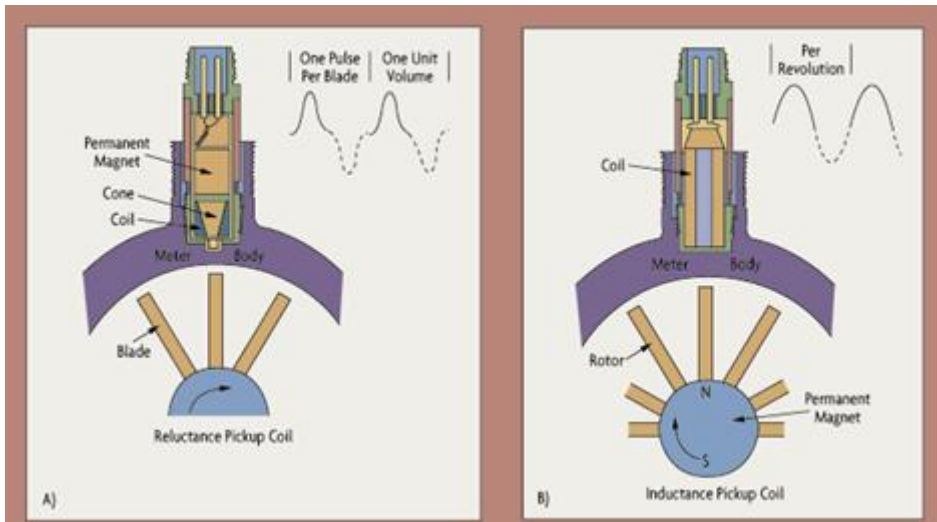


Figure 3.4 - Turbine flow meter: A) with reluctance pickup coil. B) with Inductance pickup coil (adapted from OMEGA, 1995).

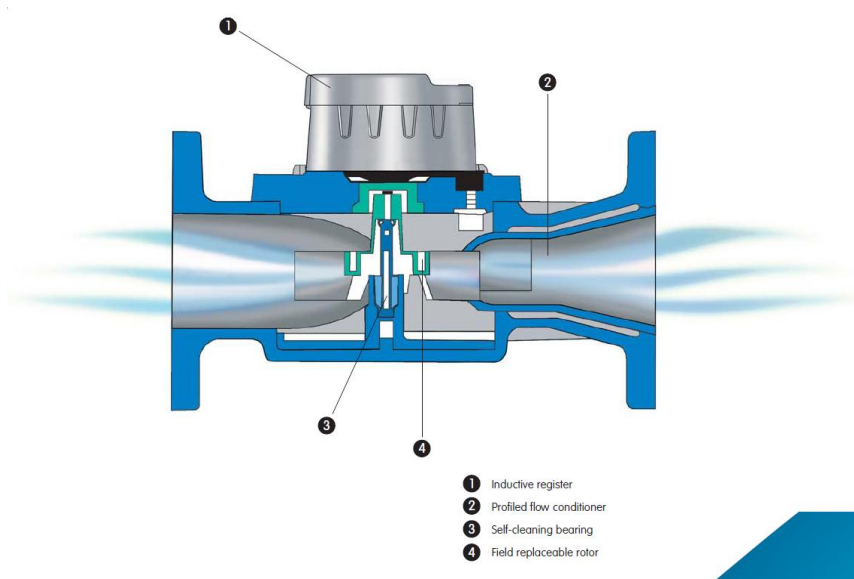


Figure 3.5 - Woltmann turbine meter (adapted from OMEGA, 1995).

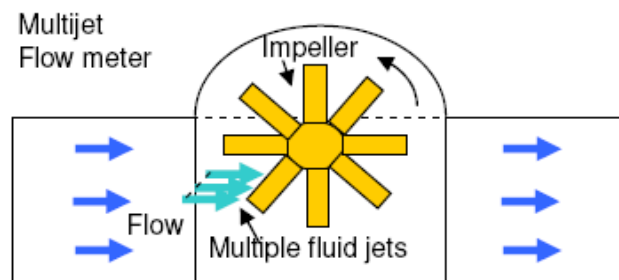


Figure 3.6 - Multijet flow meter.

Differential pressure flow meters

Measurement of stream-flow is done by using a primary element or restrictions to cause a pressure drop and accelerate (the energy of this acceleration is obtained from the fluid's static pressure), thus measuring the differential pressure within a restricted area. Flow rate changes with the pressure drop across the primary element. In simpler words, the basic operating principle is based on the idea that the drop in pressure across the meter is proportional to the square of the flow rate. This is measured using a differential pressure transmitter or by observing a scaled ruler. Other means of measurement are done by measuring static and stagnation pressures to originate dynamic pressure. This is done by stagnating the fluid and transforming all kinetic energy into pressure energy (isentropically). Pressure-based meters have a primary and secondary element. The primary element causes a change in kinetic energy, causing the differential pressure in the pipe, whilst the secondary element measures the differential pressure and provides a signal that is converted to the real flow value.

The most commonly used pressure-based meters are (Ripka and Tipek, 2007):

- Venturi meters (Figure 3.7);
- Variable area meter (Figure 3.8);
- Orifice plate (Figure 3.9);
- Dall tube;
- Pitot tube (Figure 3.10);
- Multi-hole pressure probe.

Venturi meters are used to measure the velocity at which liquid flow's in a pipe. The meter consists of short length of pipe shaped like a vena contracta (the point in a fluid stream where the diameter of the stream is at its least and fluid velocity is at its maximum). A local pressure drop is provoked in the throat of the Venturi meter when liquid passes through caused by an obstruction that narrows the width of the meter, thus accelerating the liquid. By observing this phenomenon and by using Bernoulli's equation, it is possible to calculate the rate of flow of the liquid flowing through the pipe, as shown in Figure 3.7 (B).

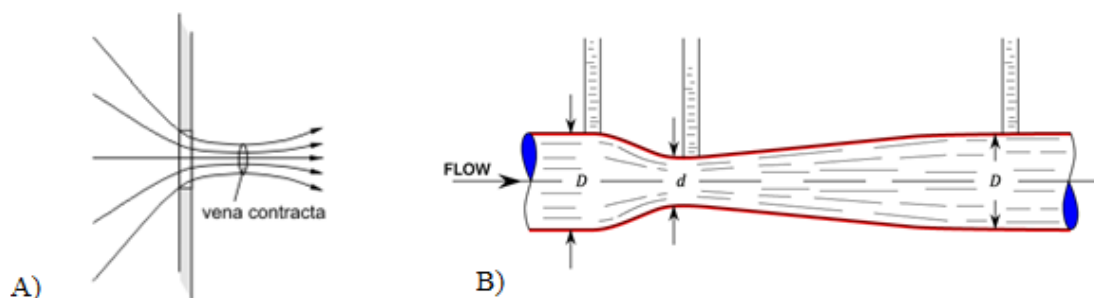


Figure 3.7 - Vena Contracta (A) and Venturi meter (B) (adapted from Falkovich, 2011).

The variable area meter measures flow by allowing liquid flow to adjust the opening within the meter. This is done by displacing an internal part. In simpler words, when there is an increase in flow the fluid generates more force and displaces the internal part farther. One of the most used variable area meters is the rotameter. This meter usually consists of a tapered tube (glass) and a “float” (which is actually a shaped weight and does not really float) inside the tube. The float is either pushed up by the drag force of the flow or pulled down by gravity, whilst the tube is in a funnel configuration, going from a narrow area to a wider area as shown in Figure 3.8.

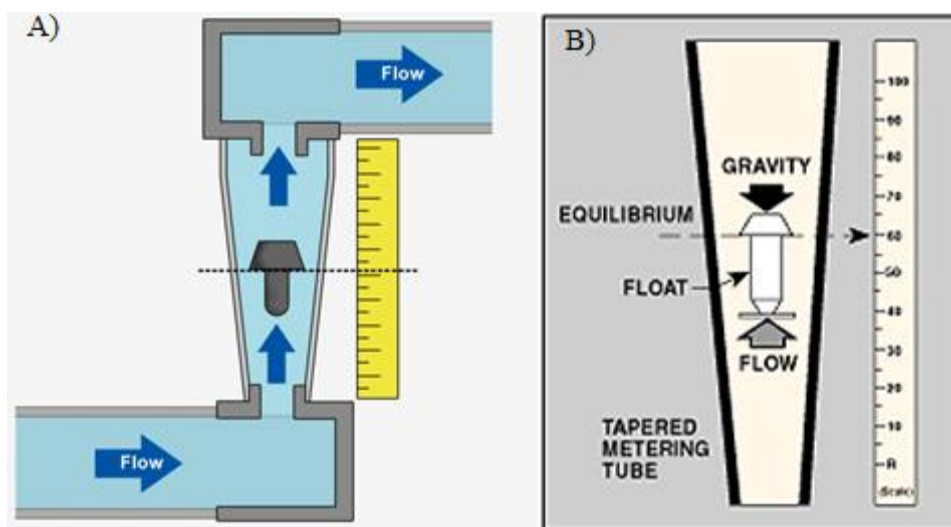


Figure 3.8 - Rotameter (adapted from Falkovich, 2011).

An orifice plate is used to obstruct the flow of liquid by narrowing the pipe diameter and thus forcing the flowing liquid to constrict, causing a pressure drop which is related to the volumetric flow based on Bernoulli's equation (Figure 3.9). In other words, an orifice plate is a sheet of metal with a specific-sized hole bored in it. The liquid flow is measured by the difference in pressure from the upstream side and the downstream side of a partially obstructed pipe. Most of the orifice plates are of a concentric type, but eccentric, conical (quadrant), and segmental orifice plates are also used, as shown in Figure 3.8 (B). The orifice plate is installed between two flanges, it acts as the primary device while it constricts the flow of liquid to produce a differential pressure across the plate. To detect the differences in pressure on each side of the plate, pressure taps on each side of the plate are used.

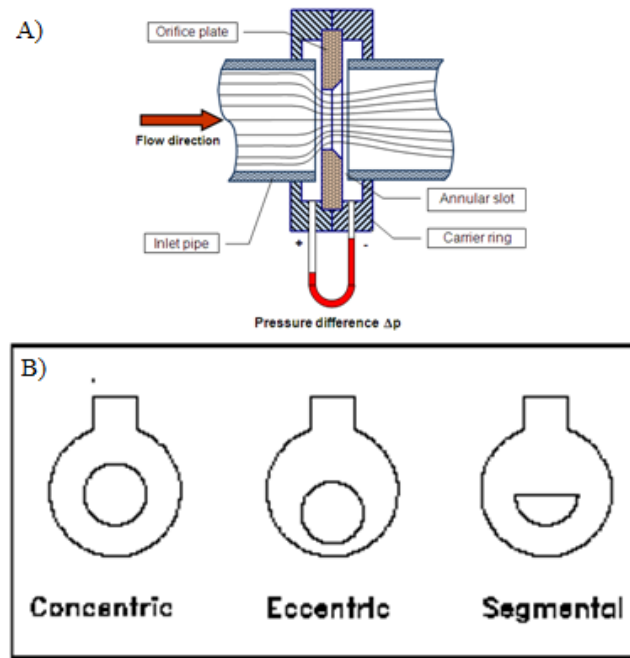


Figure 3.9 - Orifice plate meter (A), Different types of orifice plates (B) (adapted from Falkovich, 2011).

The Pitot tube (Figure 3.10) is a pressure measuring instrument used to measure fluid flow velocity by determining the stagnation pressure (static pressure at a stagnation point in a fluid flow) located at the pitot tube entrance. The liquid flow velocity is measured by converting the kinetic energy of the flow into potential energy. Thus the utilization of Bernoulli's equation is used to calculate the dynamic pressure and consequently the liquids velocity and volumetric flow. The pitot tube is a curved tube with an inlet that points towards the flow direction, there is no outlet. On most pitot tubes there is a second pressure port on the side of the tube that senses the static pressure. The difference between the total pressure and static pressure can be used to determine liquid velocity.

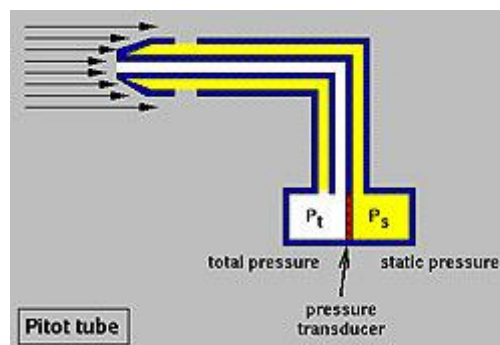


Figure 3.10 - Pitot tube (adapted from Falkovich, 2011).

Optical flow meters

In this type of meters, light is used to determine the flow rate, in other words, two laser beams or infrared diodes are focused at a short distance apart in the flow path in a pipe by illuminating optics. This technology measures the actual speed of particles in liquid and does so by having laser light scattered when a particle crosses the first beam. Detecting optics then collect dispersed light on a photo detector, producing a pulse signal. When the same particle passes through the second beam, a second pulse is registered through the same way as the first. By measuring the time interval between the two pulses, the velocity of the liquid in the pipe is calculated by dividing the distance between the lasers by the time the particle took to cross that distance, as shown in Figure 3.11.

They are used for point level sensing of sediments, liquids with suspended solids and liquid-liquid interfaces. They detect the decrease or change in transmission of infrared light emitted either from an infrared diode (LED) or laser. Because the distance between the two lasers does not change, there is no need for periodic calibration. Optical flow meters are very stable and do not possess any moving parts while delivering a high repeatability for measurement of liquid. The optical flow meter can be mounted in very different types of liquids, being those liquids aqueous, organic and even corrosive. A common application of this type of sensors is used for detecting sludge/water interface in settling ponds. The LED lights are better bet because they are cheaper to build and maintain when compared to laser beams. One disadvantage is that the optics must be frequently cleaned to maintain performance.

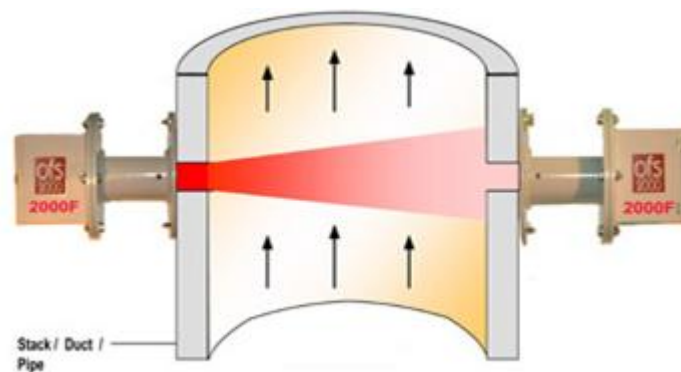


Figure 3.11 - Optical flow meter (adapted from OMEGA, 1995).

Open channel flow

Flow in open channels is not only common in industrial applications, but are also very common in urban applications (irrigation, water and wastewater works), as well as in natural streams (rivers). Open channel flow takes place when liquid flows in conduits or channels with a free surface. The liquid that runs in culverts or channels underneath streets are also

considered open channel flow, as well as liquid flow in sewers and tunnels which are partially full and not under pressure. Classical examples of open channel flow are found in treatment plants, storm and sanitary sewer systems, industrial waste applications, sewage treatment plants and irrigation systems.

A simple way to understand the difference in open channel flow and closed pipe flow is to think of it as the difference between gravity-induced flow and pressurized flow. The determination of flow rate may be carried out from two different ways:

- Using a weir and measuring the water depth (water level or water table) upstream the weir, being the flow rate given by the weir equation.
- By measuring the flow velocity that passes a cross section of the channel, and multiplying the value by the section area;
- Using a tracer experiments;

A weir consists on an overflow structure which is built across a channel and is perpendicular to the flow of liquid (Figure 3.12-A). Some weirs have opening of fixed dimensions cut at the top edge (called the weir notch). The overflowing sheet of water is known as the nappe. Weirs are designed to change the flow characteristics by causing water to group behind the structure, which runs across the channel/river, but unlike a dam it allows water to flow over the top.

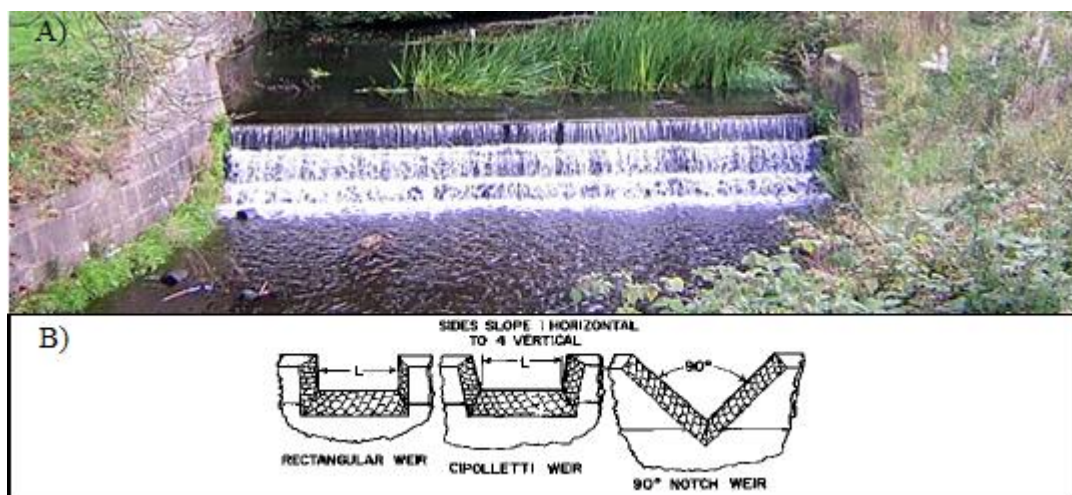


Figure 3.12 - Weir in a natural stream (A) and different shape weirs (B) (adapted from Smajstrla et al., 2002).

Since weirs are easy to design and to use, they are used for measuring volumetric flow rate in small to medium-sized streams and water works or in industrial applications. Measuring the flow rate consists in measuring the water table upstream of the weir (using an ultrasonic or electromagnetic meter, for example), followed by conversions to flow rate using the weir equation.

There are usually two types of weirs that are most commonly used: the sharp-crested weirs and the broad-crested weirs. A sharp-crested weir allow for water to fall cleanly away from the weir, they are typically 0.6 cm thick and come in many different shapes such as rectangular, V-notch and Cipolletti weirs, as shown in Figure 3.12-B. The sharp-crested weir is considered not very accurate or reliable especially when reading and measuring from an orifice. The sharp edge in the crest causes the liquid to spring clear of the crest making it possible to acquire accurate measurements. The broad-crested weir can be described as a flat-crested structure, with an extended crest compared to the flow thickness. Because the crest is broad, the streamlines become parallel to the crest invert and the pressure distribution above the crest is hydrostatic.

Practical experience showed that the weir overflow is affected by the upstream flow conditions and the weir. Broad-crested weirs are commonly used in hydraulic structures. Weirs are usually used to alter flow regime of a river, to prevent flooding, to measure discharge and to help make a river navigable, whilst inspecting and checking critical parts of weir structures degradation and improper operation are easy, making this type of flow measurement an easy solution to upkeep.

The area-velocity method is a common method in medium-large rivers, where the section is not regular. The section of irregular section may be measured using partial measurements (depth x width) and applying an integration method for area estimation. The velocity may be measured using Doppler equipment or a rotameter device.

Tracer experiments consist in injecting a known concentration of tracer (saline, dye or radioactive reagent) into the liquid and the measurement of tracer concentration at time intervals downstream the injection point. If properly executed, an accurate measurement of a stream's velocity and dispersion coefficient can be determined. The dilution factor/rate is then utilized to accurately calculate the flow rate for that specific test section. However, it is a time consuming method and, many times, is expensive and difficult to replicate for the same conditions.

The Doppler device records instantaneous velocity components at a single point with a relatively high frequency by measuring the velocity of particles that pass by. The device sends out a beam of acoustic waves at a fixed frequency from a transmitter probe (Figure 3.13). These waves bounce off of moving particles in the water and three receiving probes "listen" for the change in frequency of the returned waves. The ADV then calculates the velocity of the water in the x, y, and z directions. This type of sensor is based upon the Doppler shift (change) effect.

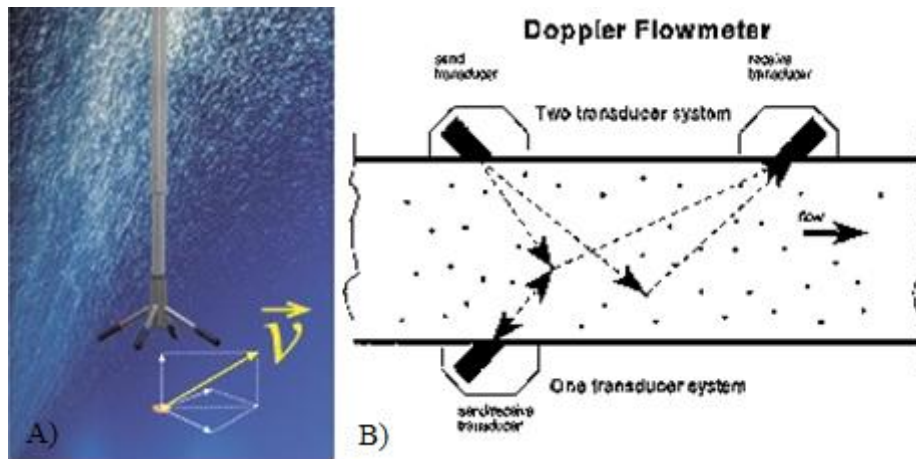


Figure 3.13 - Doppler calculating velocity.

Thermal mass flow meters

The thermal mass flow meters usually use an arrangement of heated elements and temperature sensors to measure the difference between static heat transfer and flowing heat transfer to a liquid and thus deduces the flow of liquid by knowing the liquids specific heat (this has been *a priori* measured by the device and compensated) and density. If the liquid keeps its density and specific heat characteristics constant, then the meter can produce direct mass flow readout and no compensation is needed.

The thermal mass flow meter has two distinctive ways of operating, either by inserting a known amount of heat into the flowing liquid and measuring an associated temperature change, or by maintaining the probe at a constant temperature and measuring the energy required to keep it that way (Ripka and Tipek A, 2007). They usually consist of two temperature sensors and an electric heater between them. There are two different methods for measuring the quantity of heat that is dissipated, one is known as the “Constant Temperature Differential” method, as shown in Figure 3.14, and the second as the “Constant Current” method.

The first method uses two temperature sensors: a heated sensor and sensor that measures the temperature of the liquid. Mass flow rate is calculated based on the amount of electrical power required to maintain a constant difference in temperature between the two temperature sensors. So as liquid flows, heat is dissipated or carried away and as the flow rate increases, more current is required to keep the element at a fixed temperature. The current requirement is proportional to the mass flow rate.

The second method uses the same sensors as the first method, a heated sensor and another one that detects the temperature in the flow of liquid, the difference lies in how mass flow is measured. The power to the heated sensor is kept constant in this case. Mass flow is then

measured as a function of the difference between the temperature of the heated sensor and the temperature of the flow stream of liquid (AWWA, 2006). The sensors are usually very small and fragile, and consist of a heated thin wire element. Hot wire anemometers have a quick response time, because they are so small and thin. However, they are fragile for very high flows. In all, both these methods thrive from the idea that greater cooling results come with higher velocity flows, while both measure mass flow based on the measured effects of cooling in the flow stream of liquid.

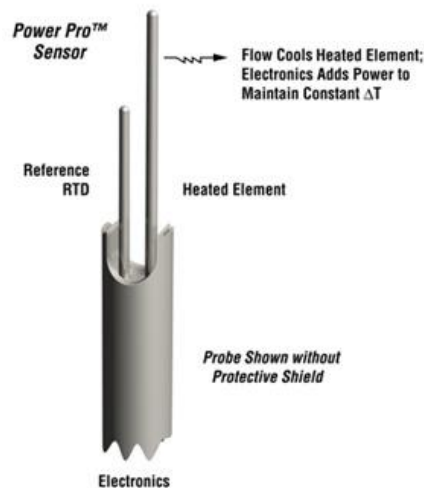


Figure 3.14 - Constant temperature differential probe (adapted from <http://www.foxthermalinstruments.com/flowmeter-technology.php>).

Vortex flow meters

This method is based on the principle of 'Kármén Vortex Street' and consists in placing a shedder bar, also known as a bluff body (non-streamlined object or broad body with a flat front), in the path of the liquid at right angles to the flow stream, thus creating disturbances in the flow called vortices or whirlpools and measuring the vibrations of the vortices downstream of the object. The vortex generating flow meter is based on simple principle where obstructions that are placed in running water generate vortex trails in the flow.

The vortices will trail behind the bluff body, alternately from each side in sequence. A simpler way of putting it is that a bluff body is placed in the path of fast-flowing stream, the liquid will then hit the bluff body and alternately divide to pass around the object. Due to viscous adhesion, the boundary layer moves slower than the outer layer and at lower flow rates these viscous forces dominate and keep the liquid attached to the wall of the object, meaning that the liquid will then recombine in a symmetrical fashion downstream. As the

flow rates increase, there comes a point where the flow cannot endure the adhesion pressure along the surface of the object and the boundary layer consequently separates from it forming rotating vortices that are then carried downstream. The distances between the vortices are constant and depend on the size of the object that is used to form the vortices. It is important to note that on the side of the bluff body where the vortex is being created, the liquid velocity is higher and the pressure is lower, whilst the vortex travels downstream it grows in size and strength and will eventually detach or shed itself from the bluff body, as shown in Figure 3.15.

Usually the sensor that is used for measuring the frequency of the vortex shedding is placed inside, atop or downstream of the bluff body and a piezoelectric crystal is used, which will produce a voltage pulse every time a vortex is created (Ripka and Tipek A, 2007). Other methods consist in using a capacitive sensor or ultrasonic sensor to detect vortices. Knowing that the frequency of the voltage pulse is proportional to the liquid velocity, a volumetric flow rate can be calculated by using the cross sectional area of the pipe and multiplying it by the flow velocity. This type of measuring uses three components, a bluff body strut-mounted across the flow meter bore, a sensor to detect the presence of the vortex and to generate an electrical impulse and signal amplification and conditioning transmitter whose output is proportional to the flow rate.

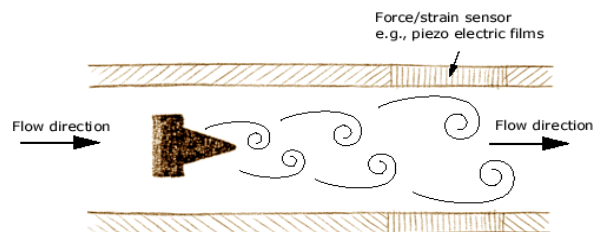


Figure 3.15 - Vortex flow meter (bluff body and sensors) (Adapted from http://www.efunda.com/designstandards/sensors/flowmeters/flowmeter_vtx.cfm).

Electromagnetic flow meter

The principle of operation of the electromagnetic flow meter is based on Michael Faraday's Law of Electromagnetic Induction. They are designed to measure the flow of electrically charged liquids in a closed pipe and are considered volumetric flow measuring devices, meaning that the liquid are obliged to be conductive. In other words, the liquid has to be electrically conductive, meaning that when it passes through the pipe it is equivalent to a conductor cutting across a magnetic field. This is based on the principle that a voltage is induced in an electrical conductor (the flowing liquid), moving through a magnetic field.

The electromagnetic flow meter (also known as a magnetic flow meter) obtains the flow velocity by measuring the changes of induced voltage of a conductive liquid passing through a controlled magnetic field (Figure 3.16). By being an electrically conductive liquid, it induces

changes in the voltage reading between the electrodes, and while the flow speed gets faster, the voltage gets higher. Usually a magnetic flow meter places two electric coils around the pipe (inline model) or near the pipe (insertion model) on each side of which the flow is to be measured, and sets up a pair of electrodes, which sense the flow-induced voltage, across the pipe wall for the inline model or at the tip of the flow meter for the insertion model (Ripka and Tipek A, 2007).

The electrodes should be in a horizontal state to prevent air from breaking the voltage measuring circuit, meaning that the meter must be correctly mounted. The meter itself consists of a nonmagnetic and nonelectrical conducting pipe, lined with an insulating material through which liquid flows through. Usually the meter has electrical circuits to measure and transform voltage into a flow rate on a meter dial, whilst flow can be measured in both directions. Properties such as temperature, viscosity, density, or even solid particles do not change the performance of the meter, however dissolved chemicals can deposit on the electrodes and cause some accuracy errors. The magnitude of the induced voltage is proportional to the velocity of the conductor (liquid), for a given field strength, thus flow velocity is obtained and flow rate can be calculated by knowing the cross-sectional area of the pipe (AWWA, 2006).

Magnetic meters can be useful for measuring untreated water, raw (untreated/unfiltered) water, and wastewater, since there are no moving parts clogged or damaged by debris flowing through the meter. Stray electrical energy flowing through the flow tube can cause inaccurate readings, therefore most magnetic meters are installed with either grounding rings or grounding electrodes to divert stray electricity away from the electrodes inside the flow tube which are used to measure the flow.

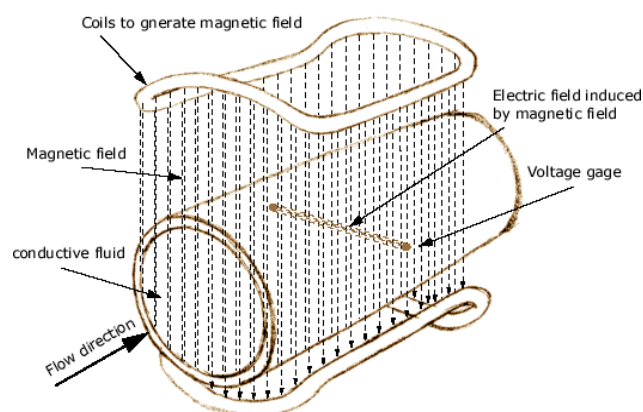


Figure 3.16 - Magnetic Flow Meter (Adapted from http://www.efunda.com/designstandards/sensors/flowmeters/flowmeter_mag.cfm).

Ultrasonic flow meters

Usually used for non-contact level sensing for highly viscous liquid like water treatment applications for pump control and open channel measurement. The ultrasonic flow meters measure the velocity at which the liquid flows by using the principle of ultrasound. By using ultrasonic transducers, the meter measures the average velocity along the path of an emitted beam of ultrasound, by averaging the difference in measured transit time between the pulses of ultrasound propagating into and against the direction of flow. They emit a high frequency acoustic waves that are reflected back to the emitting transducer and are thus detected by the transducer.

There are two types of ultrasonic flow meters, one is to measure the traveling times of ultrasonic waves and are known as transit time ultrasonic flow meters whilst the other is used to measure the frequency shifts of ultrasonic waves, known as the Doppler flow meters, in a pre-configured acoustic field in which the flow passes through to determine flow velocity. Since the Doppler flow meters were already mentioned and scrutinized above, here attention will be given to the transit time ultrasonic flow meters.

The transit time ultrasonic flow meter is based on the principle that transit time of an acoustic signal along a known path is altered by the fluid velocity. It is usually composed of a pair or pairs of transducers, each has its own transmitter and receiver and are placed on the pipe wall, as shown in Figure 3.17. One set is placed on the upstream and the other set on the downstream at a pre-defined angle. The time it takes for the acoustic waves to travel from the upstream transducer to the downstream transducer is always shorter than the time it takes for the same distance but from the downstream transducer to the upstream transducer. This occurs because of the flow direction, whereas sound waves will travel faster going downstream than going upstream. The larger the difference between the times, the higher the flow velocity is. For an example, if the flow is stationary, the time that it takes for the signal from the transducer upstream to reach the transducer downstream is the same for the signal from the downstream transducer to reach the upstream transducer.

When there is flow, the effect will boost the speed of the signal travelling downstream while decreasing the signal emitted by the downstream transducer's speed travelling upstream (OMEGA, 1995). Then, by knowing the path angle with respect to the direction of flow, the average velocity can be obtained and thus by multiplying the cross-sectional area of the pipe by the average velocity, the flow rate can be calculated. This method is not dependable on particles or bubbles in the flow stream as the Doppler meter is.

Ultrasonic flow meters are however affected in terms of response and accuracy by temperature, density, moisture, pressures, turbulence, foam, steam, chemical mists (vapour), changes in the concentration of the process material and viscosity of the liquid flow, but are easy to maintain because they don't have any moving parts. To ensure the best

results, proper mounting of the transducer is required. The speed of sound in liquids is in function of both density and temperature and have to be compensated for by calibration (AWWA, 2006).

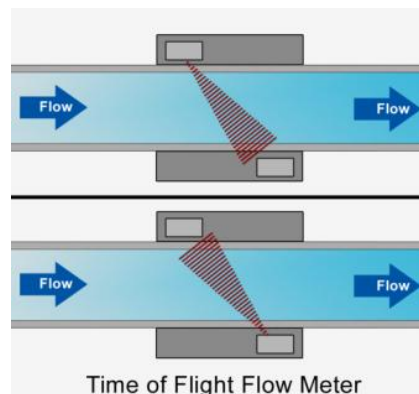


Figure 3.17 - Ultrasonic Flow Meters (Adapted from http://www.alicatscientific.com/types_of_devices.php).

Coriolis flow meters

The Coriolis flow meters are based on the Coriolis Effect which was discovered by Gaspard-Gustave de Coriolis, when noted that all bodies moving on the surface of the planet tend to drift sideways because of the eastward rotation of the planet. For example, in the Northern Hemisphere the deflection is to the right of the motion, thus when a toilet is flushed its angular rotation is from left to right, whilst in the Southern Hemisphere the deflection is to the left of the motion, meaning that when a toilet is flushed in the Southern Hemisphere its angular rotation is from right to left. Since the equator has to rotate around a larger circle per day than any point closer to the poles, a body travelling towards the South Pole or North Pole will bear eastward, this happens because it keeps its higher (eastward) rotational speed as it passes over the more slowly rotating surface of the earth. This drifting effect is known as the Coriolis force (OMEGA, 1995).

The Coriolis flow meters artificially introduce the Coriolis acceleration into the flowing stream and measure the amount of mass flow by detecting the resulting angular momentum. The Coriolis flow meters measure the amount of mass flowing through the tubes and not the volume of liquid. It uses the Coriolis Effect to measure the amount of mass travelling through the tube. The liquid that is going to be measured will run through parallel tubes, usually U-shaped that are caused to vibrate in an angular harmonic oscillation. The tubes will deform due to the Coriolis forces and an additional vibration component will be added to the oscillation.

A phase shift or twisting occurs on some places of the tube due to the additional vibration component caused by the liquid flowing through the tubing. The mass flow is directly proportional to the amount of tube vibrating/twisting. A simpler way of putting it is, in the Coriolis flow meter, liquid is restricted in two small tubes which are parallel to one another and are curved. These tubes vibrate, which is normally driven by two electromagnetic coils located at the bend of the tube, at their resonant frequency in opposite directions. When mass flows through the tubes it delays the vibration at the incoming side and accelerates the vibration at the outgoing side, this creates a torque and twists the tube. In other words, while the tube is vibrating upward, the fluid flow forces down on the tube and when the fluid flows out of the tube, it forces upward. The inverse process happens when the tube is vibrating downward. This will cause a small time delay between the two ends of the tube due to the amount of twist that is occurring. The time delay that is produced is measured and used to calculate the mass flow through the tubes.

One of the main advantages of using a Coriolis flow meter is that it measures mass flow and not volumetric flow. Accuracy which is extremely high and thus unaffected due to the fact that mass is not affected by changes in pressure, temperature, viscosity and density, meaning that it can measure virtually any type of liquid at any pressure and temperature. But the meters accuracy is its downfall because it makes this type of meter relatively expensive when compared to other meters. Volumetric flow rate metering is proportional to mass flow rate only when the density of the fluid is constant (Ripka and Tipek, 2007).

Optical fibre meters

Water level measurement through optical fibre has been growing substantially in the last decade, due to the fact that components such as glass and light emitters have become available more easily. An optical fibre can be described as a flexible, transparent fibre made out of pure glass (silica), not much wider than the hair of a human and it functions as a wave guide to transmit light between two ends of the fibre. The problems with this type of technology consist in manufacturing robust, reliable and safe devices at a low cost. For level measurement most of these types of sensors are either level controllers because of their limited range and accuracy.

Betta *et al.* (1995) have proposed a digital level transducer based on optical fibre, which can measure continuous water levels on a step index fibre (double cladded for fibre in the air; W-type when in liquid) where the cladding was removed in n zones at fixed distances from each other. The requirements for this technology are a light source, measurement hardware (not cheap) and different calibration curves for each type of liquid and range. The liquid level

measurement is then done by variations of transmitted power through the optical fibre, this happens when liquid touches or leaves one of the cladding zones.

In other words, power propagates through an optical fibre which suffers a reduction in power if a part of the fibre cladding is removed and if the external media (liquid) has a refractive index greater than the one found in the core. So the variation in power decreases as soon as the liquid touches one of the “without-cladding” zones, thus reducing the power and giving a level reading. It is important to note that a cladding zone and a zone without cladding when in the absence of liquid have the same refractive index, so when the zone without cladding is immersed in liquid, the laser beam meets the core-liquid interface and consequently the ray is refracted, resulting in a reduction in power due to the liquid present in that zone which is later detected by a photo-detector.

In the accuracy field manufacturing processes and location of the sensor in the tank need special attention while the resolution of the sensor depends on the distance between the zones without cladding, in this case the prototype possesses a 25mm distance between the zones without cladding, for static characterization of the sensor. Hysteresis was practically absent while repeatability was considered good. No testing was done with wastewater, thus it is not possible to know how the system would behave in these circumstances, but it's easy to predict that the sensor will need frequent maintenance due to the existence of impurities in the liquid.

Dynamic characterization of the sensor was evaluated through its response time, the maximum time interval between the crossing of a zone without cladding and the updating of the display, which had an average response time of 370ms, whilst the maximum level variation speed is determined by the duration of the monostable output impulse (2.5 s). The maximum level variation speed of this prototype is about 10 mm/s. No testing was done with wastewater, thus it is not possible to know how the system would behave in these circumstances, but as mentioned before it's clear that in terms of maintenance this sensor is not indicated for wastewater measurement. By manufacturing the sensors through more sophisticated techniques, the dynamic and static sensor limits may be overcome, while on the other hand the resolution can be enhanced by constructing thinner zones without cladding.

A new non-intrusive optical technique to measure transparent liquid level and volume was proposed by Singh et al. (2010) for continuous measurement in a cylindrical container. The measurement technique is based on the principle of inducing modulation on the liquid level, where a solid angled divergent light beam is focused on the liquid's surface. Therefore, when transparent liquid is put in the container the variation of liquid level in the container induces modulation in the cone of the divergent light focused on the liquid surface, this results in transmission of an intense modulated light beam through the bottom end of the surface of the container (the light is refracted). A photodetector (PD) then captures the focused beam and the response of the PD changes proportionally. A divergent beam of light coming from the LED is collimated (made straight) into a parallel beam by using two lenses. The beam is split into

two beams by a splitter (50:50), one beam is used for reference and the other as a sensing beam, liquid variation, as seen in Figure 3.18.

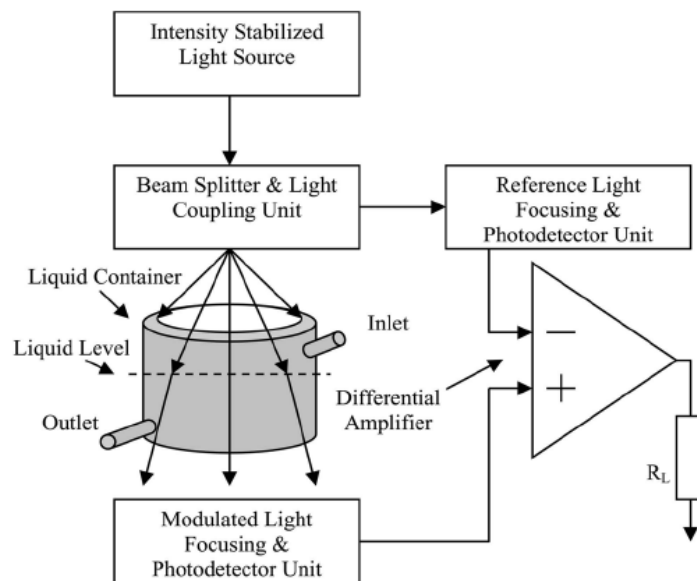


Figure 3.18 - Proposed liquid level and volume measurement system (Adapted from A New Non-Intrusive Optical Technique to Measure Transparent Liquid Level and Volume (Hidam Kumarjit Singh et al., 2010)).

The reference beam goes straight to a Light Dependent Resistor (LDR), designated as PD1, while the sensing light beam is focused to another LDR with the designation of PD2. The light beam for sensing will only reach the PD2 after passing through the liquid and bottom end surface of the container. Measurement is done from the bottom end of the container to the level of the liquid whilst the variation that the liquid volume suffers is measured in terms of proportional change in the DC voltage. Only the volume of liquid is determined, thus each DC voltage obtained corresponds to a volume of liquid. In terms of liquid level measurement, the level can be obtained by applying mathematical formulas to calculate volumes, this is done by knowing the diameter of the cylinder and the volume of liquid in the container then by utilizing the mathematical formula for calculating the volume of a cylindrical cylinder, the liquid's level/height can be calculated. The components that were used for the construction of this prototype are:

- A red-coloured LED;
- Slits;
- A beam splitter;
- Objective lens;
- Liquid containers (beaker's), three of them with volumes of 100, 250 and 500mL ;
- Plane mirrors;

- Light dependent resistors (LDR) - PD1 and PD2;

The liquid containers are internally coated in black so they can be used as a light-wave guiding structure. The black paint eliminates the entry of external light as well as it suppresses light reflection from the internal surface of the container, noting that the light reflection coefficient of the blackened internal surface of the container is considered zero to eliminate reflection effects.

The bottoms of the containers are flattened and transparent to allow light transmission through whilst the liquid container gets light source from a red-coloured LED and acts as an active sensing medium with the change of liquid level and volume in it. The sensitivity varies with the diameter of the liquid containers because liquid level varies very little in larger containers for a given volume, whereas a small container will show considerably larger liquid level variation for the same change in liquid volume. This means that the intensity of the LED is controlled by changing the applied steady voltage for each liquid container separately. When there is no liquid, the light intensity falling on the bottom end of the surface of the container is proportional to the solid angle of the light cone.

Thermal resistance measurement

Another way of level measurement is done through thermal resistance which can be described as a heat property and a measurement of temperature difference by which an object or material resists a heat flow. In other words thermal resistance is analogous to electrical resistance. Electrical resistance is computed as the difference in voltage between two points divided by the electrical current flowing between them. This analogy is based on the fundamental similarity between voltage and temperature, current conduction and heat conduction, whilst electrical conduction occurs in response to a voltage difference the heat conduction occurs in response to a temperature difference (Sofia, 1995).

Lazuardi Umar (2010) has proposed a smart level sensor based on thermal resistance measurement with self-calibration, which is based on the thermal resistance of liquids and gases by using modelling of the current-voltage-curve. This model directly examines the thermal resistance of the sensor when exposed to a specific medium, being this medium gas or liquid. In comparison to air, the thermal resistance of water drops by 82%. The sensor while measuring will present its status on a display as being “empty” - in the air - or “full” - in fluid - consonant its surroundings.

Another factor to have in account is the overall thermal resistance due to dirt which drops the overall performances of the sensor meaning that it will need to be recalibrated, cleaned

or even changed. The variation of thermal resistance whether it is in the air or water is calculated by using a mathematical model based on heat transfer concept.

There are two ways of operating this type of sensor, either by direct or indirect heating. Indirect heating consists in registering the ambient temperature to determine the temperature of a thermistor, and therefore the current flowing through the component is low, while with direct heating implies the direct measurement of the temperature. A simpler way to put it is that the electrical energy is converted into heat, which then affects the temperature of the thermistor and consequently the resistance of the thermistor. For a given voltage applied to the PTC thermistor it self-heats from electrical power resulting from the electrical sensor load. This self-heating effect depends on the load applied and the thermal resistance factor. The delivered thermal output resulting from the temperature increases in relation to the ambient temperature.

The solution proposed by Lazuardi Umar (2010) gets rid of these problems through direct measurement of the thermal resistance independently of the ambient temperature, thus eliminating the need to measure the ambient temperature. With direct heating the current which flows through the sensor heats it. The electrical energy is directly converted into heat which affects the temperature and thus the resistance of the thermistor. When the component is only surrounded by air, very little heat is dissipated. When the liquid rises to the level of the thermistor more heat is dissipated because of the liquid's higher thermal conductivity. This is based on the hot wire anemometer which consists in using a very fine wire which is electrically heated up to a temperature above the ambient temperature. As liquid/air flows past the wire it has a cooling effect on the wire.

When sensors are dirty, more heat is dissipated to the surroundings, this happens because the dirty diameter increases consequently the I - V characteristics are shifted toward a higher current and may induce error readings. This can be fixed by cleaning, recalibrating or even changing the sensor. The main advantage of this new approach is that the thermal resistance of the sensor exposed to a specified medium can be directly determined and consequently the sensor characteristics are monitored instantly, being very important for long-term stability and sensor lifetime. This method is very good for protection of overfills in liquid containers, being able to then display the liquid level as "immersed" or "not immersed" on a display screen. On the other hand, one of the main disadvantages of this method is the quantity of energy need to heat the sensor.

3.3 Capacitive sensor level measurement

A capacitor generally consists of two conductors (plates or electrodes) that are isolated electrically from each other by a non-conductor (dielectric). An electrical charge is stored when the two conductors are at different potentials, in other words when the water level rises, the air normally surrounding the electrode is displaced by material that has a different dielectric constant leading to a change in the value of the capacitor due to the fact that the dielectric between the plates/electrodes has changed.

This change is detected by radio frequency capacitance instruments which works at a low frequency range (MHz) and converted into a relay or proportional output signal. Measurement is done by measuring admittance of an alternating current (ac) circuit which changes with the water level. The use of a low frequency proves beneficial because it allows for dielectical constant of the material not to change with the frequency. The storage capability of a capacitor is measured in farads. This technology is used to sense material with dielectric constants such as water which possesses a dielectric constant of 88 whilst sewage slurry has a dielectric constant of approximately 50. Capacitance sensors apply an electrical field to measure the dielectric constant of a given medium in the water level measurement field. Generally these sensors have no moving parts, are considered rugged, simple to use and easy to clean.

Guirong, and Shuyue (2010) have developed a capacitive liquid level sensor with four electrodes fixed on the inside wall of a cylindrical vessel. This method detects the level changes of liquid in a vessel and the gradient status of that vessel. In short, this sensor can detect the liquid level and the gradient status of the vessel, whether it is in a vertical or gradient state. It can even give a detailed gradient direction and gradient angle of the vessel if this is inclined.

This sensor has no moving parts and the electrodes are made to suit the vessel's shape. If the vessel is located in a dynamic state, by detecting the change of the liquid inside the vessel the status at which this vessel is at can be estimated as vertical or gradient. By detecting the change of liquid level in the cylindrical vessel, capacitances between electrodes depending on the liquid level height and status of the vessel can be described by the gradient direction and the gradient angle. Hence, capacitances are different for various liquid levels and so is the status of the vessel, therefore the liquid level information and the status of the vessel can be obtained resulting from capacitance measurements.

The cylinder consists of a plastic pipe with thin walls (0.5mm). On the inside of the pipe's surface are four rectangular copper plates all with the same size and gaps (Figure 3.19). The output sensor, C0, is used to detect the level at which the liquid is at, whilst the other outputs, C1, C2, C3 and C4 are used to estimate the status of the vessel (gradient direction and gradient angle), as shown in Figure 3.20.

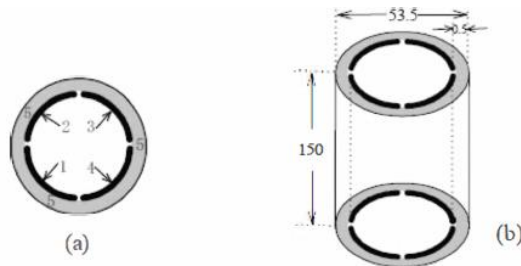


Figure 3.19 - Sensor structure. (a) view of the top of the sensor (1, 2, 3, 4: electrodes; 5: plastic pipe); (b) profile view of the sensor (mm); (adapted from Guirong and Shuyue, 2010).

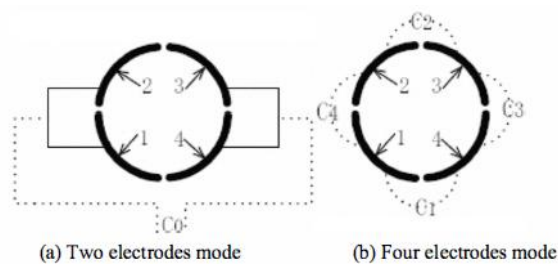


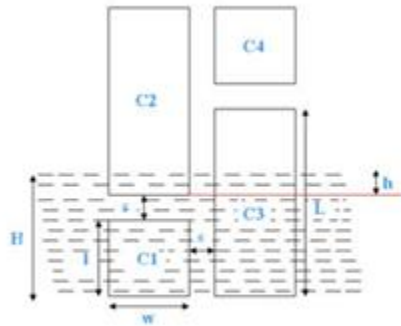
Figure 3.20 - Two electrodes mode and four electrodes mode (adapted from Guirong and Shuyue, 2010).

This sensor can be used as a two electrodes mode sensor or a four electrodes mode sensor, whereas for the four electrodes mode, C_1 corresponds to the capacitance between electrodes 1 and 2, C_2 is the capacitance between electrodes 2 and 3 and finally C_3 is the capacitance between electrodes 3 and 4. In the two electrodes mode, there is only one capacitance which is C_0 and this is formed through the combination of electrodes 1, 2 and 3, 4. Both these modes have different measurement techniques because they deliver different measurement results.

Measurement is done by pouring liquid into the sensor which is fastened on the inside of a wall rather than being inserted into the liquid. In the two electrodes mode only the level of the liquid is determined and not the gradient status of the vessel. In the four electrodes mode the gradient of the vessel can be determined and consequently the gradient direction and the gradient angle of the vessel. This type of sensor measures three different variables, liquid level, gradient direction and gradient angle. The big advantage of this sensor is that no extra components are needed to measure the gradient direction and gradient angle.

A low-cost capacitive sensor for wells level measurement was designed by Blander *et al.* (2010) to replace an existing level sensors mounted on dam wells. It is a capacitive sensor composed of eight independent copper pour (plates) areas distributed in mirror format from each other. To read the height of the liquid it is necessary to determine the capacitance. An AVR microcontroller is used to measure the capacitances as well as a LT1011 comparator for the capacitor charging time calculation. The transducer is made up of two individual

rectangular plates, parallel with each other which represent the capacitor armatures as shown in Figure 3.21. Each armature is divided into four copper pour zones.



where: C_1 – The first capacitor capacitance (completely immersed into the water).

C_2, C_3 – the capacitance of the partially immersed capacitors.

C_4 – the capacitance of the fourth capacitor (with air as dielectric).

H – the water level value.

h – the height of the liquid column corresponding to the capacitor three immersion.

L – the C_2 and C_3 armature length.

l – the C_3 and C_4 armature length.

w – the capacitors width (for all the capacitors).

s – the distance between two consecutive capacitors.

Figure 3.21 - Schematics and principal of measuring (adapted from Blander et al., 2010).

The capacitance of all four capacitors can be evaluated by Eq. (3.1), where ϵ_0 - the vacuum electrical permittivity, ϵ_r - the dielectric electrical permittivity, A - the capacitor's armature area, d - the distance between the armatures.

$$C = \epsilon_0 \epsilon_r \frac{A}{d} \quad (3.1)$$

Where C is the capacitor's capacitance, ϵ_0 the vacuum electrical permittivity, ϵ_r the dielectric electrical permittivity, A the capacitor's armature area and d the distance between the armatures.

As can be observed in Figure 3.21, the first capacitor (C_1) is completely immersed in water, thus the capacitance is calculated. The second capacitor (C_2) has as dielectrical material both water and air, it is similar to two parallel connected capacitors, one with water's permittivity and the other with air's permittivity. The third capacitor (C_3) is virtually the same as the second capacitor where the only difference resides on the areas and heights of parts of the plates which are under water and which are in the air. The fourth capacitor (C_4) is in the air and its equation is the same as the first.

All of the capacitors can be calculated through relating heights, distances, dielectric electrical permittivity and vacuum electrical permittivity as shown in Eq. (3.2).

$$\begin{cases} C_1 = \frac{\epsilon_{rw} \epsilon_0 h w}{d} \\ C_2 = \frac{\epsilon_0 w [\epsilon_{rw} H + \epsilon_{ra} (L - H)]}{d} \\ C_3 = \frac{\epsilon_0 w [\epsilon_{rw} (H - l - s) + \epsilon_{ra} (L - H + l + s)]}{d} \\ C_4 = \frac{\epsilon_{ra} \epsilon_0 h w}{d} \end{cases} \quad (3.2)$$

Where, **C1** is the first capacitor capacitance (completely immersed into the water). **C2**, **C3** the capacitance of the partially immersed capacitors. **C4** the capacitance of the fourth capacitor (with air as dielectric). **H** the water level value. **h** the height of the liquid column corresponding to the capacitor three immersion. **L** the **C2** and **C3** armature length. **l** the **C1** and **C4** armature length, **w** the capacitors width (for all the capacitors) and **s** the distance between two consecutive capacitors.

Water level then can be calculated by making the ration between the first and second capacitances. The capacitance measuring procedure is done by using a system built around an AVR ATTiny 2313 microcontroller with a clock frequency of 16MHz. The measuring system consists of a RC circuit in which the resistance has 1 Mohm. For the capacitor charging time calculation a LT 1011 analogue comparator is used.

Figure 3.22 shows an example from Blander *et al.* (2010) of measured capacitances (only air dielectric) and the values mathematically calculated through Eq. (3.2), which are similar.

No.	Measured level [m]	Scale level [m]	Absolute error [m]	No.	Measured capacitances [pF]		Mathematically calculated capacitances [pF]	
					C ₁	C ₂	C ₁	C ₂
1.	0.076	0.083	0.007		C ₁	C ₂	18 pF	85 pF
2.	0.071		0.012	1.	19	83		
3.	0.079		0.004	2.	19	83		
4.	0.076		0.007	3.	20	83		
5.	0.073		0.010	4.	20	82		
6.	0.079		0.004	5.	19	81		
7.	0.075		0.008	6.	20	84		
8.	0.071		0.012	7.	19	83		
9.	0.073		0.010	8.	19	84		
10.	0.071		0.012	9.	20	82		
				10.	19	83		

Figure 3.22 - Experimental results (dielectric air) (adapted from Blander *et al.*, 2010).

Finally, an experiment was done that consists in measuring the combined dielectric of water and air by immersing the capacitive transducer into water and obtaining a level reading. This was compared with the real value of the water level in which there was a slight error.

The exiting methods of level measurement are approximations based on large differences between the dielectric constants of liquid and air. An innovative level measurement technique using three capacitive sensors for liquids is proposed by Canbolat (2009), which eliminates the effect of air (vapour or condensation) and thus produces a closer to reality reading of the liquid level. This new level measurement technique can be used in any kind of nonconductive liquid without calibration. To obtain level measuring accurately through capacitance technology, three parallel plate capacitive structures are used, each designated as level, reference and air sensor. The measurements of the capacitance are done by a capacitance-to-digital converter (CDC) integrated circuit, which has a small error of ± 4 fF.

Liquid level is determined through capacitance sensors by using the differences of dielectric constants in liquid and air. The dielectric constants in liquid are much superior to the ones found in the air. When measuring different types of liquid levels in different liquids, the sensor usually needs to be recalibrated due to different dielectric constants. Another parameter to have in account is the temperature of the liquid as this also changes the dielectric constant. Sometimes vapour comes out of tanks and changes the dielectric constant considerably, resulting in faulty and unreliable readings. Using one capacitive sensor does not resolve this problem, but this problem is reduced because of the high dielectric constants of the liquid. On the other hand, the sensor should also be calibrated for different types of liquids, which can be costly and time consuming. The solution that the author presents is to use two reference capacitors that compensate for all the factors that liquid and air can produce. Like so, an accurate reading of the liquid level can be measured in any type of liquid, liquid dielectric and environment.

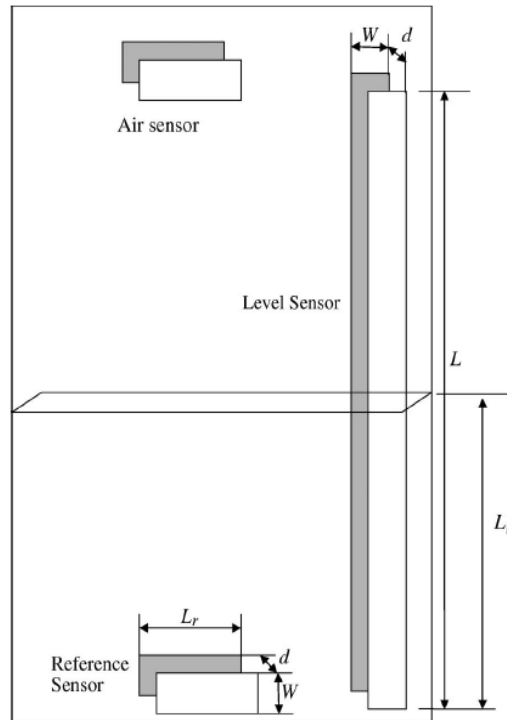


Figure 3.23 - Sensor setup (adapted from Canbolat, 2009).

The setup of this sensor uses three sensors (Figure 3.23), a reference sensor which will always be in the water, an air sensor which will be always in the air and a level sensor. The reference sensor is placed at the bottom of the container to measure liquid dielectric while the air sensor is placed at the top of the container to measure air dielectric as a reference. The two sensors are identical. Finally the third sensor is a level sensor which is placed along the height of the tank. All sensors have the same distance d and same width W while L is the total length of the level sensor and L_l is the length of the sensor submerged under the liquid. The dielectric values are converted into digital information by a Clock Distribution Circuit (CDC).

The accuracy of the readings depends on the accuracy of the distance d and width W . The capacitances measured by the CDC are fed to the microcontroller to perform the calculations, and then the result is sent to a display. An AD7745 integrated circuit is used which is especially designed for capacitance measurements. A CDC is used for each level, liquid and air sensors. All of the CDC's are connected to the inputs of a PIC16F877A. The sensor reading is independent of air humidity, temperature and dielectric constant of the liquid. This sensor can be used for any conducting, non-conducting and inflammable liquids. For conducting liquids the sensor can be put in a flexible container filled with non-conducting liquid and consequently obtain a level reading for the conducting liquids, as shown in Figure 3.24.

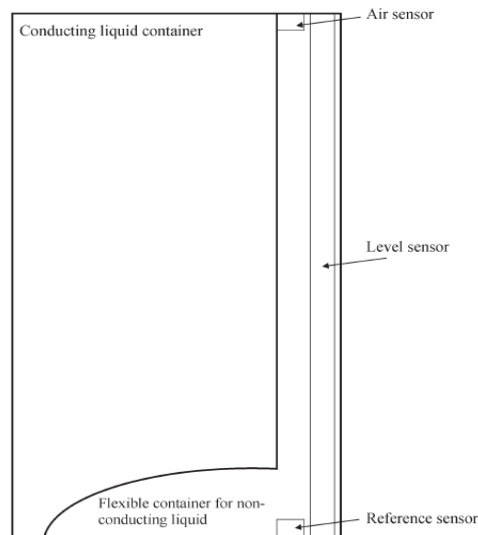


Figure 3.24 - Setup for level measurement of conducting liquids (adapted from Canbolat, 2009).

Wang and Shida (2006) developed a multifunctional self-calibrated sensor for brake fluid condition monitoring, which uses capacitive technology and is characterized by having a self-calibration ability to influence factors such as temperature, water content in the brake fluid and the variety of brake fluids. This sensor was developed to be a multifunctional self-calibrated online monitoring system for brake fluid condition. The sensor measures the liquid level and water content in the brake fluid by using capacitive technology. There are four electrodes which form three capacitances and from which three common calibrated functions are composed. The sensor is self-calibrated for liquid level, water content measurement, temperature influence (no temperature sensor involved) and for the variety of brake fluid. The sensor has a half-pipe form structure with a pipe form enclosed cavity at the end part. Four electrodes are used (Figure 3.25):

- Electrode one (E1) is a steel pole passing through the whole sensor in the middle;
- Electrodes two (E2), three (E3) and four (E4) are three half-pipe form electrodes made from copper;

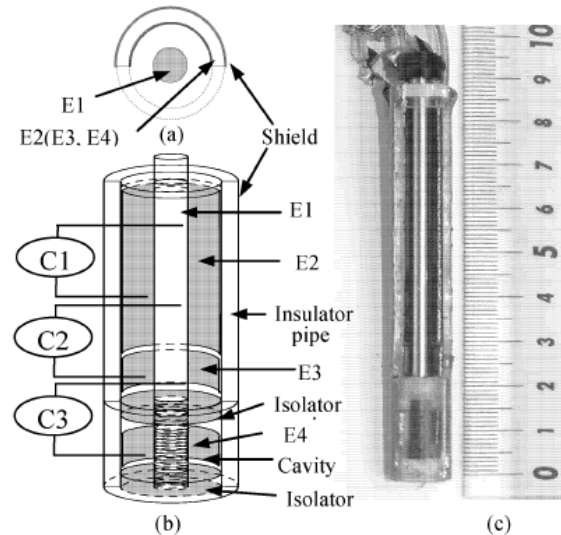


Figure 3.25 - Structure of sensor: (a) plan form of sensor; (b) sensor's structure; (c) prototype sensor; (adapted from Wang and Shida, 2006).

E2 and E3 are placed in the half-pipe form body sensor so that they are exposed to the outside. E3 is placed in the enclosed cavity and is the same size as E2. E1 is common to all the other three electrodes, thus creating three capacitances (C1, C2, and C3). C1 is used for liquid level measurement which is dependent on the liquid level and the relative permittivity of the liquid which is influenced by temperature, water content and variety of the liquid. C2 is used for water content measurement in the fluid and the calibration reference for liquid level sensing, it doesn't depend on level of the liquid because it is always submersed, but it is dependent on the relative permittivity of the measured fluid which is influenced by water content, temperature and brake fluid variety. Finally C3 is used as reference sensor which depends on the temperature and brake fluid variety. The sensor is designed to integrate the cover of the brake fluid reservoir.

By using the three mutual calibrated functions the sensor is able to self-calibrate to influence factors such as temperature, water content and brake fluid variety. Both liquid level sensing and water content sensing are well calibrated without resorting to any calibration arithmetic as in conventional intelligent sensor systems.

A low-cost non-contact capacitance type level transducer for a conducting liquid was developed by Bera *et al.* (2006). The sensor is comprised of a circular cylinder form and is made up of insulating material like glass, ceramic or plastic. The sensor is connected to a metallic or non-metallic liquid storage tank, in which the conducting liquid column is made up of one electrode and a short-circuited non-inductive wound coil outside the tank is the other electrode of a variable capacitor. When the liquid level changes, so does the capacitance and this is measured by a modified linear operational-amplifier based on De' Sauty bridge network with adjustable bridge sensitivity.

In conventional noncontact capacitance type liquid level transducer, the air column between the conducting liquid and the sensing electrode rely on dielectric constants. This technique appears to suffer from frequent changes of the dielectric constants properties of the air and also due to its low permittivity. The material used was a uniform circular cylinder made of insulating material like glass and polyvinyl chloride (PVC) which acts as a dielectric cylindrical capacitor.

The level-sensing probe (Figure 3.25) consists of a hollow cylinder made of an insulating material and is connected to a metallic storage tank. The insulating material of the sensing cylinder is considered as the dielectric cylinder capacitor, whereas the liquid inside the cylinder is considered as the grounded electrode of the capacitor because liquid is generally stored in a metallic grounded vessel. Thus the whole vessel itself may be considered as a cylindrical capacitor electrode, whereas the outer double-layer short-circuited non-inductive wound coil may be considered as another capacitor electrode. The capacitance between the liquid column and the short-circuited non-inductive wound two-layer coil may be assumed to have the same capacitance between the liquid column and only the outer layer of the coil. This is because the outer and inner layers of the coil are made from the same material.

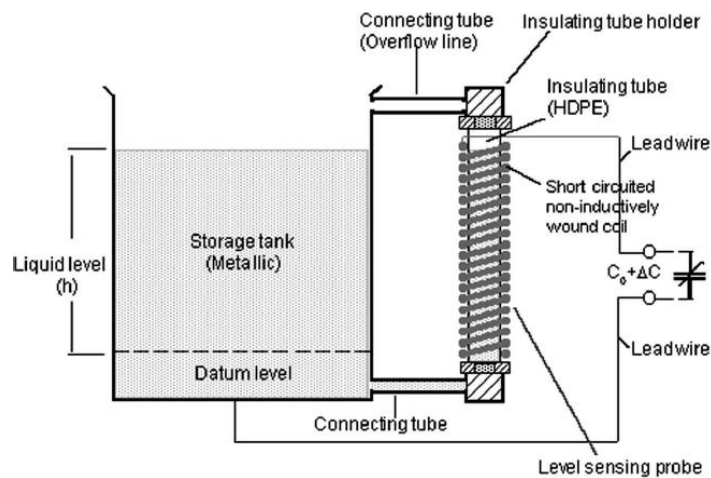


Figure 3.26 - Sensor setup (adapted from Bera et al., 2006).

Both the glass and HDPE tube level sensors presented linear tendencies and very good repeatability within a 1mm resolution in comparison to the theoretical equations for both metallic and non-metallic storage tanks (Figure 3.26).

Some errors may be caused by some manufacturing defects of the sensing cylinder. The overall sensitivity of the level sensors was 0.95pF/mm for the glass sensor and 0.65pF/mm for the HDPE sensor. The permittivity of the sensing tube material varies with temperature and operating frequency significantly. This can be eliminated by using a temperature correction

technique from the knowledge of the variation of the permittivity with the temperature. The effect caused by frequency can be eliminated by using a frequency-stable oscillator but permittivity correction is required when this is used in a wide range of varying temperatures. For a temperature region of 25-45 °C the error due to permittivity lies between +0.25% and -1.5%. This can be corrected by using a suitable temperature correction technique from knowing the variation of the permittivity with the temperature. The life span of the level sensor is expected to be long compared with other non-contact level gauges because there is no wear and tear of the sensor during the operation. It was concluded that the repeatability, linearity and resolution were satisfactory within the limits for industrial level measurement.

A new capacitive precision liquid-level sensor was presented by Toth et al. (1996). It is a high resolution capacitive sensor that allowing measures the level of both conducting and non-conducting liquids with equal accuracy (Figure 3.27). It includes a planar electrode structure, a capacitance-controlled oscillator and a microcontroller. It can measure liquid levels of conducting and non-conducting liquids with an accuracy of 1mm over a 4 m range. The resolution of the system is high (0.1mm) at short measuring times (0.2s).

The capacitances consist of a long electrode (E_0) and one that is divided into insulated segments (E_1-E_n). All capacitances are either connected to a low impedance voltage source, low impedance measurement system input. The level of the liquid can be calculated by finding the interface segment l , which has a value between C_{i-1} (capacitance in the air), and C_{i+1} (capacitance in the liquid). In order to measure conducting liquids the electrodes are covered by an isolator. This material protects the electrodes from the environment, but can also cause some electric field bending around the interface. Assuming a parallel plate electrode structure, covered with an infinitely thin isolator, the conducting liquid can be regarded as a shield that is connected to the ground. The capacitance between a single electrode segment E_i and the opposite electrode E_0 can be calculated as a function of the interface level.

The sensor has two printed circuit boards (PCBs) with 48 electrodes of 8 mm each and PCB with the sensor electronics glued to a glass filled plastic substrate (a supporting material on which a circuit is formed or fabricated). The capacitances are connected to a capacitance controlled relaxation oscillator using a multiplexer that is controlled by a microcontroller. The microcontroller also measures the period of the oscillator and calculates the capacitances. It measures capacitances of 100fF with an accuracy of 50aF.

Table 3.1 presents a capacitive analysis of different capacitive sensors.

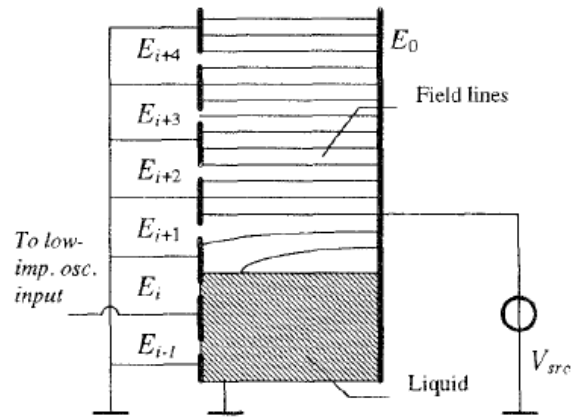


Figure 3.27 - Schematics of the sensor with the conductive liquid connected to the ground (adapted from Toth et al. (1996)).

Table 3.1 - Capacitive sensors.

Technology	Conductive or non-conductive liquid	Suitable for wastewater treatment	Observations
Digital Level Transducer Based on Optical Fibre	Both, as long as they are transparent	No, because the water cannot contain any impurities.	Continuous measurement; Needs different calibration curves for different liquids; Good repeatability; Dynamic and static limitations; Resolution could be higher; Intrusive measuring;
New Non-Intrusive Optical Technique to Measure Transparent Liquid Level and Volume	Both, as long as they are transparent	No, because the water cannot contain any impurities.	Continuous measurement; Use of one reference sensor beam and one sensing beam, and two photodetectors; Sensitivity varies with the size of containers, thus needing different LED intensities. Simple, low cost, very sensitive; Best container is the 100ml; Large dynamic range of measurement; Good linearity and repeatability; Non-intrusive measuring;
Smart Level Sensor Based on Thermal Resistance Measurement with Self Calibration	Both	Only for controlling overflow systems.	Dirt will drop overall performance of the sensor; Heat transfer concept (water contains higher thermal conductivity than that of air); Based on the hot wire anemometer; Needs a lot of energy to heat the sensor; Intrusive measuring;
Capacitive Liquid Level Sensor with Four Electrodes	Both.	Yes.	Determines liquid level measurement and gradient status of the vessel; No moving parts; Two electrodes mode is used for measuring liquid level; Four electrodes mode is used for measuring the status of the vessel (direction and angle); Doesn't need additional parts for measuring the vessels status; Intrusive measuring;
Low-Cost Capacitive Sensor for Wells Level Measurement	Both	Yes, rain water.	Made up of eight copper pour plates; Very good capacitance results; High repeatability in terms air capacitance; Slight errors when comparing real liquid level height to measured liquid level height. This can be resolved by using thicker plates; Intrusive measuring;

Table 3.2 – Capacitive sensors (continues)

<p>Novel Level Measurement Technique using Three Capacitive Sensors for Liquids</p>	<p>Both, no calibration needed for nonconductive liquid.</p>	<p>Yes, in tanks.</p>	<p>Eliminates the traditional capacitive level measuring which is based on large differences between dielectric constants of liquid and air; Has in account different liquid dielectric constants as well temperature influence; Uses two reference capacitor sensors that compensate for different dielectric constants in the air and liquid; Vapour could alter dielectric constants; Accuracy depends on the dimensions of the plates; The reading of the level sensor is independent from air-humidity temperature and dielectric constants of liquids; The level sensor put inside a flexible container filled with non-conducting liquid can be used for measuring inflammable liquids; Intrusive measuring;</p>
<p>Multifunctional Self-Calibrated Sensor for Brake Fluid Condition Monitoring</p>	<p>Conductive</p>	<p>No, because it's specifically designed for brake fluid monitoring.</p>	<p>Self-calibration ability; Uses four electrodes to form three capacitances; No temperature sensor involved; No need for any calibration arithmetic; Intrusive measuring;</p>
<p>A Low-Cost Non-contact Capacitance Type Level Transducer for a Conducting Liquid</p>	<p>Conductive</p>	<p>Yes.</p>	<p>The whole cylinder is considered as a cylindrical capacitor electrode, and the liquid inside the cylinder is considered as the grounded electrode of the capacitor; The outer double-layered short-circuited non-inductive wound coil is considered as the other capacitor electrode; Linear tendencies and good repeatability within a 1mm resolution; Permittivity of the sensing tube material varies with temperature and operating frequency. Not suitable for varying temperatures as it will need permittivity correction; Lifespan is considered good; Repeatability, linearity and resolution were considered satisfactory; Non-intrusive measuring;</p>
<p>New Capacitive Precision Liquid-Level Sensor</p>	<p>Both</p>	<p>Not specified</p>	<p>High Resolution; Non-linearity is caused by field bending effects; Measurement with an accuracy of 1mm over a 4m range; Intrusive measuring;</p>

Capacitive measurement techniques

There are several techniques for measuring the capacity value of a capacitive probe. By using either an RC circuit and determining the charging times of the condenser, in function of the capacitive value, or by creating an RC oscillator and counting the number of oscillations produced by the oscillator over a fixed period of time. It's considered that in both techniques that the oscillation frequency is sufficiently low enough so that the dielectric constant of the medium can be considered constant.

The charging time of the capacitor in a RC circuit depends on the C_x capacity value. It's considered that the resistance value R is maintained, that the power V_{in} circuit is regulated and kept constant, and that the stored energy of capacitor/condenser C_x is initially zero. The timer that is used, as shown in Figure 3.28, is for measuring the time that the V_{out} voltage of the C_x condenser/capacitor takes to reach the reference voltage value V_{ref} . Once the V_{in} output of the logical control and processing unit is put into high logic state, the timer commences. The C_{out} output comparator transits from a low logic state to a high logic state, the timer is thus inhibited from counting and the counting registration content T_{count} is collected. The count registration value is proportional to the counter's capacitance value. The count registration value is proportional to the counter's capacitance value. The capacitor C_x voltage (V_{out}) is given by Eq. (3.3).

$$V_{out} = V_{in} \left(1 - e^{-t/RC} \right) \quad (3.3)$$

Where, V_{out} is the voltage out of the capacitor, V_{in} is the voltage in of the capacitor, t is the time required and RC is the resistance capacitance value.

The time required for V_{out} to reach V_{ref} can be computed through Eq. (3.4).

$$t = RC_x \ln \left(\frac{V_{in}}{V_{in} - V_{ref}} \right) \quad (3.4)$$

Where, t is the time value, RC_x is the resistance capacitance value, V_{in} is the voltage in and V_{ref} is the reference voltage.

Considering the clock Clk frequency as being 1MHz. For a given resistance value of 220kOhm and a variable capacity between 482.2pF and 1482pF, the timer will return a counting value of 254 to 781, respectively.

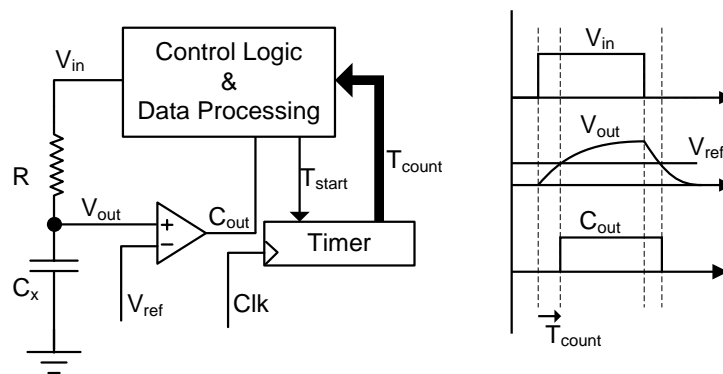


Figure 3.28 - Capacity measurement with a RC circuit.

The oscillator circuit is an important component of the sensor and requires three essential components:

- A capacitor;
- A resistor;
- A switching device;

As shown in Figure 3.29, the V_{out} voltage level to the capacitor terminals is monitored continuously in order to toggle the switch. The switch frequency is in function of the C_x variable capacitance value. The oscillator of Figure 3.28 is built around a CI555 in an stable configuration. The charge of the C_x capacitor is performed through the R_c resistance requiring a $t_c=0.7R_cC_x$ time. On the other hand, the discharge path is performed through the R_d resistor over the $t_d=0.7R_dC_x$ time. Due to this configuration, the duty-cycle is 50% with a time period of $T=t_c+t_d$.

For the R_c and R_d resistor values equal to 220kOhm, and considering the probe C_x variable capacity between 482.2pF and 1482pF, the oscillation frequency of the output from the CI555 *Out* is ranging between values of 6733.1Hz and 4381.6Hz, respectively. Every time the logic and process control unit needs to determine the C_x capacity value, it enables the counting operation of the timer in a time interval already set in advance. The frequency variation *Out* will vary the T_{count} registration.

This operating principle can be found in processors with special entries that integrate this feature by using an internal timer and oscillator. An example of another unit using this technology is the MSP430 which supports capacitive touch interface

Capacitance probe sensors are an attractive technique for estimating water level in filtration systems. However, there are several factors that can influence the capacity variation and its measurement and, therefore, the final measurement of the water level. According to

Kelleners et al. (2004), the media salinity, the characteristics of the wastewater and the temperature might affect the accuracy of a capacitive sensor.

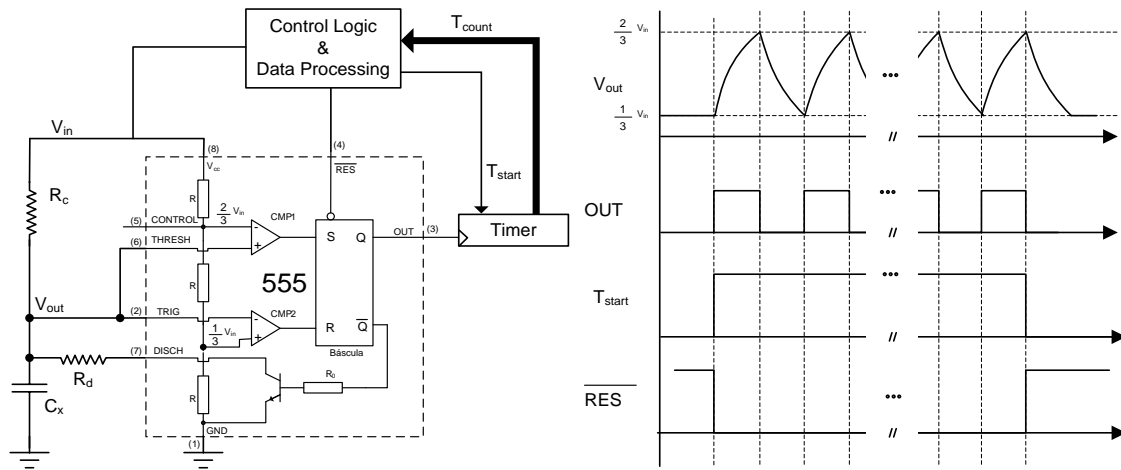


Figure 3.29 - Capacity measurement with an oscillator.

4 Material and Methods

4.1 Development of the capacitive sensor

4.1.1 Architecture of the system

A capacitive sensor was developed to measure the water depth in multiple points of a filtration bed for wastewater treatment (the HSSF-CW of Vila Fernando, Guarda). The sensor has a probe (made of aluminium), a data-logger and an interface to pass stored data to a computer. The principle of measurement follow the determination of the charging times of the condenser, in function of the capacitive value, or by creating an RC oscillator and counting the number of oscillations produced by the oscillator over a fixed period of time, as described in the point 3.2 (see Figures 3.28 and 3.29).

The data-logger is considered the centrepiece of the measurement system. This component, which was developed over a MSP430F2231 MCU device, converts the capacity values in depths, according to a calibration curve, and stores all the values in a data-logger at regular time intervals. The main advantages of using this MCU are the low energy consumption and the use of integrated peripherals (RAM, UART, ADC and flash memory).

The whole system was thought-out to be powered by a nine volt battery. The MCU device can operate most of the time in power save mode. Since the required operation time for measuring the capacity and registering the data is very short, it may be admitted that the processor passes great part of time in power save mode. The interaction with a computer is achieved through a docking bay (interface to pass the stored data from the data-logger to a computer).

4.1.2 Capacitive probe theoretical model

A capacitive probe should be accurate, robust and highly sensitive. The main component is the condenser, whose dielectric material characteristics vary due to the influence of the surrounding characteristics (e.g. temperature, pressure and salinity). In a capacitive probe for water level measuring, the dielectric constant may be, in a limited situation, very low for the air and water levels. As the water level rises, the air dielectric is progressively substituted by the water dielectric.

Analytically, the capacitance value of a cylindrical capacitor is given by Eq. (4.1).

$$C = \frac{2\pi k \epsilon_r \epsilon_0 l}{\ln \left[\frac{b}{a} \right]} \quad (4.1)$$

Where a is the internal radius, b the external radius, l the length, ϵ_0 the dielectric constant of the vacuum (approximately equal to the unit), ϵ_r the relative dielectric constant of the medium, in this case it is either air or water.

It is considered that the dielectric constant of air, ϵ_{r_air} , is approximately equal to the unit. In the case of water the dielectric constant, ϵ_{r_water} , varies with temperature, ranging from 88 at 0 °C, to 80 at 20 °C and to 78.4 at 25 °C.

This physical principle is schematically presented in Figure 4.1 (with the values of l , a , b and c given in Table 4.1) and was used for the construction of the capacitive probe for this work. Therefore, its construction is based on a cylindrical condenser, where an aluminium rod is placed within a tube made up of the same material. The fact that aluminium is used for probe construction will increase its durability. Since tap water has a typical conductivity between 35 and 45 $\mu\text{s}/\text{cm}$, the two aluminium elements should be isolated by a heat-shrinking sleeve, which should be placed around the rod.

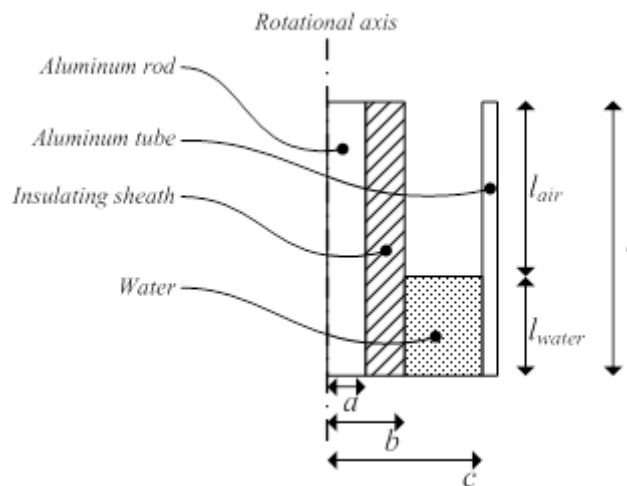


Figure 4.1 - Capacitive probe structure.

Table 4.1 - Physical dimensions

Physical Dimensions (mm)			
<i>l</i>	<i>a</i>	<i>b</i>	<i>c</i>
900	3.75	4.375	6.4

An equivalent diagram for the capacitive probe is proposed in Figure 4.2. This diagram takes into account the variation of the medium level, where measurement is intended to be done. Actually, two capacitors C_1 and C_3 in series are considered. Capacitor C_1 with an air dielectric (ϵ_{r_air}) and capacitor C_3 with a dielectric ϵ_{r_sh} associated to the material used for the heat-shrinking sleeve. It was also considered that in parallel with these two capacitors there are two other capacitors in series, C_2 and C_4 , which also have variable capacity values depending on the medium. However, the value of the dielectric constant of capacitor C_2 is dependent on the medium in which the measurement is performed. As the medium is wastewater, the dielectric constant of water (ϵ_{r_water}) is considered. For any event, the dielectric constant of capacitor C_4 is considered equal to that of C_3 due to the fact that they are made from the same material.

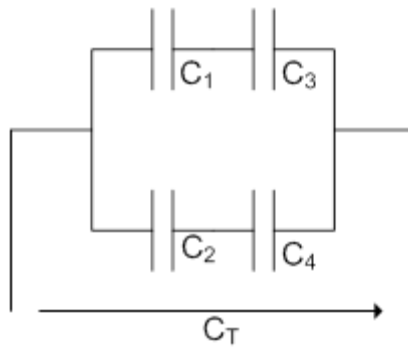


Figure 4.2 - Theoretical model of the capacitive probe.

The proposed model of the capacitive probe includes a combination in series of capacitors C_1 and C_3 , designated as C_A , and a combination in series of capacitors C_2 and C_4 , referred to as C_B , as presented in Eq. (4.2) and (4.3).

$$\frac{1}{C_A} = \frac{1}{C_1} + \frac{1}{C_3} = \frac{C_1 + C_3}{C_1 C_3} \quad (4.2)$$

$$\frac{1}{C_B} = \frac{1}{C_2} + \frac{1}{C_4} = \frac{C_2 + C_4}{C_2 C_4} \quad (4.3)$$

Where C_1 is the capacitance produced by the air, C_3 is the capacitance produced by the shrinkable sleeve, C_2 is the capacitance produced by a given medium and C_4 is the capacitance also produced by the shrinkable sleeve.

The association in parallel of C_A and C_B capacities allow determining the total capacity of C_T through Eq. (4.4).

$$C_T = C_A + C_B \quad (4.4)$$

Thus by inserting Eq. (4.2) and (4.3) into Eq. (4.4) results Eq. (4.5)

$$C_T = \frac{C_1 C_3}{C_1 + C_3} + \frac{C_2 C_4}{C_2 + C_4} = \frac{C_1}{C_1/C_3 + 1} + \frac{C_2}{C_2/C_4 + 1} \quad (4.5)$$

Where, C_1 is the capacitance produced by the air, C_3 is the capacitance produced by the shrinkable sleeve, C_2 is the capacitance produced by a given medium and C_4 is the capacitance also produced by the shrinkable sleeve.

Assuming that capacitors C_3 and C_4 have the same dielectric material of the dielectric constant ϵ_{r_sh} , it is possible to replace their value for an equivalent expression of the capacitor (Eq. (4.6)).

$$C = \frac{2\pi\epsilon_{r_sh}\epsilon_0 l}{LN\left(\frac{a}{b}\right)} \quad (4.6)$$

Where, C is the capacitance of the capacitor, ϵ_{r_sh} is the sheath's dielectric constant, ϵ_0 is the vacuum electrical permittivity and a and b are dimension sizes.

By inserting Eq. (4.6) into Eq. (4.5) results Eq. (4.7),

$$C_T = \frac{C_1}{C_1 \frac{\ln(a/b)}{2\pi\epsilon_{r_sh}\epsilon_0 l_{air}} + 1} + \frac{C_2}{C_1 \frac{\ln(a/b)}{2\pi\epsilon_{r_sh}\epsilon_0 l_{water}} + 1} \quad (4.7)$$

where l_{air} and l_{water} depend on the water level. By factorizing the parameter ϵ_{r_sh} and introducing the factors α and B (Eq. (4.8) and (4.9)) results Eq. (4.10).

$$\alpha = \frac{2\pi\epsilon_0 l_{air}}{\ln(a/b)} \quad (4.8)$$

$$\beta = \frac{2\pi\epsilon_0 l_{water}}{\ln(a/b)} \quad (4.9)$$

$$C_T = \frac{C_1 \epsilon_{r_{sh}}}{C_1 \alpha + \epsilon_{r_{sh}}} + \frac{C_2 \epsilon_{r_{sh}}}{C_1 \beta + \epsilon_{r_{sh}}} \quad (4.10)$$

Finally, the equation for calculating the dielectric constant of the insulating sheath material, $\epsilon_{r_{sh}}$ was developed and is presented in Eq. (4.11)

$$[(C)_T - C_1 - C_2] \epsilon_{r_{sh}}^2 + (\alpha C_T + \beta C_T - \beta C_1 - \alpha C_2) \epsilon_{r_{sh}} + \alpha \beta C_T = 0 \quad (4.11)$$

4.1.3 Probe construction

30 probes were constructed using a 0.90m aluminium tube with an external diameter of 0.016m and an internal diameter of 0.0128m, a 1m solid aluminium rod with a diameter of 0.075mm, a black insulator used to wrap around the solid aluminium rod increasing the diameter of the solid aluminium rod to 0.0875m, plastic caps, electrical wire and a plastic vessel to house the data-logger and power source.

A black insulator was used to isolate the solid aluminium rod from the hollow aluminium rod, this was done by inserting the solid rod into the sleeve of insulator, cutting it to the right size and applying a heat source to make the insulator retract and cover the rod tightly as can be seen in Figure 4.3.

As illustrated in Figure 4.3-d), the solid aluminium rod has a hole drilled on one of its extremities, in order to connect the electrical wiring that is needed at a later stage, while the bottom part was sealed tightly with the heat shrinkable sleeve, as shown in Figure 4.4-a). The solid aluminium rod was then housed in a hollow aluminium rod (Figure 4.5), where plastic caps were used on the top and bottom to help keep the solid aluminium rod in the middle of the hollow aluminium rod. The plastic caps were drilled to the right diameter size so that they fitted tightly and snugly around the rod at the bottom and at the top as it can be seen in Figures 4.4 b) and 4.6.

The hollow aluminium rod had to have slits cut into it, one at the top and one at the bottom, ensuring that water could get in and air out (Figure 4.7). It also had a hole drilled into it so to connect the vessel that houses the data-logger and power source to the sensor, as illustrated in Figure 4.7-a).

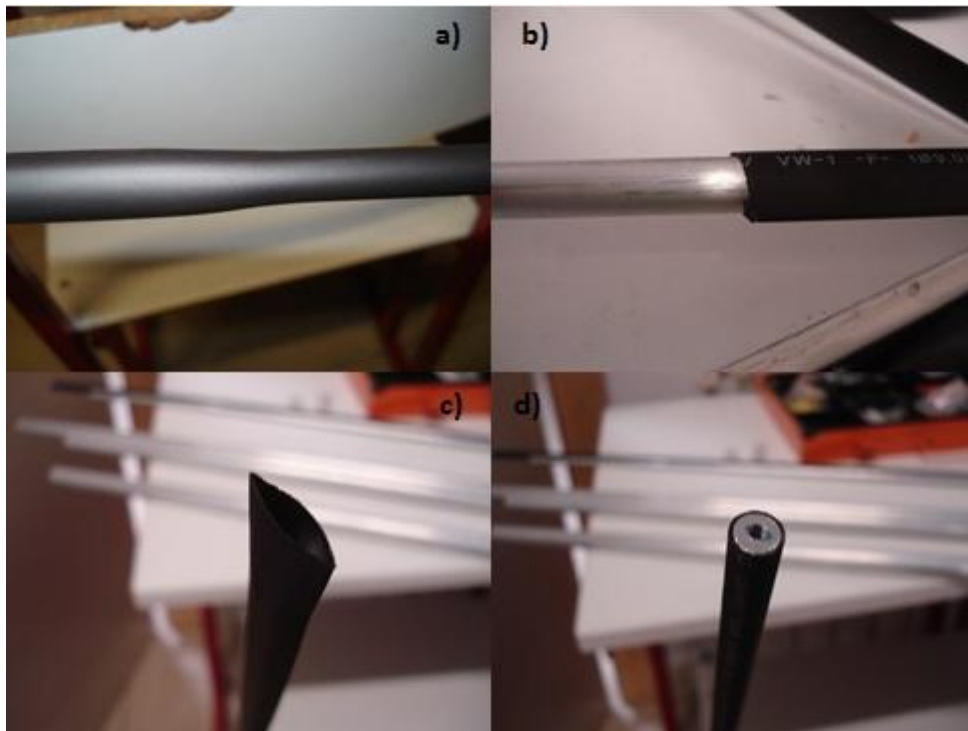


Figure 4.3 - Heat retracting sleeve over solid aluminium rod; a) heat applied to sleeve; b) sleeve inserted over rod; c) sleeve inserted over rod top view; d) sleeve inserted over rod after applying heat source to retract the sleeve.

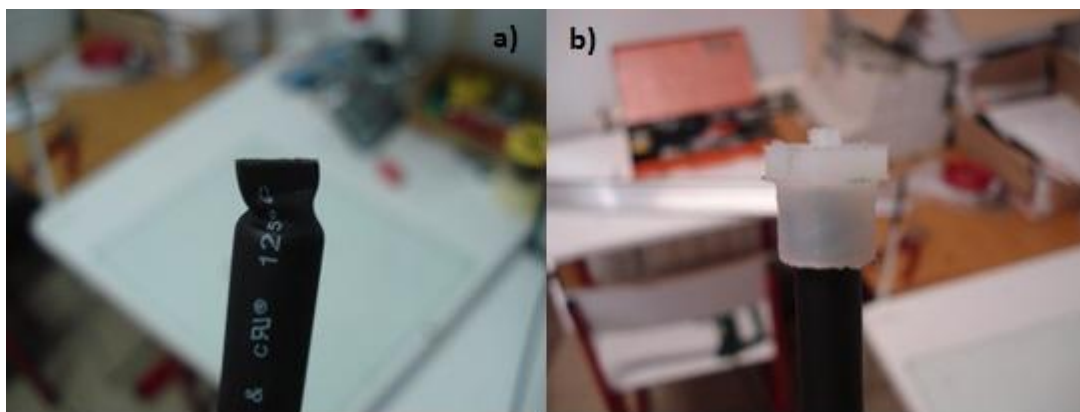


Figure 4.4 - Heat shrinkable sleeve; a) sealed tightly around the bottom end of the solid aluminium rod; b) plastic cap placed on the bottom of solid aluminium rod after sealed tightly.



Figure 4.5 - Solid aluminium rod being inserted into hollow aluminium rod.



Figure 4.6 - Plastic cap placed on the top part of the sensor.

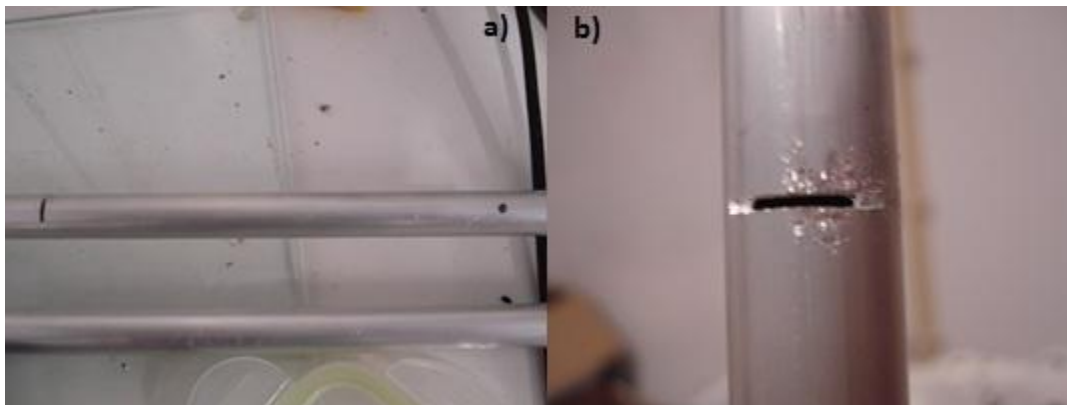


Figure 4.7 - Slits; a) slit incision at the top of the sensor and hole for attaching vessel that houses data logger and power source; b) slit incision at the bottom of the sensor.

The next phase consisted in attaching the plastic vessel that houses the data-logger and power source and the wiring to the sensor (Figure 4.8). This procedure involved the use of screws and O-rings. The terminals that were used on the wiring needed to be insulated by the same material and method that was used on the solid aluminium rod whilst the other part of the wire used O-ring terminals with a plastic cover, as seen in Figures 4.8-b) and 4.8-c).

The plastic vessel was drilled in two places, on the back in the middle and on the top and middle, one hole is used to connect the vessel and wiring to the external hollow aluminium rod while the other hole has a second wire that passes through it to connect to the data-logger which is connected to the solid aluminium rod with insulator. The wire passes through the inside of the vessel.

The final sensors are presented in Figure 4.9.

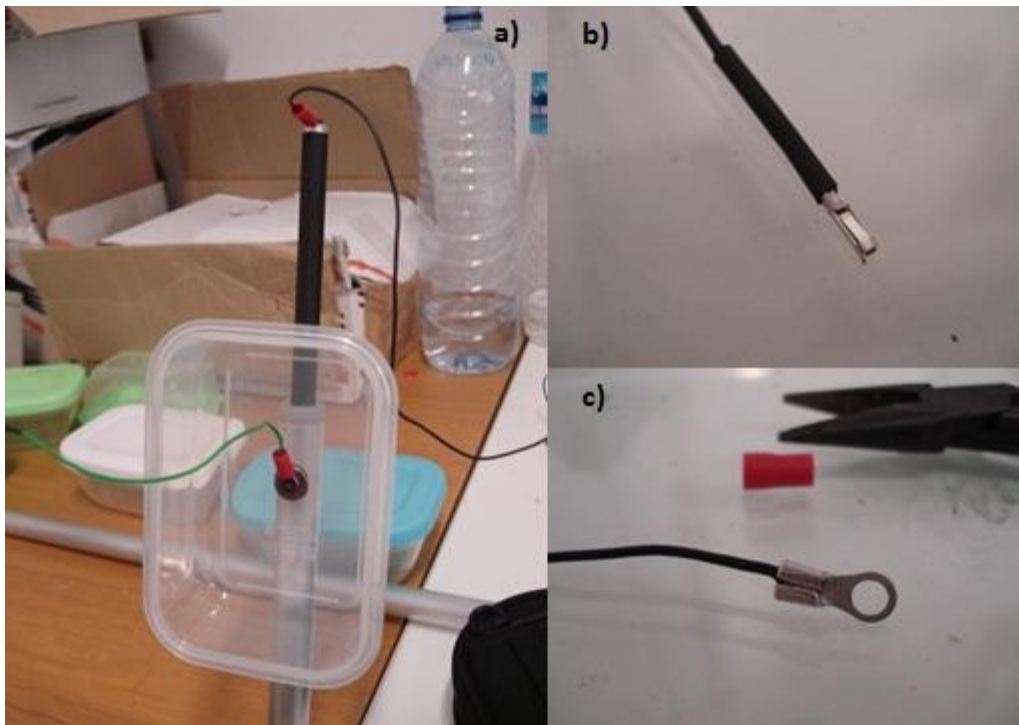


Figure 4.8 - Details on sensor construction. a) vessel connected to sensor; b) terminal with electrical wire to connect to data logger; c) O-ring terminals with wire to connect to sensor.



Figure 4.9 - Capacitive water level sensors.

The sensors were then calibrated according to the procedure presented in the point 4.1.6 and then were placed in the measuring tubes of the HSSF-CW of Vila Fernando (see point 4.3.2) for water level measurements.

4.1.4 Data-logger development

The capacity measured by the probe is then stored in a data-logger (Figure 4.10) on flash memory, which is the more sensitive part of the sensor. The overall storing capacity is 5378 measurements.

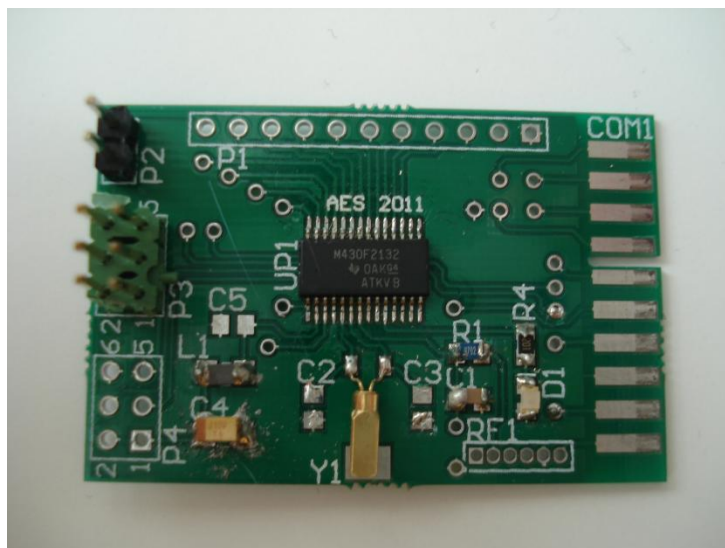


Figure 4.10 - Data-logger.

The processor will be in hibernation state most of the time. Periodically the processor is activated from its sleep state to perform the measurement procedure and data storage. By using this methodology, it allows to extend the battery life span. The measurement process is expected to follow the curve of Figure 4.11, starting by raising the *P1.2* line, initiating the voltage increment in the capacitive probe connected to terminal *P1.3* (V_{Cx}) of the processor. Simultaneously, the counting process of the Timer_A0 begins by using as a clock source the *SMCLK* signal, which operates at 1MHz. The stability of this clock is very important for overall measurement quality and it's important to note that, the higher the clock's frequency signal, the greater the resolution of the measuring process.

The measuring process then waits for the logic state of the *P1.3* input to transit from a low logic state to a high logic state. This situation occurs when the voltage V_{Cx} reaches the $V_{CC}-0.3 V$ value. Upon the occurrence of this event, the counting process of the timer is inhibited. The number of cycles of the *MCLK* clock signal is accounted for and registered whilst the *TAR* count is in function of the charging time.

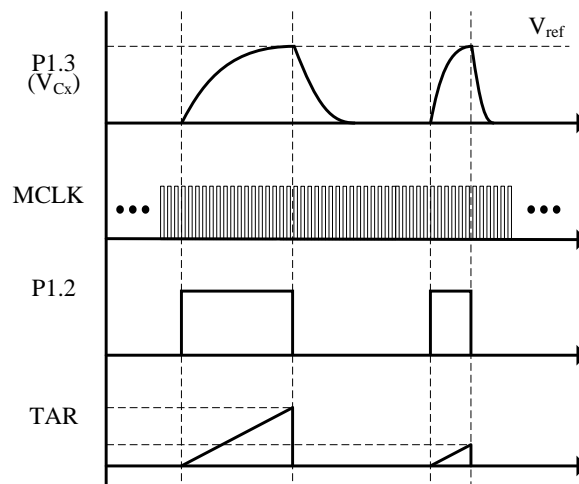


Figure 4.11 - Expected measurement process.

The measurement process is repeated several times in order to make an effective dispersion of the error. The average value is scaled down to 8-bits. The decision to only retain 8-bits of the 16-bits timer is justified by two reasons:

- Firstly, 8-bits means 256 different measuring levels, since the amplitude of the measurement is 90cm, the theoretical resolution will be $900/256 = 3.56\text{mm}$;
- The second reason is memory related, where by just storing only 8-bit data, we're able to use less memory space when compared to 16-bit data storage;

4.1.5 Computer interface

The computer interface is essential to pass the stored data from the data-logger to a computer. This procedure can be achieved through a docking bay. This unit, in addition to permitting the interface with a running application on the computer, also allows for firmware updating. The decision to separate the measuring features from communication features was done to reduce energy consumption, complexity, and manufacturing costs.

The data-logger and computer interface is accomplished via a USB port. Once the data-logger is inserted into the docking bay, the computer will automatically detect it and open a communications port through the USB device. This interface is developed around a TUSB3410 device and converts the TX/RX signals into a USB format. Figure 4.12 shows the interface between the data logger and the docking bay.

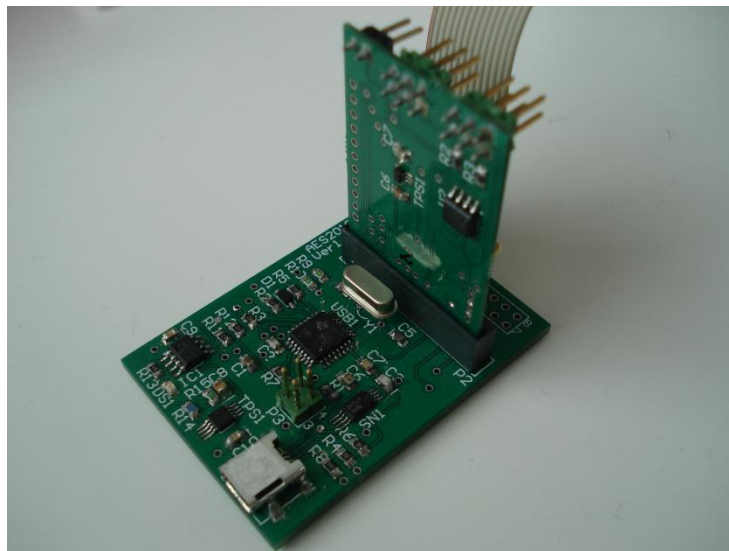


Figure 4.12 - Interface for data data-logger.

4.1.6 Sensor calibration

Calibration is an important step for accurate measurements of probes. The calibration of the sensor was done in laboratory using a measuring tube similar to the ones used in filed work. The measuring tube is a cylindrical format and is made from PVC. A clear plastic tube was connect from the bottom to the top of the tube with a scaled ruler to read the height of the water level inside the tube (i.e. it acted as a piezometer), as shown in Figure 4.13-a).

The sensors were hung at a fixed height when calibration was being done in order to have correct height values of water for the sensor. The procedure involved measuring the response time for a given height of the water level, as well as the corresponding capacitance value for the same water level. Calibration was done with the sensor connected to the data logger and

the data logger connected to the docking bay which in turn was connected to a computer (Figures 4.13-b) and 4.13-c)). The calibration curve (water level vs. number of cycles) for all the sensors are given in Annex I. and were obtained by linear regression.

A *Mat Lab* routine was used to retrieve data from the data logger to the computer, which was displayed on the computer screen while water was poured into the PVC tube with intervals of five centimetres (from 0 to 70cm). For each interval, the *CLK time* (number of cycles) corresponded to the water level was retrieved. The respective calibration curves for several sensors are presented in Figure 4.14.

Figure 4.15 shows the relationships between capacitance values and water levels for several probes. It can be seen a good linear relationship between both variables for all the probes, which was accepted for the calibration curves. These curves were then retrieved by using a Philips PM6304 programmable automatic RCL meter. Therefore, any further capacitive values stored at data-logger can then be converted to water depth values. Table II.1 of Annex 2 shows all the results obtained from regression analysis of water level data and capacitance data for several sensors.

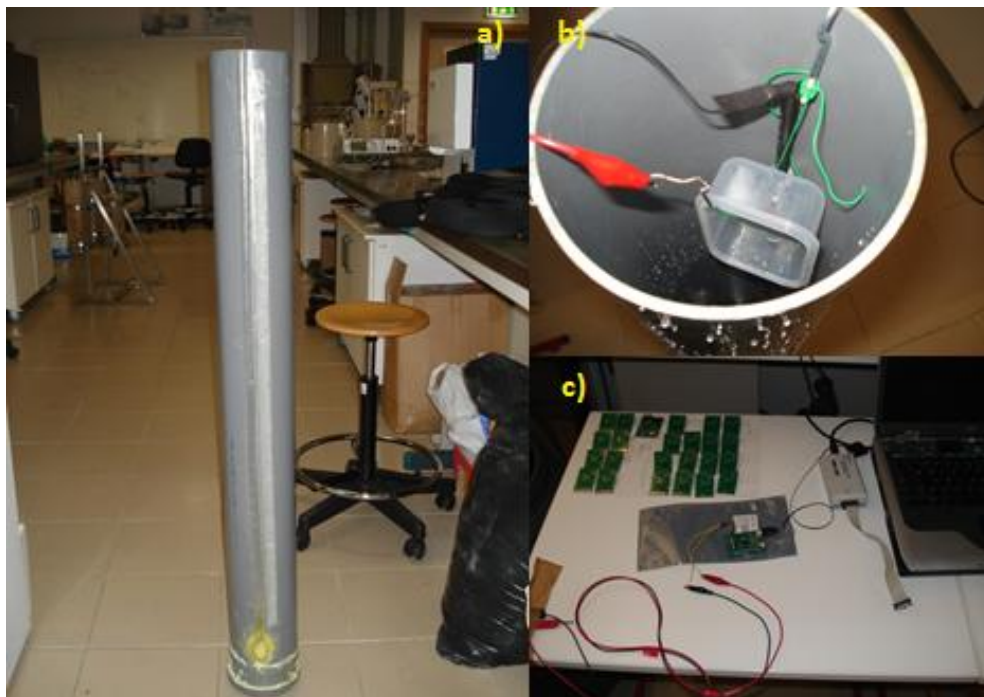


Figure 4.13 - a) Measuring tube used for sensor calibration; b) Sensor inside the tube and connected to the data-logger; c) Data-logger and interface for computer.

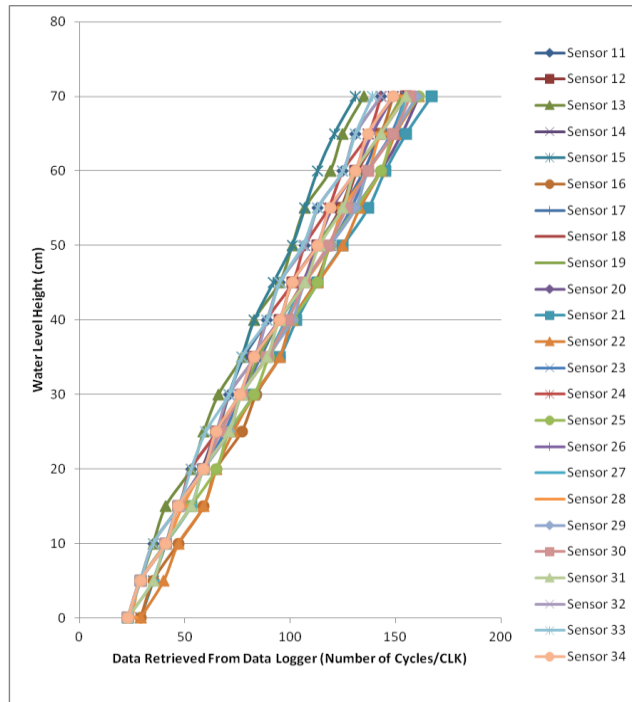


Figure 4.14 - Calibration curves for water depth and number of cycles.

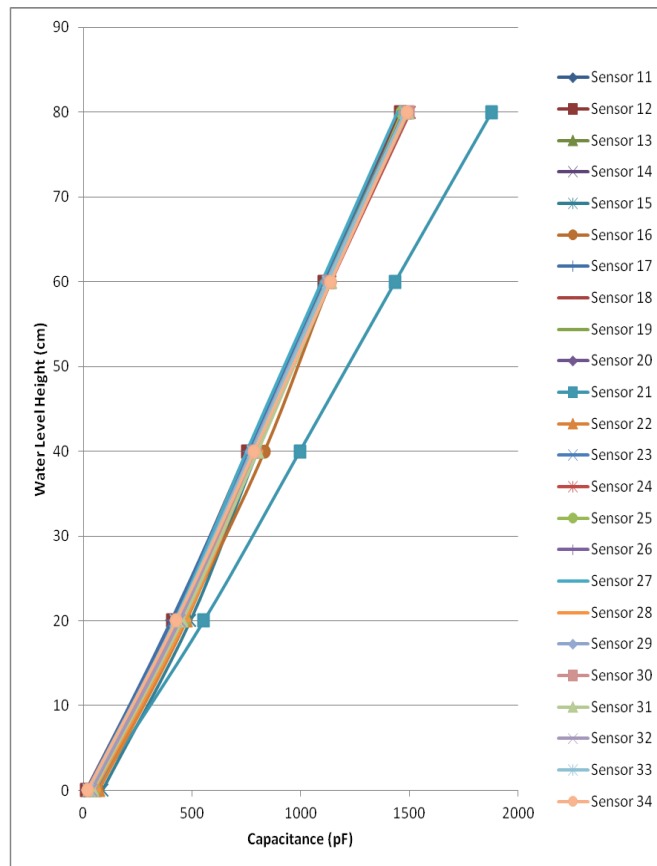


Figure 4.15 - Capacitance calibration curve.

4.2 Effect of water characteristics

4.2.1 Introduction

Since some factors (*e.g.* water salinity, characteristics of the wastewater and temperature) may influence the accuracy of capacity probes (Kelleners *et al.*, 2004; Bera *et al.*, 2006), several experiments were carried out in order to evaluate the influence of the salinity (measured as electrical conductivity), temperature and the characteristics of the wastewater on probe accuracy.

These tests were carried out in laboratory and the real scale WWTP of Vila Fernando. A smaller probe was built following the procedure of points 4.1.3 and 4.1.6. 4 mini-sensor were built, consisting in a 0.10m hollow aluminium rod with an external diameter of 0.016m and an internal diameter of 0.0128m, a 0.16m solid aluminium rod with a diameter of 0.075m, a black insulator used to wrap around the solid aluminium rod increasing the diameter of the solid aluminium rod to 0.0875m, plastic caps, wiring, as show in Figure 4.16.



Figure 4.16 - Mini-sensors.

A series of tests was carried out to measure the total capacity, C_T , of the probes at different water levels (between 200 and 800 mm), using a Philips PM6304 programmable automatic RCL meter. The results are shown in Table 4.2. It was also included the theoretical values of C_1 and C_2 for different water levels, as well α and β values. Using Eq. 4.11 it was possible to determine the dielectric constant of the insulating sheath material, ϵ_{r_sh} , which gave an average value of 5.94.

Table 4.2 - Capacitive probe theoretical model parameters.

l_{water} (mm)	C_{T_exp} (pF)	C_1 (pF)	C_2 (pF)	a	β	ϵ_{r_sh}
200	452,2	102,4	2352	0,405	32,6	5,82
400	792,4	73,13	4703	0,405	32,6	5,92
600	1136,0	43,88	7055	0,405	32,6	5,98
800	1482,0	14,63	9407	0,405	32,6	6,02

Using FEEM programme based on finite element method, the theoretical model was validate for the characteristics of the probe. The model used the same dimensions of the proposed probe and the dielectric constants of the water and air were considered $\epsilon_{r_water}=80$ and $\epsilon_{r_air} = 1$. It was considered a potential difference of 1V between the aluminium rod and aluminium tube. The height of the water considered for this simulation was 600mm.

The results of the numerical simulation are presented in Figure 4.17. The capacity values retrieved during model simulation for different water heights were compared to the experimental measured values as presented in Table 4.3, where it can be noted that there is a close proximity between the values retrieved from the finite element method model and the values measured through experimental means, which validates the model.

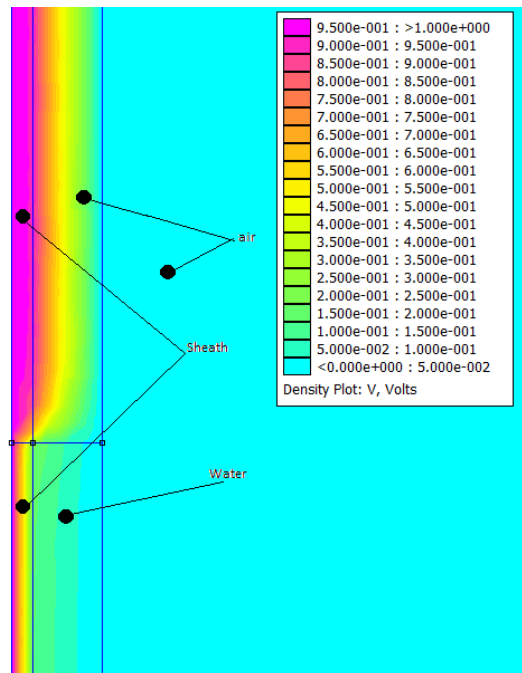


Figure 4.17 - Capacitive probe finite element method.

Table 4.3 - Experimental and theoretical results.

l_{water} (mm)	C_{T_FEM} (pF)	$C_{T_experimental}$ (pF)	$C_{T_theoretical}$ (pF)
200	460,6	452,2	458
400	796,5	792,4	794
600	1132,0	1136,0	1129
800	1468,0	1482,0	1464

4.2.2 Effect of salinity

The mini-sensor was immersed in different solutions of different salinity (distilled water, tap water, water from constructed wetlands and 8 solutions with different NaCl concentrations) and the relationship between capacitance and electrical conductivity (parameter used to measure salinity) was measured.

11 solutions were prepared in vessels with 2 L, an external diameter of 0.11m and a height of 0.24m (Figure 4.18) as follows:

- Distilled water at 20°C;
- Tap water at 20°C;
- Water collected at the interior of a HSSF-CW (laboratory set-up);
- 8 saline solutions prepared with NaCl with the following concentrations: 0, 11.2, 27.8, 56, 277.8, 555.6, 1666.7 and 2777.8 mg/L.

The electrical conductivity of each solution was measured by using a TetraCon 325 probe and a Multi 340i meter both from WTW. The electrical capacity was measured using a Philips PM6304 programmable automatic RCL meter.



Figure 4.18 - Capacitance measurement with samples from HSSF-CW.

4.2.3 Effect of temperature

The temperature may change the capacitance of sensors and, therefore, is important to evaluate the changes as the water temperature changes. The data-logger is itself temperature sensitive and can easily detect the changes in capacitance of probe according to the temperature.

Therefore, to overcome his problem is necessary developing an experimental methodology to assess the influence of temperature on the performance of capacitive measuring technology. A protocol to be implemented on field work was developed and is expected to provide results to allow assessing the influence of temperature on capacitance measuring, as well as to identify possible technical solutions to fix this problem

4.3 File work measurements

4.3.1 Wastewater treatment plant

The WWTP used for sensor tests is located in Vila Fernando (district of Guarda, Figure 4.19.).



Figure 4.19 - WWTP location.

The WWTP is operated by the company Zêzere and Côa and consists of a preliminary treatment stage (a screening and grit chamber channel), primary treatment (Imhoff tank) and a secondary treatment (two HSSF-CW in parallel), as shown in Figure 4.20. The sludge, after being digested at the Imhoff tank, is discharged through hydrostatic pressure into drying beds for a final dehydration process. The plant receives mainly domestic wastewater from the populations of Vila Fernando and Albardo (approximately 770 equivalent-population).

The filtration system (the two HSSF-CW) is filled with 0.7 m of an homogeneous layer of light expanded clay aggregates (LECA) with the commercial name of Filtralite NR 4-8 (i.e. effective diameter between 4 and 8 mm), but only one is colonized with reeds (*Phragmites australis*) and in operation as it can be seen in Figure 4.21. The outlet pipe was adjustable allowing for total control of the water level within the bed.

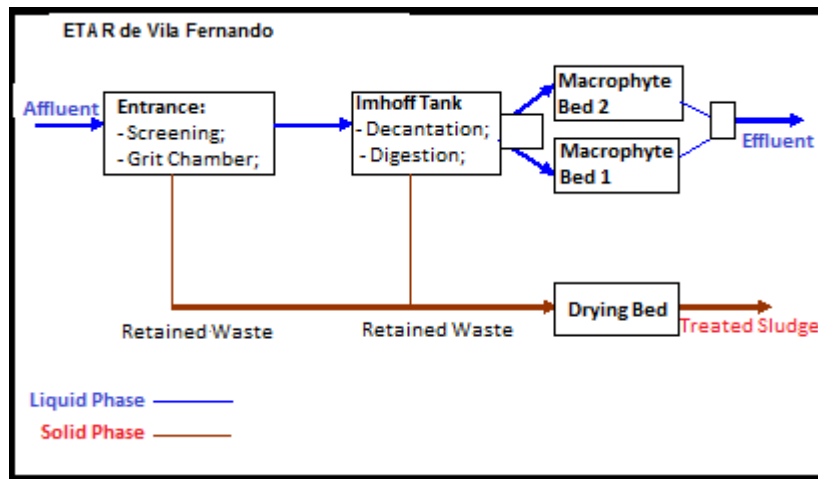


Figure 4.20 - Wastewater Plant Setup



Figure 4.21 - General view of the unvegetated filtration bed of Vila Fernando (A); HSSF-CW bed of Vila Fernando with *Phragmites australis* (B).

4.3.2 Installation of measuring points

In order to evaluate the variations of water level over time and space, 35 measuring points were setup in the CW as presented in Figure 4.22 (7 rows perpendicular to the flow direction, numbered from 1 to 7; and 5 rows parallel to the flow direction, identified from A to E). The piezometers are made of PVC material with a diameter of 125mm and 1.20m in height. Each piezometer is perforated with holes with 20mm in diameter and 80mm apart from each other and coated with a meshed net with 5x5mm square holes in order to prevent clogging of the holes and consequently preventing the filling material from getting into the tubes.

Figure 4.23 shows a general view of the bed with the 35 measuring points installed, whilst Figures 4.24 and 4.25 present a schematic representation of the vegetated bed and its longitudinal section, respectively.

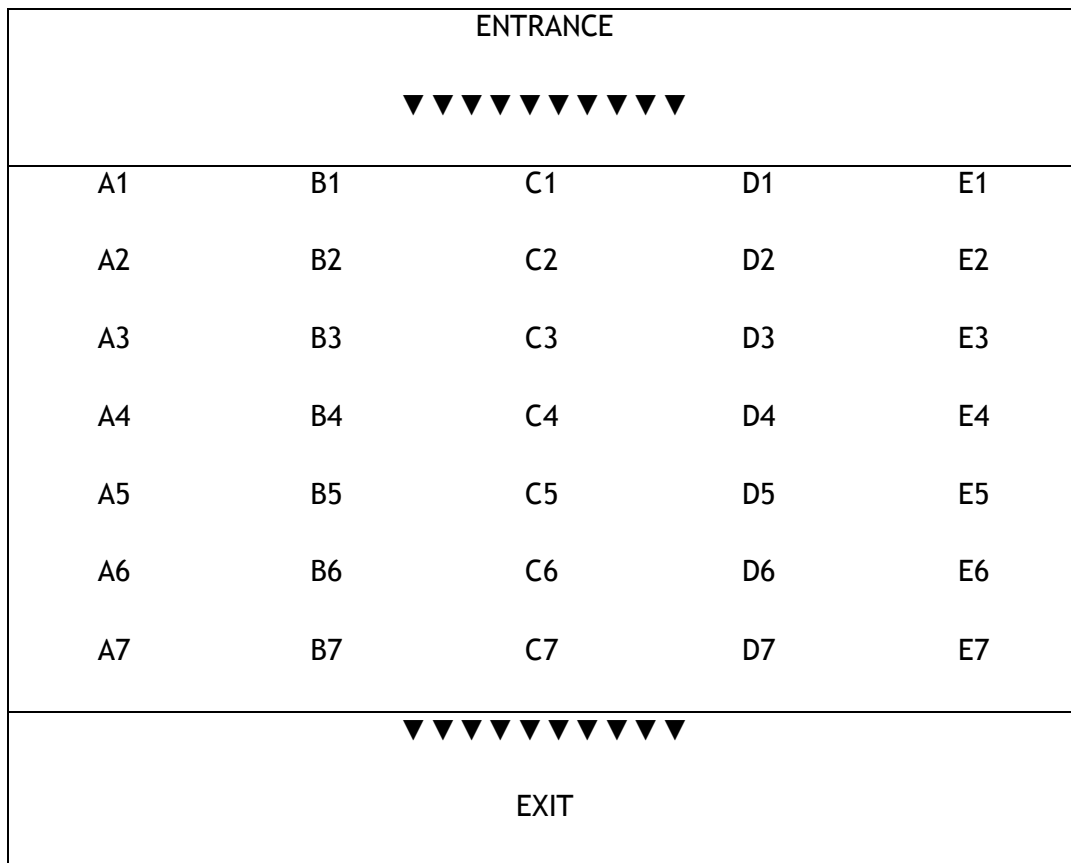


Figure 4.22 - Measuring point's layout at the CW of Vila Fernando.



Figure 4.23 - General view of the HSSF-CW bed with measuring points installed.

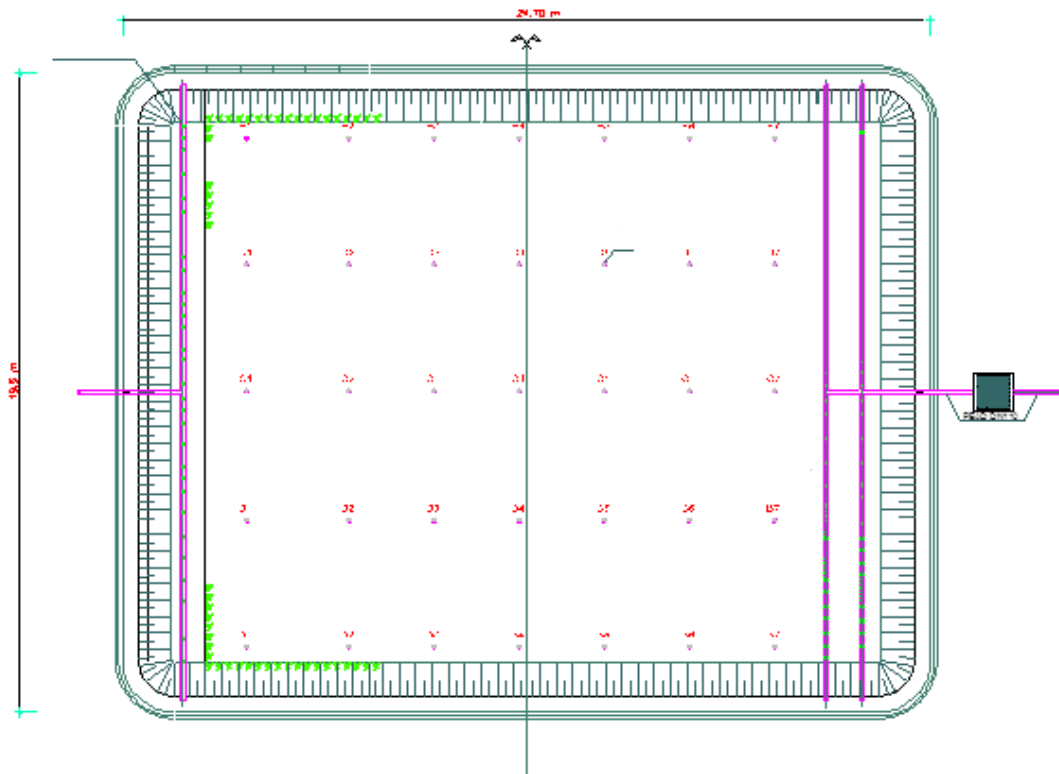


Figure 4.24 - Schematic representation of the HSSF-CW bed of Vila Fernando.

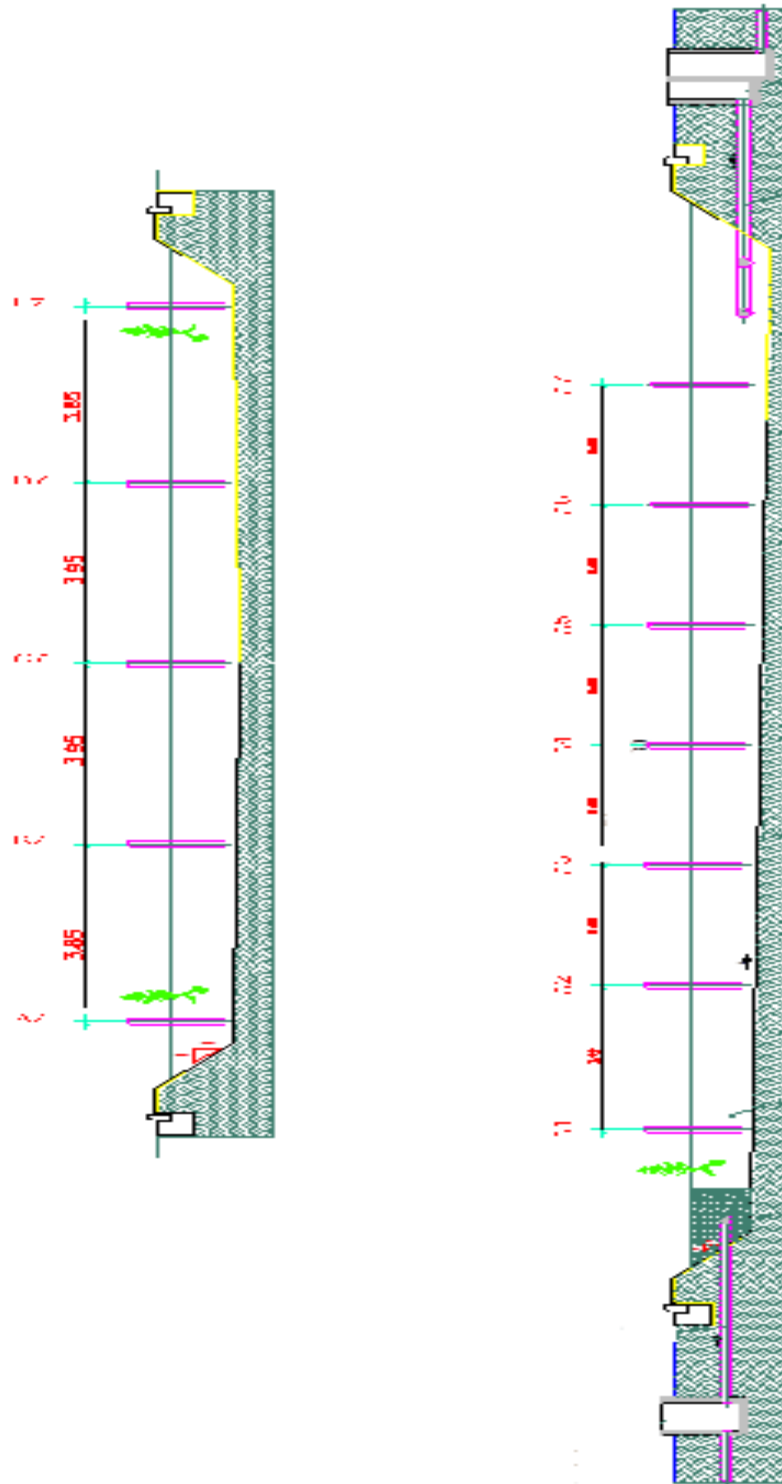


Figure 4.25 - Longitudinal section of the HSSF-CW of Vila Fernando.

4.3.3 Installation of the sensors

The probes were inserted into the measuring tubes of the HSSF-CW of Vila Fernando, as shown in Figure 4.26. Each position in which the sensors were installed was registered in order to know where the data came from. The starting measuring time and the measuring time for each sensor was annotated in order to create a network of sensors working in symphony.

Two sensors were also placed into feeding box (CRC), located upstream the HSSF-CW, in order to quantify the amount of water entering the bed.



Figure 4.26 - A) Network of measuring tubes with sensors. B) Sensors inserted into a tube.

4.3.4 Water level measurements

The measurements were made during February and March of 2012. 27 sensors were measuring the water table during week days (Monday-Friday). On Friday, the data-loggers were collected and the data were retrieved in laboratory.

5 Results and Discussion

5.1 Effect of water characteristics

The results of the salinity tests show that for concentrations of NaCl over than 277.8 mg/L (i.e., conductivity values higher than 553 $\mu\text{s}/\text{cm}$), the capacitance values of the probe remained virtually unchanged (260-265 pF), as shown in Table 5.1. This occurrence can be justified due to the fact that when the medium becomes conductive, its capacity to store energy is zero.

Table 5.1 - Sensor capacitance for different salinities solutions.

NaCl (mg/l)	Conductivity ($\mu\text{s}/\text{cm}$)	Probe capacity (pF)
0	1	79
11.2	25	214
27.8	65	224
56	118	252
277.8	553	260
555.6	1133	262
1666.7	3210	260
2777.8	5220	265

Comparing the conductivity value of tap water (42 $\mu\text{s}/\text{cm}$) and its capacitance value (215 pF) to the values retrieved when measuring the conductivity and probe capacitance for different NaCl concentrations, it can be stressed that as the tap water conductivity is between the values observed in the saline solutions 11.2 to 27.8 mg/L (conductivity from 25 to 65 $\mu\text{s}/\text{cm}$), which have capacitance between 214 and 224 pF. Therefore, the sensor is measuring well the capacitance for the different solutions, and salinity solutions over 553 $\mu\text{s}/\text{cm}$ seem to not influencing the probe capacity.

Using Eq. 4.1, it's was possible to compute the theoretical capacity to compare with the experimental reading. Table 5.2 shows an example for the solution with 11.2 mg NaCl/L and 214 pF. Looking at the theoretical model, the probe works with the overall capacity of the capacitor in series, which is formed by the dielectric air capacitor (C_1) and the dielectric insulating sheath capacitor (C_3).

Therefore, the capacity will vary linearly from a minimum capacity value of 247.1 pF (corresponding to a water level of 80 cm) to a value of 1714.9 pF (corresponding to a water

level of zero). That means, the capacity decreases with the increase of the water level. This behaviour can also be used to detect the operating regime of the capacitive probe.

Table 5.2 - Theoretical and experimental probe capacity for a solution with 214 pF.

	$l_{water} (mm)$			
	200	400	600	800
Theoretical capacity (pF)	95,84	68,46	41,07	13,69

A mini-sensor was immersed into 1.8 litres vessels with the 3 solutions, and the conductivity, capacitance and dielectric constant were measured. The values of electric conductivity and probe capacity for each water solution are presented in Table 5.3. The dielectric constants were computed according to Eq (4.11).

Table 5.3 - Sensor capacitance for different mediums with probe totally submerged.

Medium (@25°C)	Medium Conductivity ($\mu\text{s/cm}$)	Probe capacity (pF)
Distilled water	1	79
Tap water	42	215
Water from C. wetlands (lab)	1268	238

5.1.1 Protocol for evaluating the effect of temperature

The experiments to evaluate the effect of temperature may follow the following protocol, which was developed in the final of this work, but was not tested due to time restrictions.

The mini-sensor developed in point 4.2.1 will be immersed in a 5 L vessel with tap water with known capacitance (as presented in Figure 5.1-a)) and the vessel will be then immersed in a box with wastewater flowing at the entrance of the Vila Fernando HSS-CW. Knowing that the capacitance of water at 20°C is 80, any change to this value is related to change in temperature.

Additionally, it will be also necessary to measure the in situ temperature of the wastewater and a data-logger will be used for this purpose. This data-logger with the temperature sensor will be inserted into a glass jar, which offered an air tight and water tight vessel, ensuring that no water will go inside. This procedure will be weighed down with sand, making sure it would stay immersed in the wastewater, while the data logger was inserted inside with a power source, as proposed in Figures 5.1-b) and 5.1-c).

Therefore, both the vessels with the mini-sensors will be inserted into the box with flowing wastewater at the Vila Fernando HSS-CW, to act as reference sensors for temperature readings only. This practice, would allow measuring the temperature of the wastewater flowing into the HSS-CW, as well as changes in the water temperature as wastewater goes into the filtration system.

The changes in capacitance and temperature were followed through the values read by the data-logger and displayed in a computer screen. The Mat lab routine will be used to pass the data from the data-logger to the computer, using the docking bay.

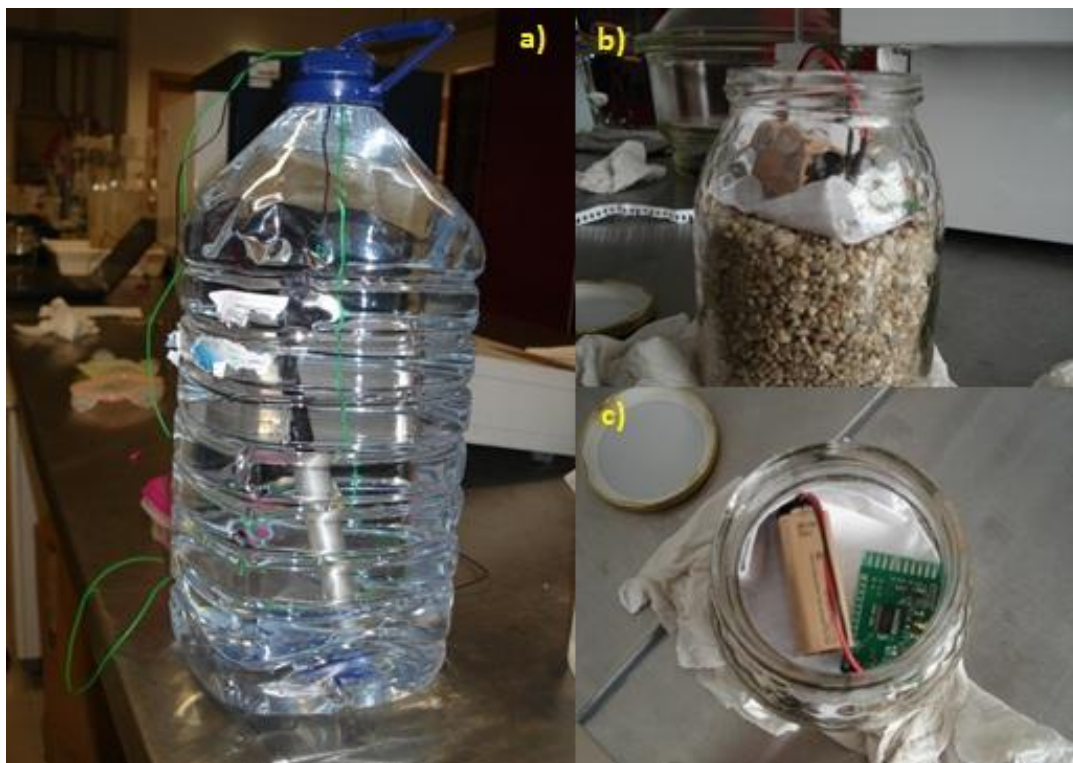


Figure 5.1 - Reference sensors for temperature; a) Sensor inserted into tap water at 20°C; b) c) Data logger inserted into a vessel to measure the temperature of the wastewater;

5.2 Water level measurements

Not all the sensors measured continuously during the weeks of measurements. The main causes of failure were the fail in battery, disconnection between components and oxidation of some circuits. However, most of the days there were obtained water level measurements in all the sensors for several days at 5 min time intervals. 23 sensors stored enough data during the two-month of measurements. Figure 5.2 shows the displacement of the 23 sensors whose data were validated for this work.

The sensors installed close the feeding point (entrance of the HSSF-CW), i.e. at lines 1 and 2, detected larger amplitude variation of water level, which is explained by the pumping periods

of wastewater to the CW bed. The amplitude decreased as the water progresses towards the bed output, what is explained by the head losses through the porous media. Therefore, the probes inserted near the exit (lines 6 and 7) registered more flat lines.

Entrance					
	<i>A</i>	<i>B</i>	<i>C</i>	<i>D</i>	<i>E</i>
<i>1</i>	<i>Sensor 11</i>	<i>Sensor 12</i>	<i>Sensor 13</i>	<i>Sensor 14</i>	<i>Sensor 15</i>
<i>2</i>	<i>Sensor 16</i>	<i>Sensor 17</i>	<i>Sensor 18</i>	<i>Sensor 19</i>	<i>Sensor 20</i>
<i>3</i>	<i>Sensor 21</i>	<i>Sensor 22</i>	<i>Sensor 23</i>	<i>Sensor 24</i>	<i>Sensor 25</i>
<i>4</i>	<i>Sensor 26</i>	<i>X</i>	<i>Sensor 27</i>	<i>X</i>	<i>Sensor 28</i>
<i>5</i>	<i>X</i>	<i>X</i>	<i>X</i>	<i>X</i>	<i>X</i>
<i>6</i>	<i>Sensor 29</i>	<i>X</i>	<i>Sensor 30</i>	<i>X</i>	<i>Sensor 31</i>
<i>7</i>	<i>X</i>	<i>X</i>	<i>Sensor 33</i>	<i>Sensor 34</i>	<i>X</i>
Exit					

Figure 5.2 - Sensor placement.

The data stored in the computer comes in vector of time (min) and number of cycles. Applying the calibration curves of Annexes I and II, data were then passed to water level values, which were treated in a spreadsheet.

All the data collected from the 23 data-logger are presented in Annex III.

Figure 5.3 shows the evolution of the water level in the first line of sampling tubes (A1, B1, C1, D1 and E1) during 6.5 hours.

It can be seen at least 3 peaks of water level, which corresponds to 3 pumping periods (the wastewater was pumped from the preliminary stage to the Imhoff tank, and flowed into the CW). Peaks are very noted in A1 and C1, but no so noted in B1, D1 and E1. These results are quite interesting since it may mean that LECA media is getting clogged at areas around B1, D1 and E1, where the water table could not reach the same values than the ones noted at points A1 and C1.

Figure 5.4 shows a similar evolution of the water level in the first line of sampling tubes (A1, B1, C1, D1 and E1) during 24 hours. This graph is clearer and shows a clear oscillation of the water level at A1 and C1, and an evident clogged area around tubes B1, D1 and E1. Each row tube has been divided into two 12 hour cycles, in order to obtain a clearer, readable and a more accurate visualization of the flow in the constructed wetland. The total time of the graphs is 24hours, corresponding to one day of continuous measuring. Each 12 hour graph has 720 minutes. The values can be seen in Annex III.

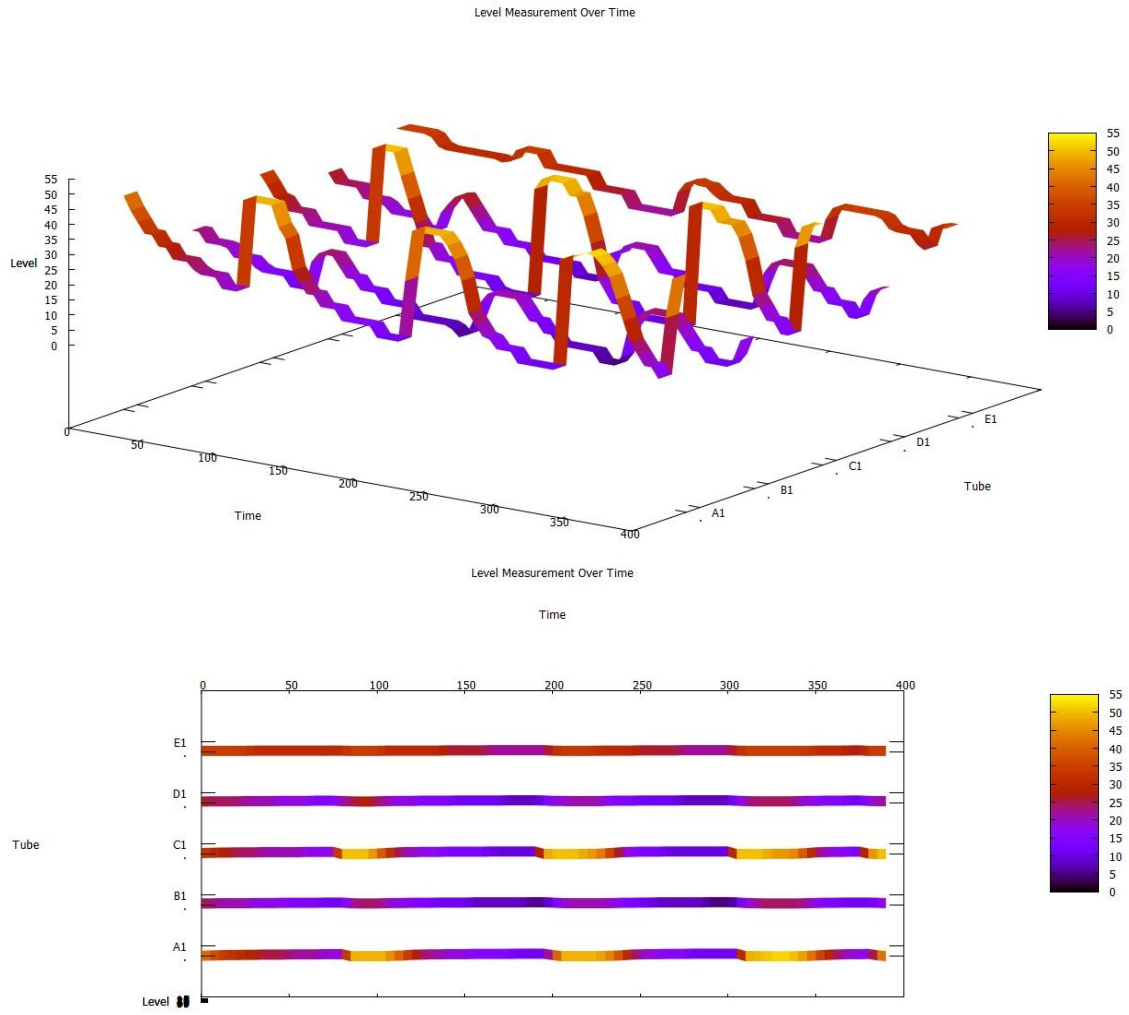


Figure 5.3 - Water level measuring in the first transversal row (11th of February 2012).

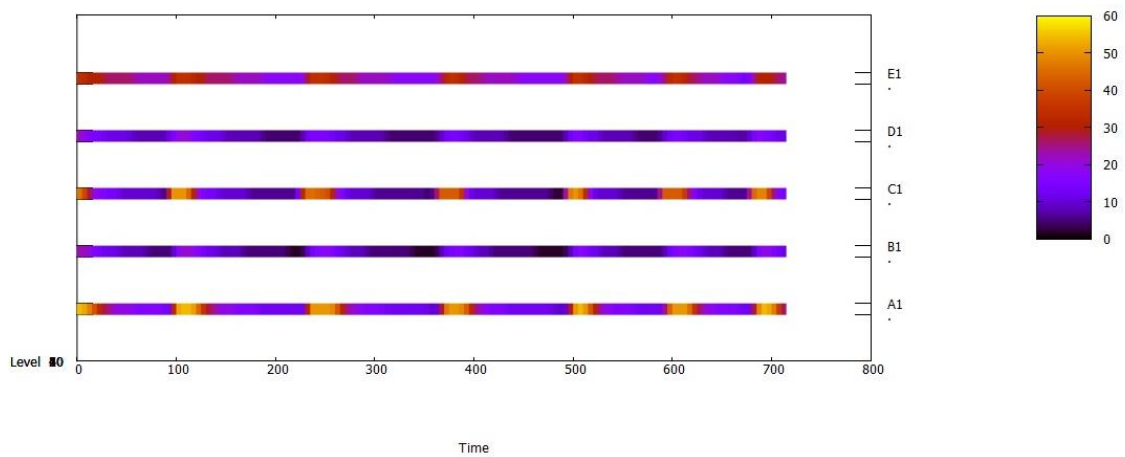
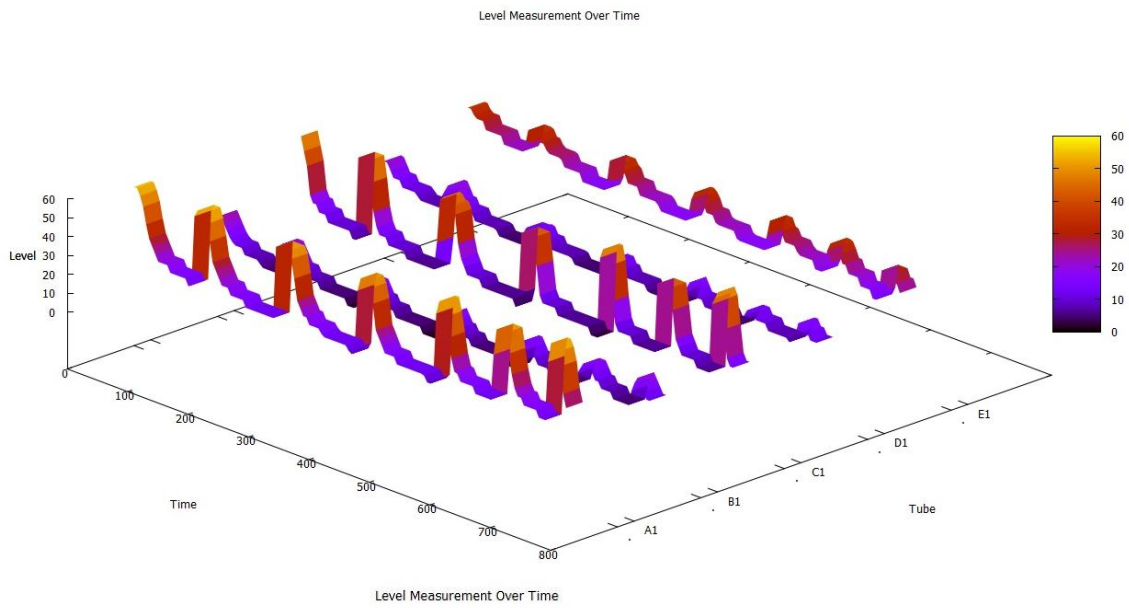


Figure 5.4 - Water level measuring in the first transversal row (12th February).

Figure 5.5 shows the water level measurements for 12 hours in the second line (A2, B2, C2 and D2). In this case, it is clear that a similar shape observed in the 4 parallel sampling tubes, which means that those areas were not clogged. Therefore, these results may allow concluding that the bed is clogged in the first 2 m from the entrance, but clogging is not expanding yet to the interior of the bed.

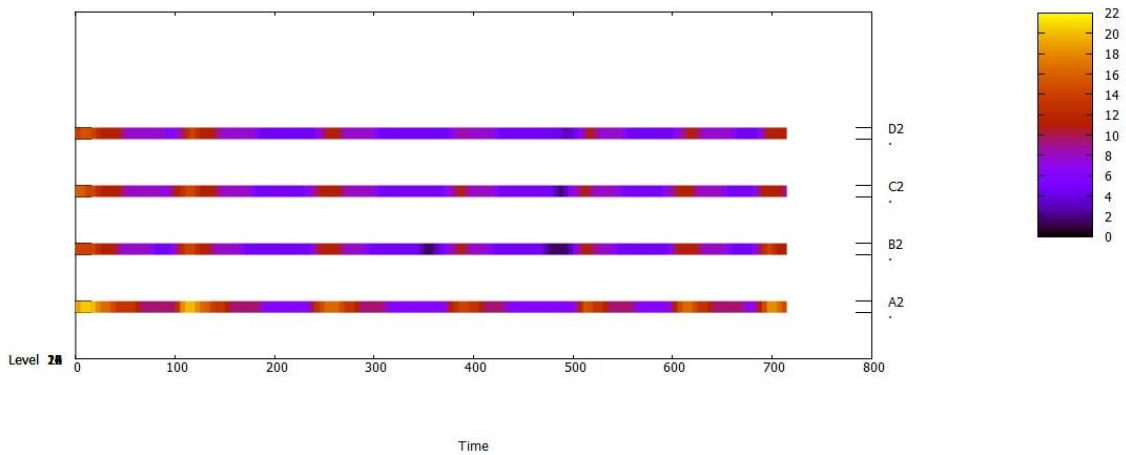
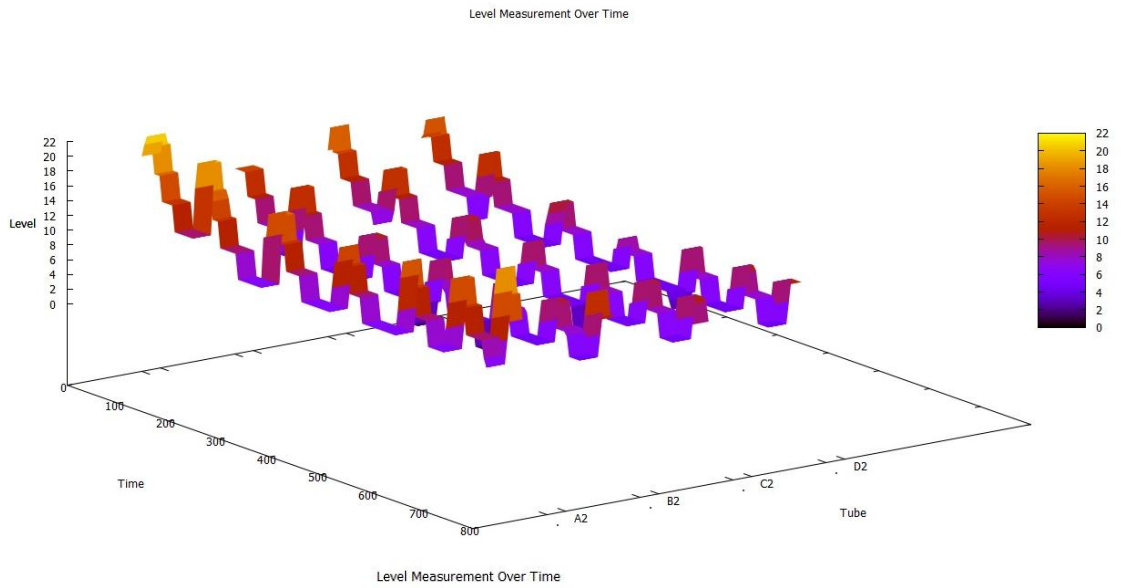


Figure 5.5 - Water level measuring in the second transversal row (12th February).

Figure 5.6 presents the variation of the water level for 12 hours in the measuring tubes A6 and C6 (sixth line), where it can be seen a very similar behaviour of the water level (i.e. there is no significant interference of media properties on flow). The flow is at this point more flat, which is explained by the head losses along the media.

The acquisition system maintenance is simple. It is needed is to ensure that the battery is in good condition, and replace batteries should always be available.

In field continuous measurements, the batteries had durability around 2 weeks. Therefore, this part should be improved in order to not have a dependence on lithium batteries. A solar battery would be a good solution for solving this problem, allowing also decreasing the costs of batteries.

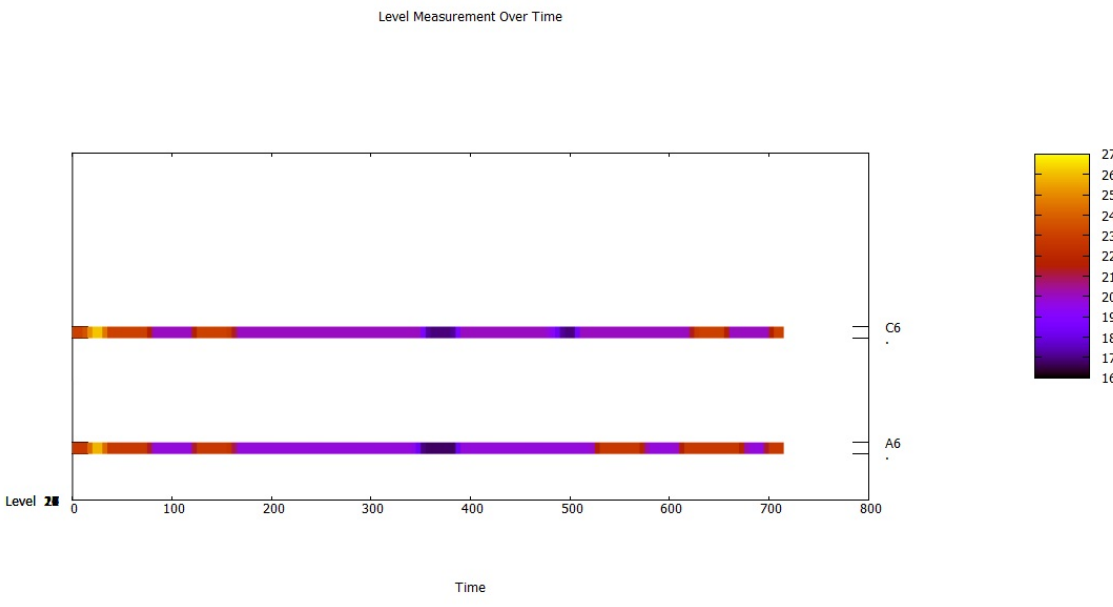
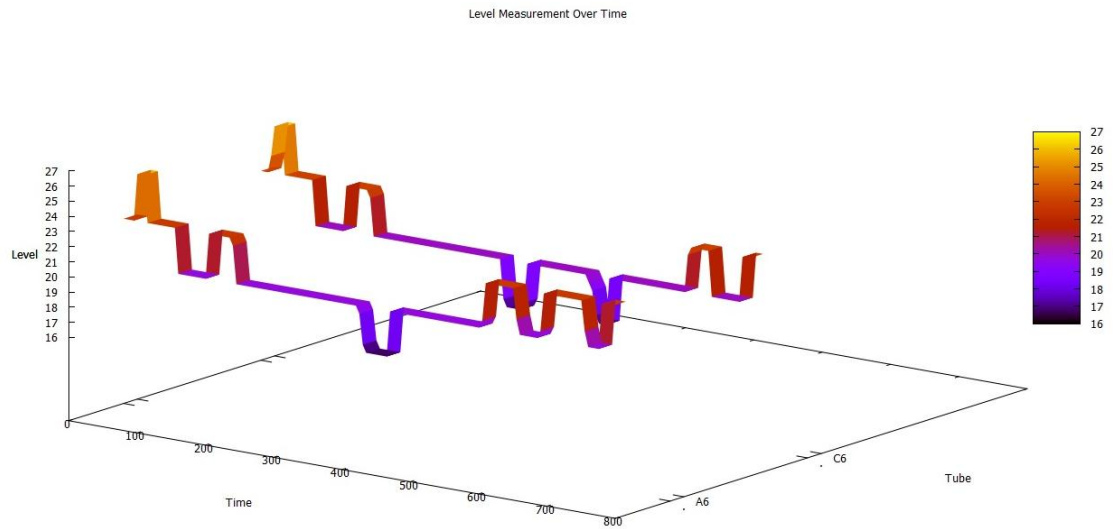


Figure 5.6 - Water level measuring in tubes A6 and C6 (12th February).

Probes need to be cleaned times to time to remove biofilm and other particles that can interfere with capacitance measurements. At the entrance of the pond there exists a higher concentration of organic matter, and some time oils, and for this reason, the probes located there require more maintenance.

The data-logger is also very robust. However, with time of operation the humidity can affect the measurements. Therefore, a properly device for data-logger storage will be developed in future.

6 Conclusions

6.1 Main Conclusions

This work is part of a larger project that aims to develop a sensor for water level measurement light, cheap, durable and with low energy consumption, which can be easily installed for the measurement of free surface water level or in porous media. The technology used involves the development of a capacitance meter (air-water), a data-logger for registering the capacity over time and an interface for data transfer to a computer.

33 capacitive sensors were developed (30 for field work, 3 mini-sensors for laboratory work), according to a theoretical model. The sensors were calibrated in the laboratory, according to the conditions used for the measurement in the field. The respective calibration curves allow passing capacitance data to water level data.

The mini-sensors were used to evaluate the effect of the characteristics of the effluent quality measurement. The sensor responded well to change in salinity, presenting capacitance measurements proportional to the different solutions (distilled water, tap water, water from an HSSF-CW and 8 and NaCl solutions).

It was proposed an experimental method that will allow evaluating the effect of temperature variation in sensor performance. However, it is also necessary to evaluate the effect of the wastewater characteristics on probe measurements over a long term operation. Some sensors had measurement errors, associated to energy depletion, an aspect that must be improved in further work.

The experimental tests carried out on the HSSF-CW of Vila Fernando (Guarda) show that the sensor made reliable measurements of the water level variation over time, and detected water level changes caused by cycles of upstream water pumping. The evolution of the water levels in several measuring points along the bed allowed also observing clogging at the initial section, a situation that could not be detected by conventional operational procedures.

6.2 Further Work

There are several aspects that can be improved on sensor developments, mainly:

- i) The development of an energy self-sufficient system (e.g. solar energy);
- ii) The study of the effect of temperature, humidity and characteristics of the wastewater over long term operation;
- iii) The development of data acquisition system using signal technology to retrieve data directly from the data-logger when installed in field;
- iv) Increase system overall robustness.

7 References

Afridi M. (2008): Phosphorus removal from wastewater using Absol - A novel reactive filter material. MSc Thesis, KTH Royal Institute of Technology, Stockholm, Sweden.

Albonico, M., Smith, P.G., Ercole, E., Hall, A., Chwaya, H.M., Alawi, K.S. and Savioli, L. (1995) Rate of reinfection with intestinal nematodes after treatment of children with mebendazole or albendazole in a highly endemic area. *Transactions of the Royal Society for Tropical Medicine and Hygiene* 89, 538-541.

Albuquerque, A. (2003a). Tratamento de águas residuais. 2ª versão, UBI, Covilhã, 167 pp.

Albuquerque A. (2003b). *Contribuição para o estudo da remoção de residuais de carbon em filtros biológicos de leito imerso e fluxo descendente*. Tese de Doutoramento na Especialidade de Engenharia Civil, Universidade da Beira Interior, Covilhã, 469 pp.

Albuquerque A., Arendacz M., Gajewska M., Obarska-Pempkowiak H., Randerson P., Kowalik P. (2009). Removal of organic matter and nitrogen in an horizontal subsurface flow (HSSF) constructed wetland under transient loads. *Water Science and Technology*, 60(7), 1677-1682.

Albuquerque A. (2012). Spatial variation of longitudinal dispersion in LECA-based vegetated beds. *Defect and Diffusion Forum*, 326/328, 279-284.

Amado L., Albuquerque A., Espirito Santo A. (2012). Influence of stormwater infiltration on the treatment capacity of a LECA-based horizontal subsurface flow constructed wetland. *Ecological Engineering*, 39, 16-23.

Andersson S., Nilsson M., Dalhammar G. e Rajara G. (2008). Assessment of carrier materials for biofilm formation and denitrification. *VATTEN*, 64, 201-207.

Armon, R., Gold, D., Brodsky, M. and Oron, G. (2002) Surface and subsurface irrigation with effluents of different qualities and presence of *Cryptosporidium* oocysts in soil and on crops. *Water Science and Technology* 46(3), 115-122.

Arregui F., Cabrera E. and Cobacho R. (2007). *Integrated Water Meter Management*. IWA Publishing, London, UK.

Asano T., Burton F., Leverenz H., Tsuchihashi R. e Tchobanoglous G. (2007). *Water reuse*. McGrawHill, Nova York, EUA.

AWWA (2006). *Flowmeters in Water Supply*. Manual M33, 2nd Edition, American Water Works Association, Denver, USA.

Ayres, R.M., Stott, R., Lee, D.L., Mara, D.D. and Silva, S.A. (1992) Contamination of lettuces with nematode eggs by spray irrigation with treated and untreated wastewater. *Water, Science and Technology* 26(7-8), 1615-1623.

Bande V., Ciascai I. and Pitica D. (2010). A low-cost capacitive sensor for wells level measurement. Proc. of the 3rd International Conference on *Computer Science and Information Technology (ICCSIT)*, IEEE, 9-11 July 2010, Changdu, China, 279-283.

Bartram, J., Fewtrell, L. and Stenström, T.A. (2001) Harmonised assessment of risk and risk management for water-related infectious disease: an overview. In: Fewtrell, L. and Bartram, J. (eds.) *Water Quality: Guidelines, Standards and Health; Assessment of Risk and Risk*

Management for Water-related Infectious Disease. International Water Association (IWA) on behalf of the World Health Organization, London, UK, pp. 1-16.

Baumhardt R.L, Lascano R.J & Evett S.R (2000). Soil, Temperature, and Salinity Effects on Calibration of Multisensor Capacitance Probes., *64*(6), 1940-1946.

Baxter, L. K. (1996). Capacitive Sensors. *IEEE*, 1-17.

Bera, S. C., Ray, J. K., & Chattopadhyay, S. (2006). A Low-Cost Noncontact Capacitance-Type Level Transducer for a Conducting Liquid. *IEEE*, *55*(3), 778-786.

Berkman, D.S., Lescano, A.G., Gilman, R.H., Lopez, S.L. and Black, M.M. (2002) Effects of stunting, diarrhoeal disease, and parasitic infection during infancy on cognition in late childhood: a follow-up study. *Lancet* *359*(9306), 542-571.

Betta, G., Pietrosanto, A., & Scaglione, A. (1995). A Digital Transducer Based on Optical Fiber, *IEEE transactions on instrumentation and measurement*, *46*(3), 551 - 555.

Beuchat, L.R. (1998) *Food Safety Issues: Surface Decontamination of Fruits and Vegetables Eaten Raw: A Review*. Food Safety Unit, World Health Organization (WHO), Geneva, Switzerland, 42 pp.

Białowiec A., Wojnowska-Baryła I. and Randerson P. (2011). Evapotranspiration in ecological engineering. In Evapotranspiration, Leszek Labeledzki (Edt)., Cap. 17, *Tech, Series on Environmental Sciences*, 395-418.

Blumenthal, U. and Peasey, A. (2002) *Critical Review of Epidemiological Evidence of the Health Effects of Wastewater and Excreta Use in Agriculture*. World Health Organization (WHO), Geneva, Switzerland. (Unpublished document available on request).

Blumenthal, U., Mara, D.D., Peasey, A., Ruiz-Palacios, G. and Stott, R. (2000a) Guidelines for the microbiological quality of treated wastewater used in agriculture: recommendations for revising WHO guidelines. *Bulletin of the World Health Organization* *78*(9), 1104-1116.

Blumenthal, U.J., Peasey, A., Ruiz-Palacios, G. and Mara, D. (2000b) *Guidelines for Wastewater Reuse in Agriculture and Aquaculture: Recommended Revisions Based on New Research Evidence*. WELL Study, Task No. 68, Part 1. Water and Environmental Health at London and Loughborough (WELL), London, UK. <http://www.lboro.ac.uk/well/resources/well-studies/well-studies.htm>.

Buechler, S. and Devi, G. (2003) *Household Food Security and Wastewater-dependent Livelihood Activities Along the Musi River in Andhra Pradesh, India*. International Water Management Institute (IWMI), Document prepared for the World Health Organization (WHO), Geneva, Switzerland, 33 pp. (unpublished)

Canbolat, H., & Member, S. (2009). A Novel Measurement Technique Using Three Capacitive Sensors for Liquids, *IEEE*, *58*(10), 3762-3768.

Carr, R. and Strauss, M. (2001) Excreta-related infections and the role of sanitation in the control of transmission (Chapter 5).

Chazarenc F., Merlin G., Gonthier Y. (2003). Hydrodynamics of horizontal subsurface flow constructed wetlands. *Ecological Engineering*, *21*, 165-173.

Chen, Z.S. (1992) Metal contamination of flooded soils, rice plants, and surface waters in asia. In: Adriano (ed.) *Biogeochemistry of Trace Metals*. Lewis Publishers, Boca Raton, Florida, pp. 85-108.

Cifuentes, E., Blumenthal, U., Ruiz-Palacios, G., Bennett, S. and Quigley, M. (2000) Health risk in agricultural villages practicing wastewater irrigation in Central Mexico: perspectives for protection. In: Chorus, I., Ringelband, U., Schlag, G. and Schmoll, O. (eds.) *Water Sanitation and Health*, International Water Association (IWA) Publishing, London, UK, pp. 249-256.

Crini, G. (2006). Non-conventional low-cost adsorbents for dye removal: a review. *Bioresource Technology*, 97, 9, 1061-1085.

Davis, Mackenzie L., Masten, Susan J. (2004) *Principles of Environmental Engineering and Science* New York, McGraw-Hill.

Falkovich G. (2011). *Fluid mechanics: a short course for physicists*. Cambridge University Press, Cambridge, UK.

E. Flow, M. Solutions. Aeroprobe Corporation. Multi-Hole Velocity Probes.

EPA (2000). Wastewater technology fact sheet. Trickling filters. U.S. Environmental Protection Agency, EPA 832-F-00-014, Washington, EUA, 7 pp.

FAO (Food and Agriculture Organization of the United Nations). (1993) *Control de aguas de riego destinadas a la produccion hortofruticola: Chile*. Technical Report of Project TCP/CHI/2251(A). FAO, Rome, Italy.

FAO (Food and Agriculture Organization of the United Nations). (2001) *Crops and Drops: Making the Best Use of Water for Agriculture*. FAO, Rome, Italy, pp. 1-22.

Fattal, B. and Shuval, H. (1999) A risk-assessment method for evaluating microbiological guidelines and standard for reuse of wastewater in agriculture. Paper presented at the WHO meeting *Harmonized Risk Assessment for Water Related Microbiological Hazards, Stockholm, Sweden, 12-16 September 1999*, pp. 1-10.

Feenstra, S., Hussain, R. and van der Hoek, W. (2000) *Health Risks of Irrigation with Untreated Urban Wastewater in the Southern Punjab, Pakistan*. Institute of Public Health, International Water Management Institute (IWMI), Pakistan Program, Lahore, Pakistan, 27 pp.

Fewtrell, L. and Bartram, J. (eds.) *Water Quality: Guidelines, Standards and Health; Assessment of Risk and Risk Management for Water-related Infectious Disease*. International Water Association (IWA) on behalf of the World Health Organization, London, UK, pp. 89-113.

Finlayson, C. M., Farrell, T. P., and Griffiths, D. J. (1982); *Treatment of sewage effluent using the water fern salvinia*; Water Research Foundation of Australia Report.

Fogler H. (1999). *Elements of Reaction Engineering*. Bk&cdr, 3rd Edition, Prentice Hall Inc., New Jersey, USA.

Frazer, A., Lapina, K., Whaley, A. Muga, H. (2007). Michigan Environmental Education Curriculum, Wastewater Treatment. Michigan Tech.

Lekang O. e Kleppe H. (2000). Efficiency of nitrification in trickling filters using diferente filter media. *Aquaculture Eng.*, 21, 181-199.

Galvão, A. F. (2009). *Comportamento Hidráulico e Ambiental de Zonas Húmidas Construídas Para o Tratamento de Águas Residuais*.

- Garzón-Zúñiga M., Lessard P., Aubry G. e Buelna G. (2007). Aeration effect on the efficiency of swine manure treatment in a trickling filter packed with organic materials. *Water Science and Technology*, 55(10), 135-143.
- Gersberg, R. M.; Elkins, B. V. and Goldman, C.R. (1986); Role of aquatic plants in wastewater treatment by artificial wetlands; *Water Research* 20 (3), 363.
- Gleick, P.H. (2000) *The World's Water 2000-2001: The Biennial Report on Freshwater Resources*. Island Press, Washington DC, 315 pp.
- Grady Jr, W., Daigger, G. and Lim, H. (1999). Biological wastewater treatment. 2^a Edition, Marcel Decker, Basel, Switzerland, 1076.
- Guirong L and Shuyue C. (2010). A capacitive liquid level sensor with four electrodes. Proc. of the 3rd International Conference on *Computer Science and Information Technology (ICCSIT)*, IEEE, 9-11 July 2010, Changdu, China, 628-632.
- Harleman, D. and Murcott, S. (2001) An innovative approach to urban wastewater treatment in the developing world. *Water* 21, 44-48.
- Havelaar, A.H. and Melse, J.M. (2003) *Quantifying Public Health Risks in the WHO Guidelines for Drinking Water Quality: A burden of disease approach*. RIVM Report 734301022/2003. Rijksinstituut voor Volksgezondheid en Milieu (National Institute for Public Health and the Environment), Bilthoven, The Netherlands, 49 pp.
- van der Hoek, W., Sakthivadivel, R., Renshaw, M., Silver, J.B., Birley, M.H. and Konradsen, F. (2001a) Alternate wet/dry irrigation in rice cultivation: a practical way to save water and control malaria and Japanese encephalitis? *IWMI Research Report 47*. International Water Management Institute, Colombo, Sri Lanka, 30 pp.
- van der Hoek, W., Konradsen, F., Ensink, J.H.J., Mudasser, M. and Jensen, P.K. (2001b) Irrigation water as a source of drinking water: is safe use possible? *Tropical Medicine and International Health* 6(1), 46-54.
- Homsi, J. (2000) The present state of sewage treatment. International Report. *Water Supply* 18(1), 325-327.
- Hussain, I., Raschid, L., Hanjra, M., Marikar, F. and van der Hoek, W. (2001) *A Framework for Analyzing Socioeconomic, Health and Environmental Impacts of Wastewater Use in Agriculture in Developing Countries*, Working Paper 26. International Water Management Institute (IWMI), Colombo, Sri Lanka, 31 pp.
- Ijumba, J.N. (1997) The impact of rice and sugarcane irrigation on malaria transmission in the lower Moshi area of northern Tanzania. PhD Thesis, Tropical Pesticides Research Institute and Danish Bilharziasis Laboratory, Charlottenlund, Denmark, 134 pp.
- Jiménez B., Noyola A., Capdeville B., Roustan M., Faup M. (1988). Design Dextran blue colorant as a reliable tracer in submerged filters. *Water Research*, 22, 1253-1257.
- Kadlec R. and Wallace S. (2008). *Treatment Wetlands*. 2nd edition, CRC Press, USA.
- Kay, M. (2001) *Smallholder Irrigation Technology: Prospects for Sub-Saharan Africa*. International Programme for Technology and Research in Irrigation and Drainage, Food and Agriculture Organization of the United Nations (FAO), Rome, Italy, pp. 1-19.

Kelleners, T. J., Soppe, R. W. O., Robinson, D. A., Schaap, M. G., Ayars, J. E., & Skaggs, T. H. (2004). Calibration of Capacitance Probe Sensors using Electric Circuit Theory, *Soil Society of America*, 430-439.

Klute, R. and Hahn, H. (eds.) (1992) *Chemical Water and Wastewater Treatment II. Proceedings of the 5th Gothenburg Symposium*, Springer-Verlag, Berlin, Germany, pp. 401-416.

Koch, J. (2002). Measurements in Sewer Systems, (November), 1-7.

Kosek, M., Bern, C. and Guerrant, R.L. (2003) The global burden of diarrhoeal disease, as estimated from studies published between 1992 and 2000. *Bulletin of the World Health Organization* 81(3), 197-204.

Krajnovic, S., & Davidson, L. (2000). FLOW AROUND A THREE-DIMENSIONAL BLUFF BODY. *Symposium A Quarterly Journal In Modern Foreign Literatures*, 177(177), 1-10.

Mano, A. P. (1996). Contribuição para o estudo do processo de desnitrificação em reactores biológicos de filme fixo. Tese de Doutoramento em Engenharia Sanitária, FCT, Universidade Nova de Lisboa, Monte de Caparica, 317 pp.

Mara, D.D. (1997) *Design Manual for Waste Stabilisation Ponds in India*. Lagoon Technology International, Leeds, UK.

Mara, D. and Cairncross, S. (1989) *Guidelines for the Safe Use of Wastewater and Excreta in Agriculture and Aquaculture*. World Health Organization, Geneva, Switzerland, 187 pp.

Martinez C., Wise W. (2003). Analysis of constructed treatment wetland hydraulics with the transient storage model OTIS. *Ecological Engineering*, 203-211.

Martins, A. M. (1998). Contribuição para o estudo dos efeitos do oxigénio dissolvido e do excesso de carbono no processo de desnitrificação. Tese de Mestrado em Engenharia Sanitária, FCT, Universidade Nova de Lisboa, Monte de Caparica, 188 pp.

Martins, A. M. (2004). Selectores biológicos em sistemas de lamas activadas. In livro de Comunicações da 8^a Conferência Nacional do Ambiente, Lisboa, Portugal. 336 pp.

Mead, P.S., Slutsker, L., Dietz, V., McCaig, L.F., Bresee, J.S., Shapiro, C., Griffin, P.M. and Tauxe, R.V. (1999) Food-related illness and death in the United States. *Emerging Infectious Diseases* 5(5), 607-625.

Merkley, G. P. (2004) Weirs for Flow Measurement, Annotations. 61-72.

Monreal, J. (1993) *Estudio de caso de Chile. Evolucion de la morbilidad entérica en Chile, luego de la aplicacion de medidas de restriccion de cultivos en zonas regadas con aguas servidas*. Presented at WHO/FAO/UNEP/ UNCHS Workshop on Health, Agriculture and Environmental Aspects of Wastewater Use, Juitepec, Mexico, 8-12 November 1993.

Montresor, A., Crompton, D.W.T., Gyorkos, T.W. and Savioli, L. (2002) *Helminth Control in School-age Children: A Guide for Managers of Control Programmes*. World Health Organization, Geneva, Switzerland, 64 pp.

Morrissey, S., and Harleman, D. (1992) Retrofitting conventional primary treatment plants for chemically enhanced primary treatment in the USA.

Munoz P., Drizob A., Hession W. (2006). Flow patterns of dairy wastewater constructed wetlands in a cold climate. *Wat. Res.*, 3209-3218.

Murray, C.J.L. and Lopez, A.D. (eds.) (1996) *The Global Burden of Disease, Vol. 1, Global Health Statistics: A Compendium of Incidence, Prevalence and Mortality Estimates for Over 200 Conditions*, Harvard School of Public Health on behalf of the World Health Organization and The World Bank, Cambridge, Massachusetts.

OMEGA (1995). *Complete Flow and Level Measurement Handbook and Encyclopedia*. OMEGA Press, Connecticut, USA.

Parr, J., Smith, M., and Shaw, R. (2000) Wastewater treatment options. *Technical Brief no. 64. Waterlines* 18(4), 15-18.

Pollution Equipment News. Open Channel Flow Measurement Using the Area Velocity Method and Doppler Technology, *Isco*.

Quintela, A. C.(1998); *Hidráulica*; Fundação Calouste Gulbenkian, 6ª Edição.

Ribeiro, João Paulo Lopes (Licenciado) (2007). Dissertação para a obtenção do grau de mestre em Engenharia do Ambiente - MODELAÇÃO DO COMPORTAMENTO HIDRÁULICO DE LEITOS DE MACRÓFITAS.

Ripka P. and Tipek A. (2007). *Modern Sensors Handbook*. Wiley-ISTE, John Wiley & Sons, London, UK.

Rodrigues, J., Galvão, A., Matos, J. and Heath, P. (2004). Sustainable Sewage Solutions for Small Agglomerations. *Water Sci Technol.* 2005; 52(12): 25-32.

Seguret M. (1998). Etude de l'hydrodynamique des procédés de traitement des eaux usées à biomasse fixée. Application aux lits bactériens et aux biofilters. PhD thesis, University of Bordeaux, France.

Shuyue, C. (2010). A capacitive liquid level sensor with four electrodes. *2010 3rd International Conference on Computer Science and Information Technology*, 628-632. Ieee. doi:10.1109/ICCSIT.2010.5564467.

Silva, J. P. C. M. A. (2010). AVALIAÇÃO DA CAPACIDADE DE TRATAMENTO DE UM BIOFILTRO COM UTILIZAÇÃO DE AGREGADOS GEOPOLIMÉRICOS ARTIFICIAIS.

Simões M. (2009). Avaliação da influência do tipo de enchimento no rendimento de leitos de macrófitas de escoamento subsuperficial e horizontal. Tese de Mestrado em Eng. Civil. UBI, Covilhã.

Singh, H. K., Chakroborty, S. K., Talukdar, H., Singh, N. M., & Bezboruah, T. (2011). A New Non-Intrusive Optical Technique to Measure Transparent Liquid Level and Volume. *IEEE Sensors Journal*, 11(2), 391-398. doi:10.1109/JSEN.2010.2068543.

Skaggs T. H., J. A. Poss, P. J. Shouse and C. M. Grieve (2006): Irrigating Forage Crops with Saline Waters: 1. Volumetric Lysimeter Studie. *Vadose Zone Journal*, August 5(3).

Smajstrla, A. G., & Harrison, D. S. (2002). Weirs for Open-Channel Flow Measurement 1.

Sofia, J. W. (1995). *Fundamentals of Thermal Resistance Measurement*, (781).

Tchobanoglous, G., Burton, F. L., Burton, F., Stensel H.D. *Wastewater engineering: treatment, disposal and reuse*. 4ª Edição, McGraw-Hill Science/Engineering/Math, Nova York, EUA, 1848 pp.

Tecnologia, F. D. E. C. E., & Oliveira, J. M. (2008). Estudo da Influência do Material de Enchimento na Remoção de Matéria Orgânica, Azoto e Sólidos em Leitos de Macrófitas do Tipo ESSH.

Toth, F. N., Meijer, G. C. M., & Lee, M. V. D. (1996). A New Capacitive Precision Liquid-Level Sensor, in conference of *IEEE 17 June -21 June, Braunschweig, Germany* 356-357.

T. U. S. G., National Nonpoint Source Monitoring Programme (2008). Surface Water Flow Measurement for Water Quality Monitoring Projects Introduction, 1-16.

Turona C., Comasa J., Poch M. (2009). Constructed wetland clogging: A proposal for the integration and reuse of existing knowledge. *Ecological Engineering*, 35, 12, 1710-1718.

Umar, L. (2010). Smart level sensor based on thermal resistance measurement with self-calibration. *2010 International Conference on Autonomous and Intelligent Systems, AIS 2010*, 1-5. Ieee. doi:10.1109/AIS.2010.5547040.

Visvanathan C. and Nhien T. (1995). Study on aerated biofilter process under high temperature conditions. *Environmental Technology*, 16, 4,301-314.

Vymazal J.; Kropfelova L. (2008). Wastewater Treatment in Constructed Wetlands with Horizontal Subsurface Flow. *Env. Pollution* 14, Springer, Germany.

Wallace S.D. and Knight R.L., (2006); Small-scale constructed wetland wastewater treatment systems: Feasibility, design, and O&M requirements, Final Report, Project 01-CTS-5; Water Environment Research Foundation: Alexandria, Virginia.

Wang, C. (2006). Multifunctional Self-Calibrated Sensor For Brake Fluid Condition Monitoring, 815-818.

Yoder, J. L., PhD., & Analyst, S. (1998). Using meters to measure steam flow, (April).

Annexes

Annex I - Calibration curves for water level and number of cycles

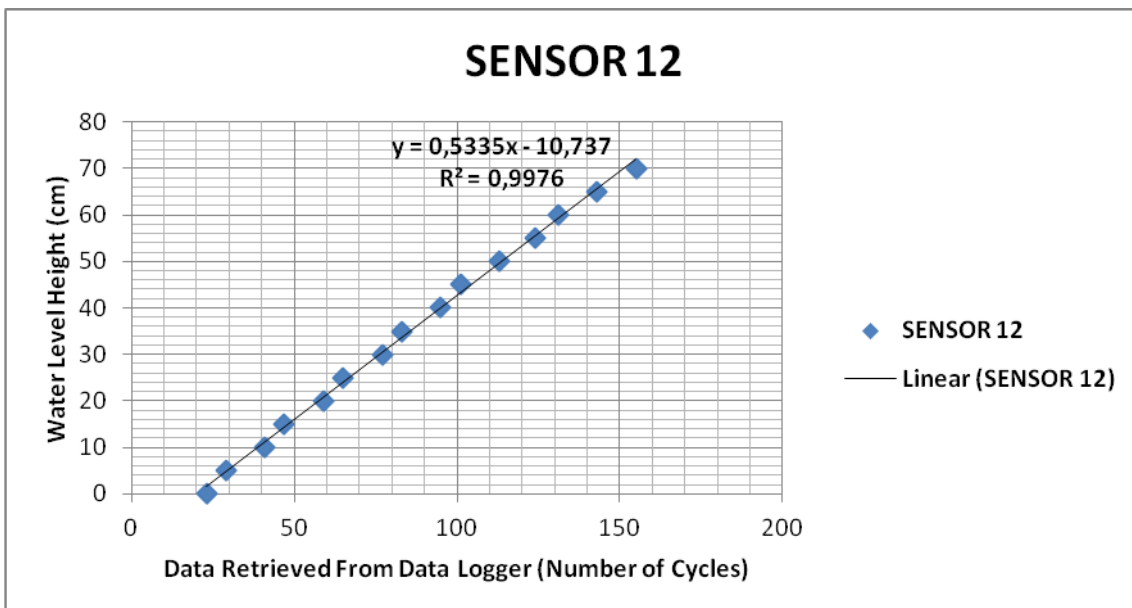
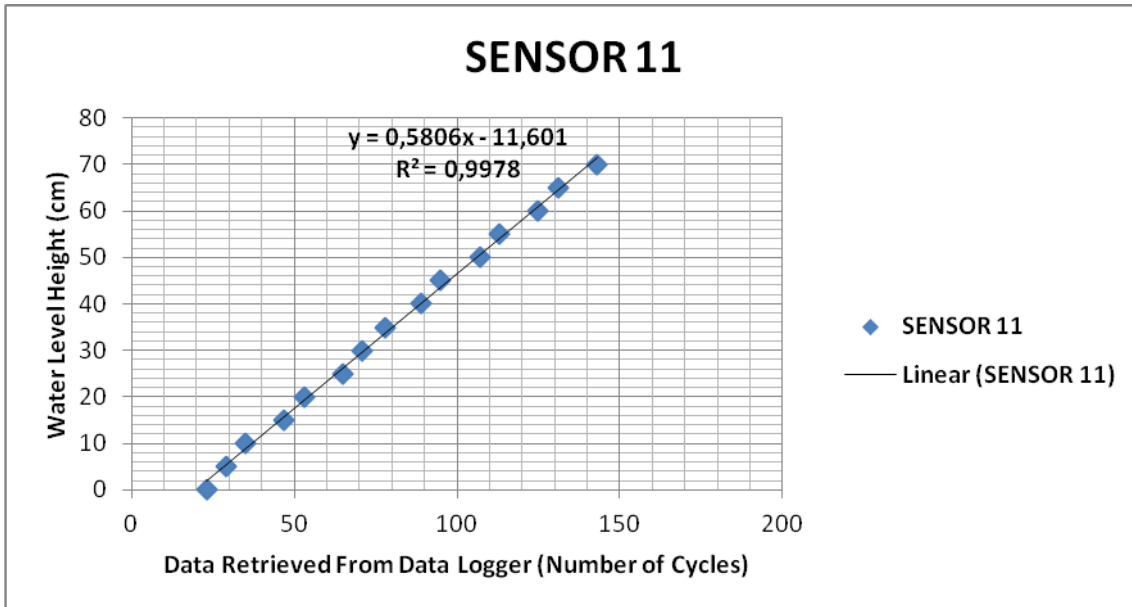
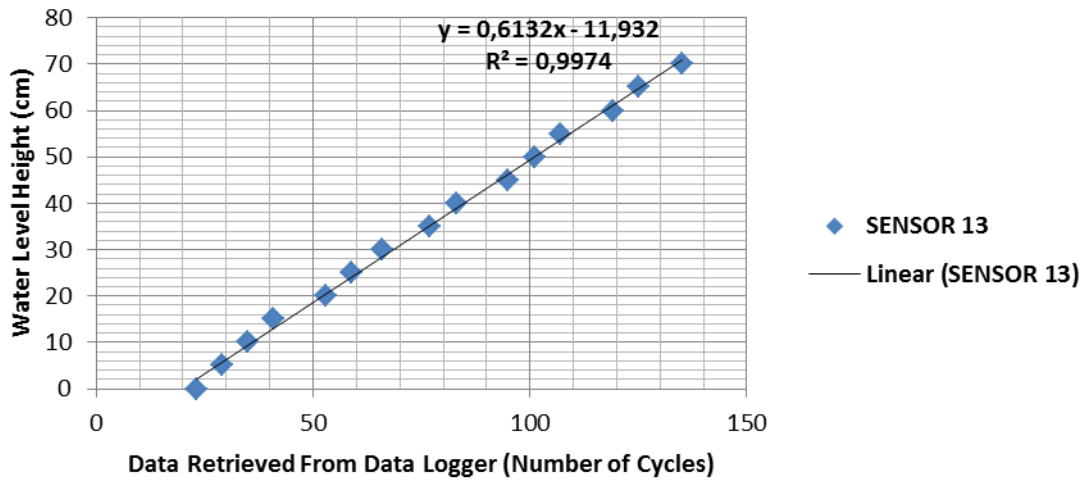
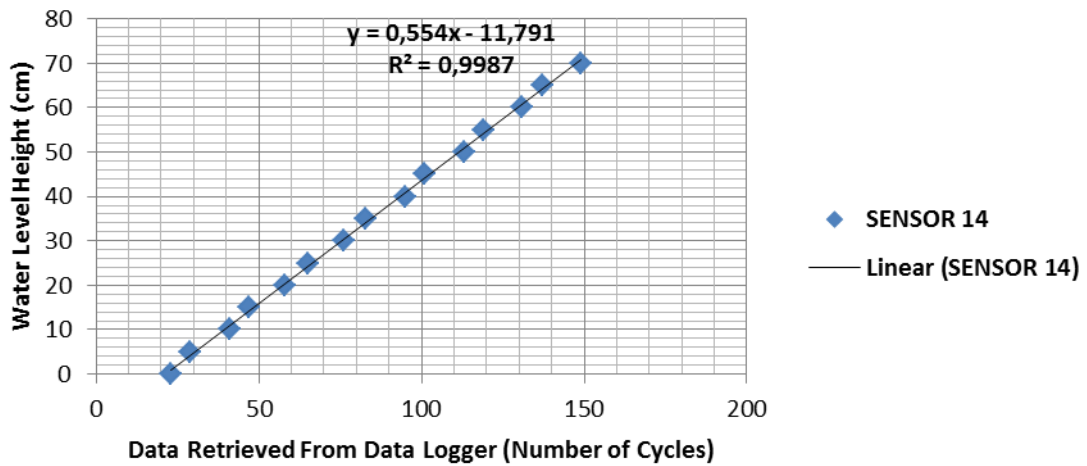


Figure 0.1 - Sensor calibration 11 and 12.

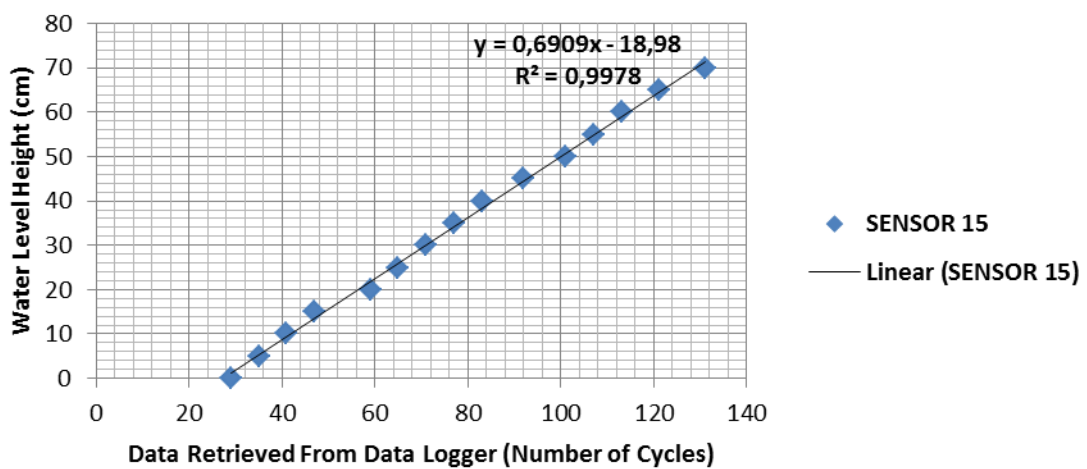
SENSOR 13



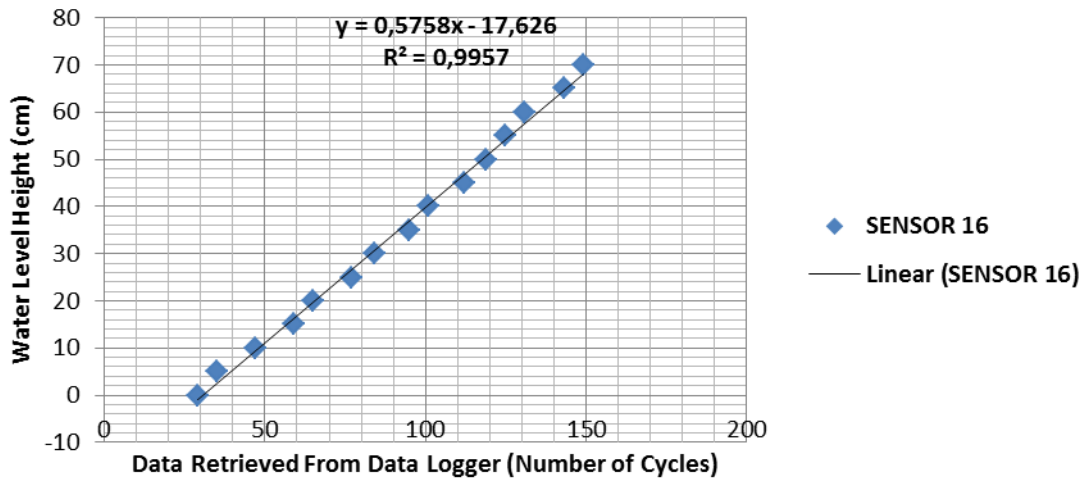
SENSOR 14



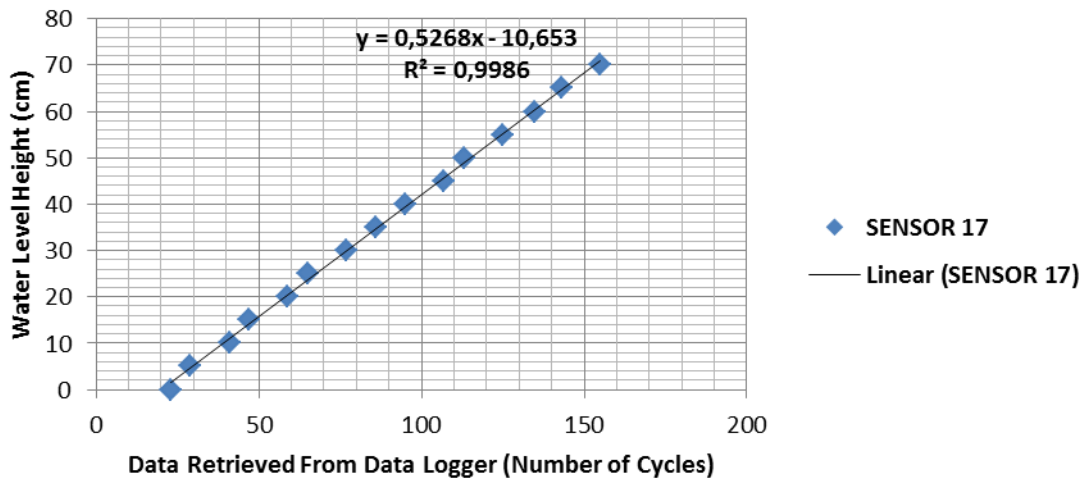
SENSOR 15



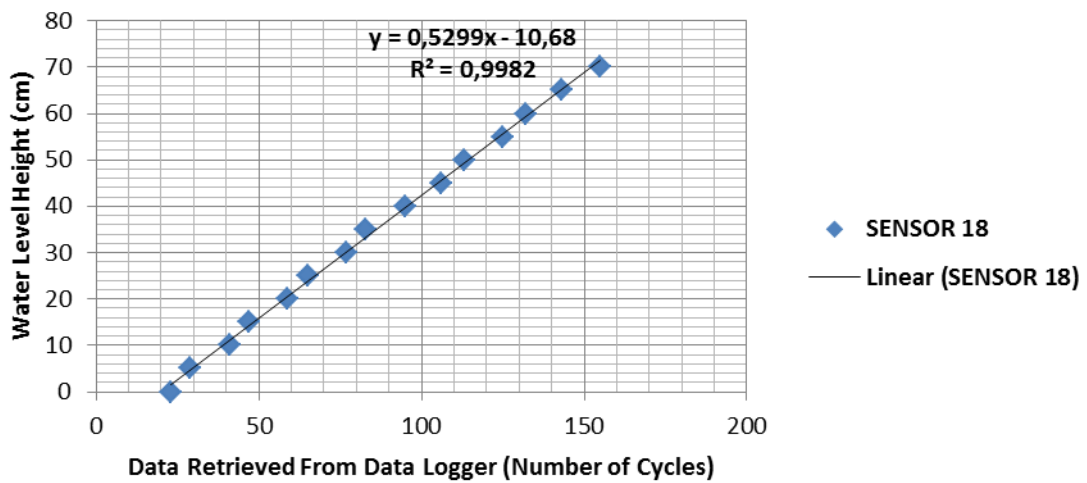
SENSOR 16



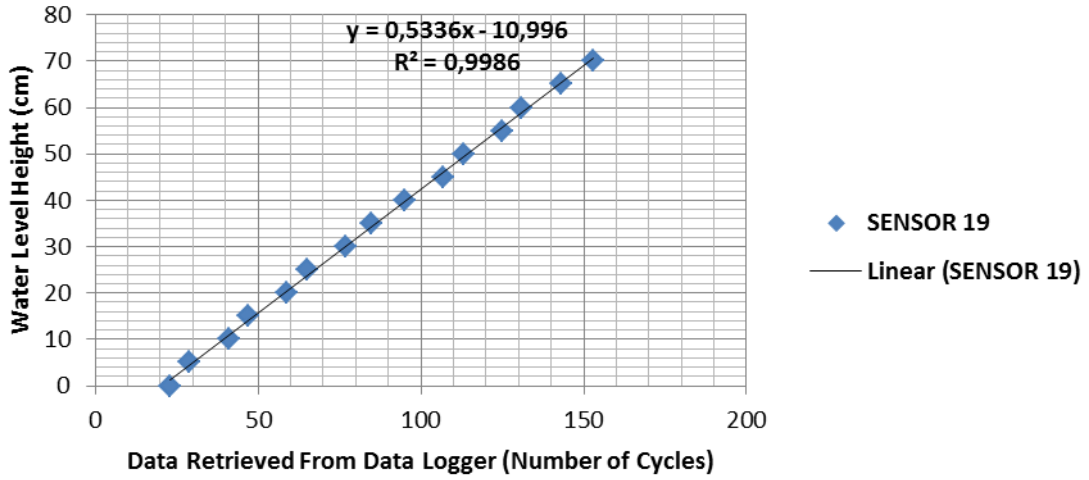
SENSOR 17



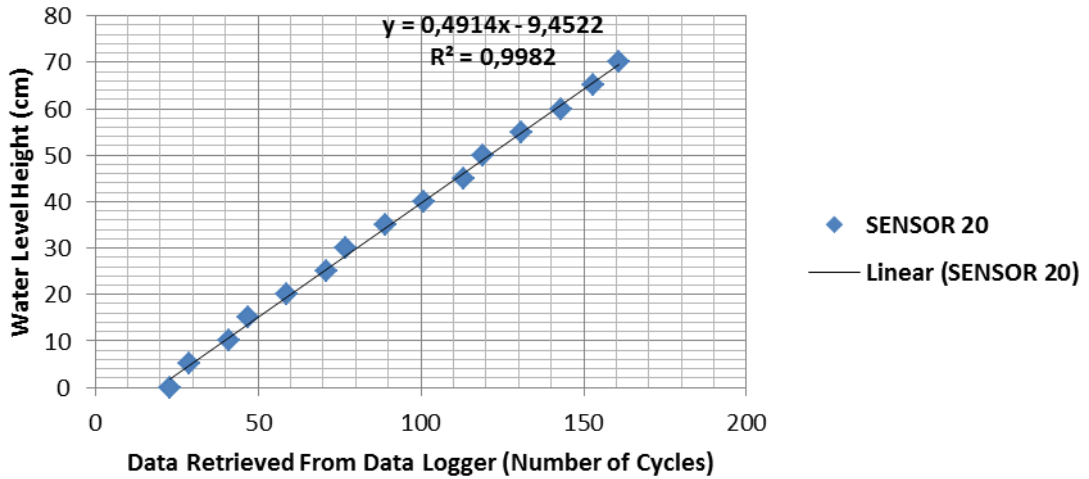
SENSOR 18



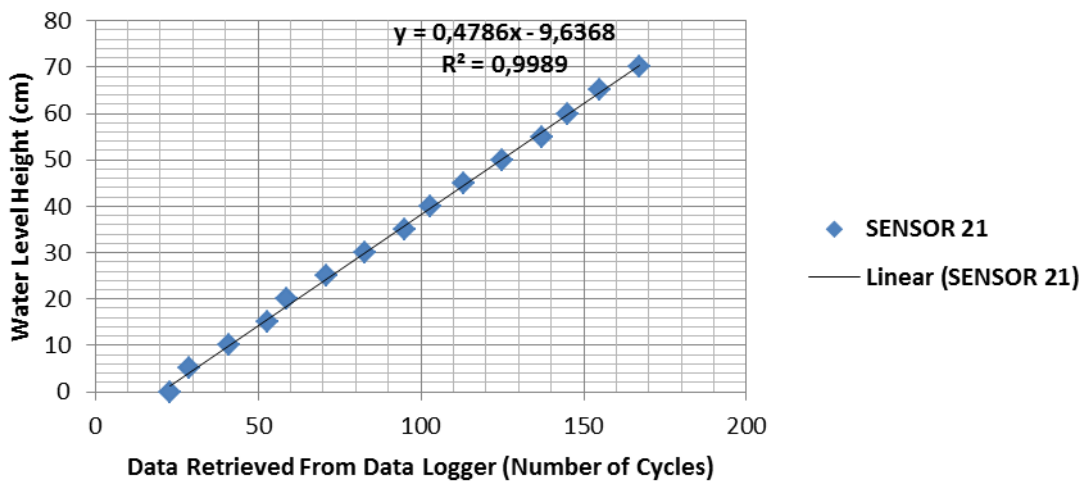
SENSOR 19



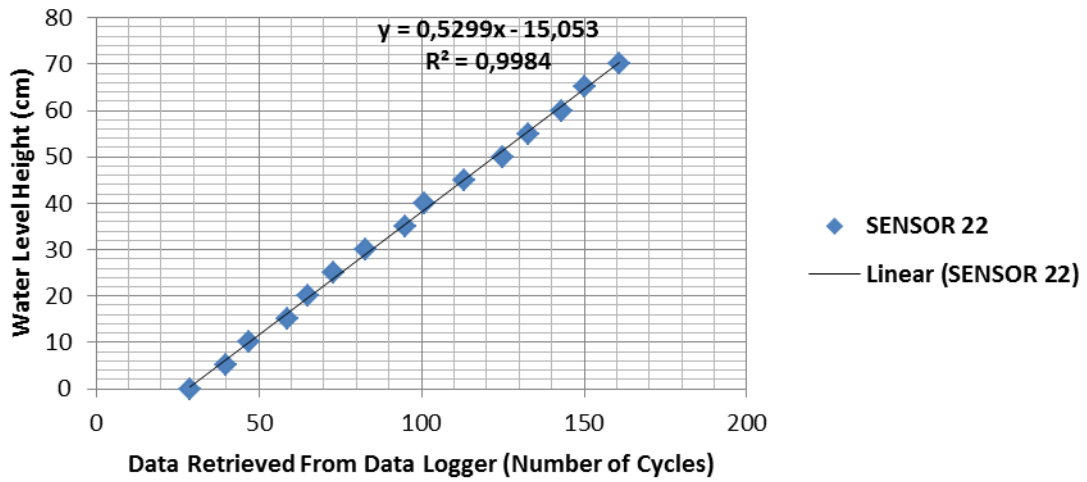
SENSOR 20



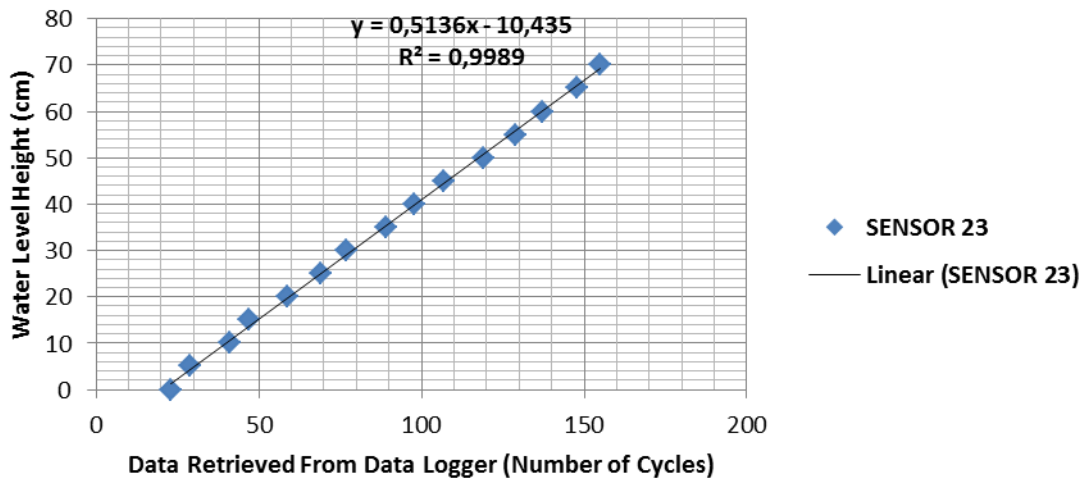
SENSOR 21



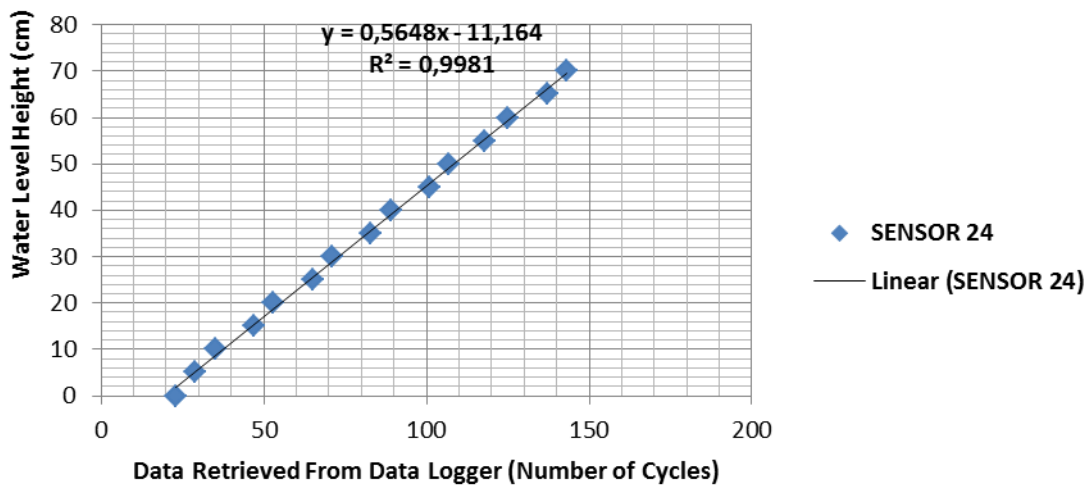
SENSOR 22



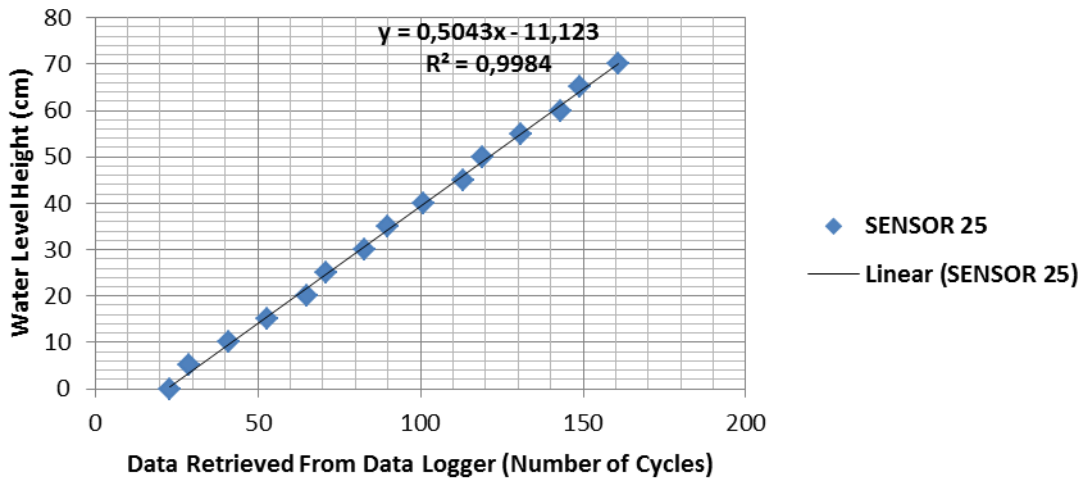
SENSOR 23



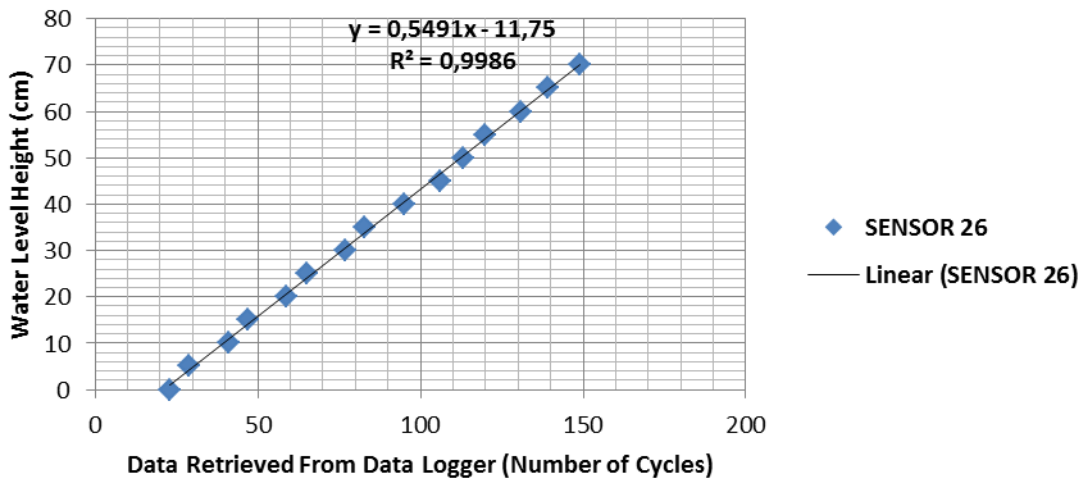
SENSOR 24



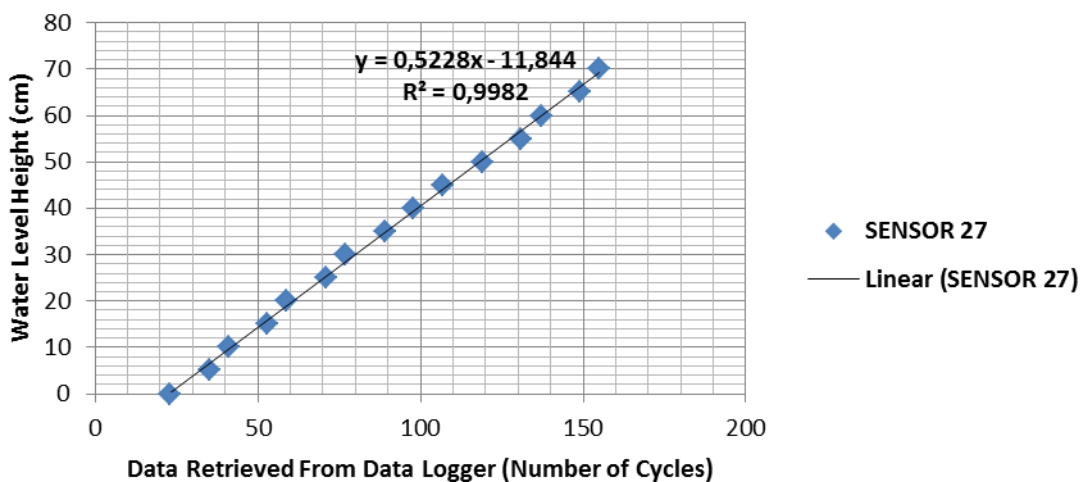
SENSOR 25



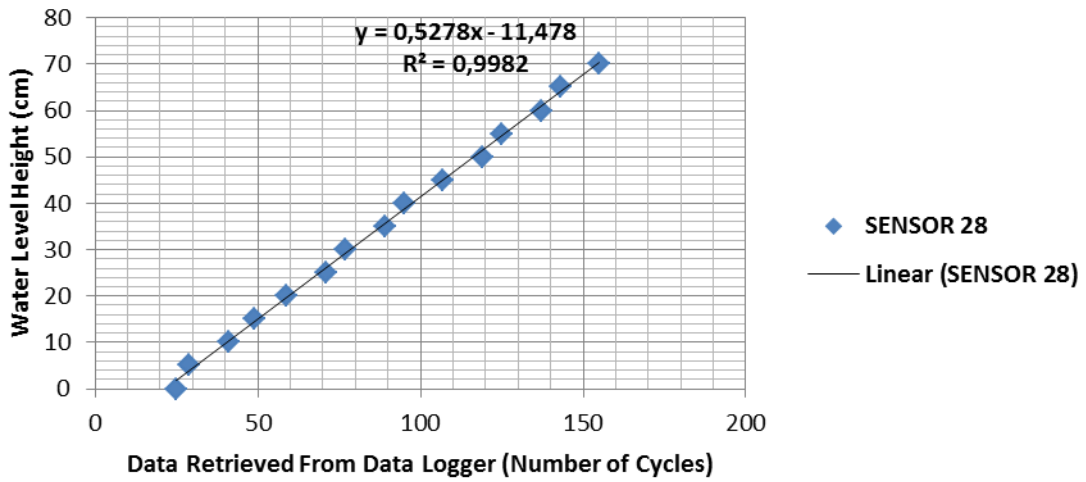
SENSOR 26



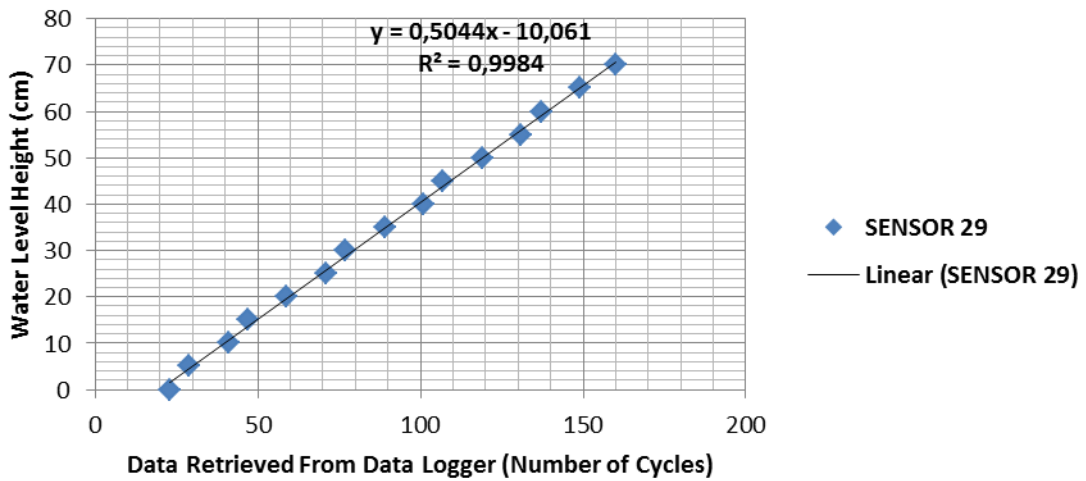
SENSOR 27



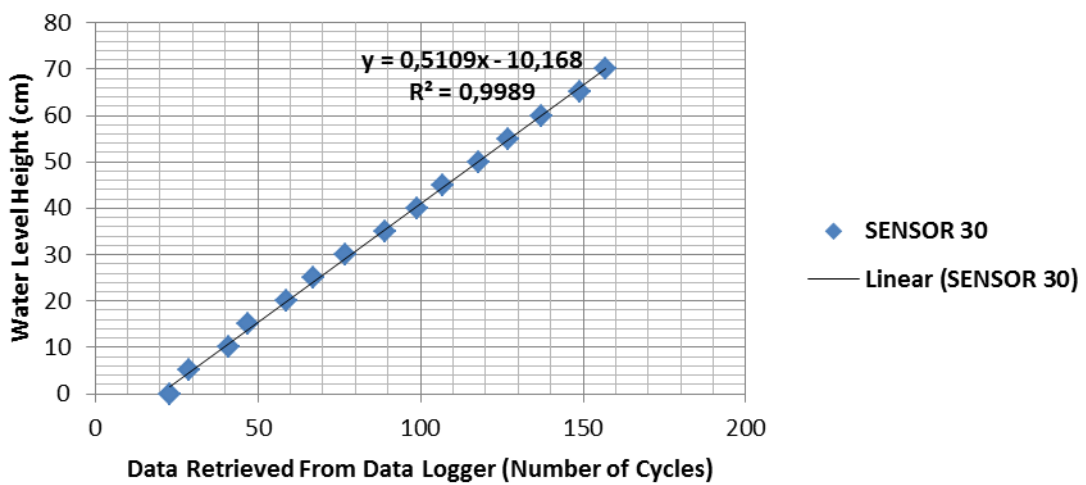
SENSOR 28



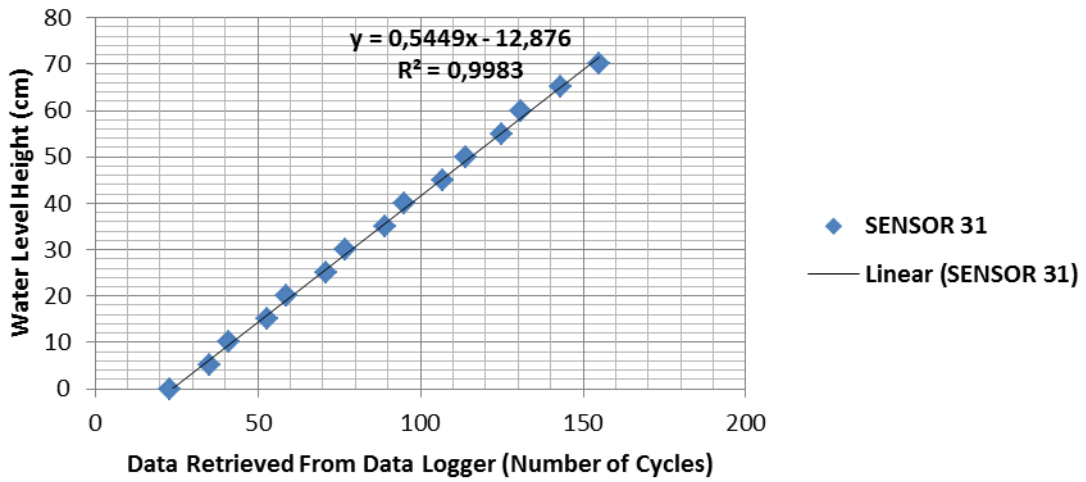
SENSOR 29



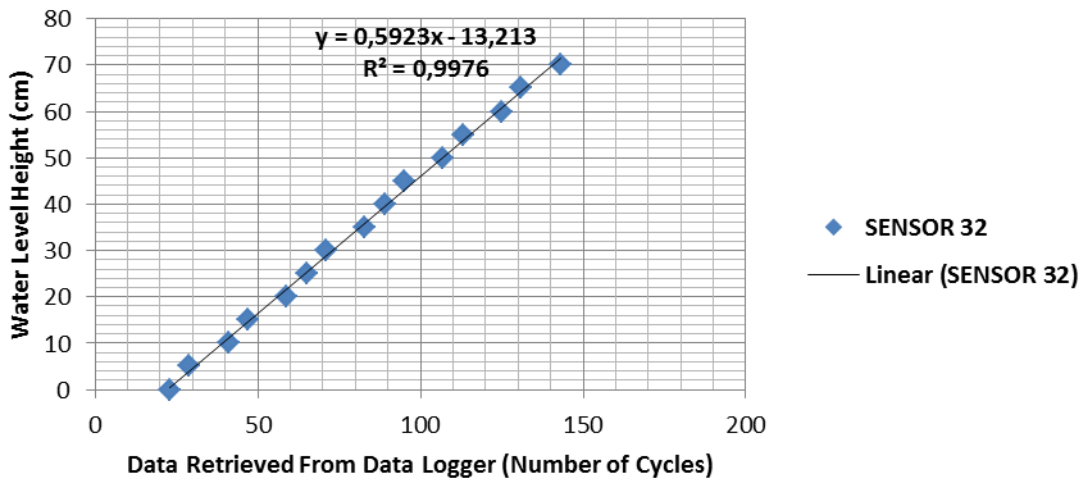
SENSOR 30



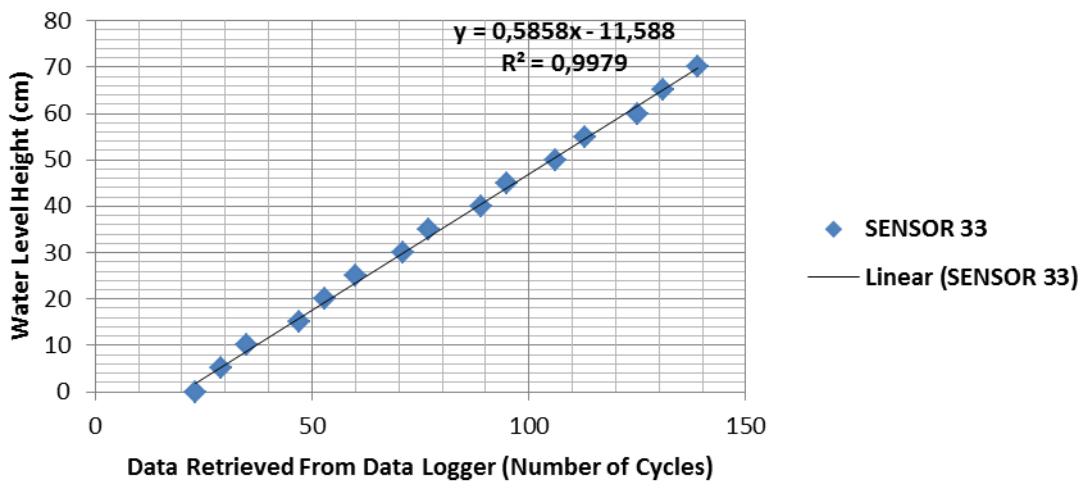
SENSOR 31



SENSOR 32



SENSOR 33



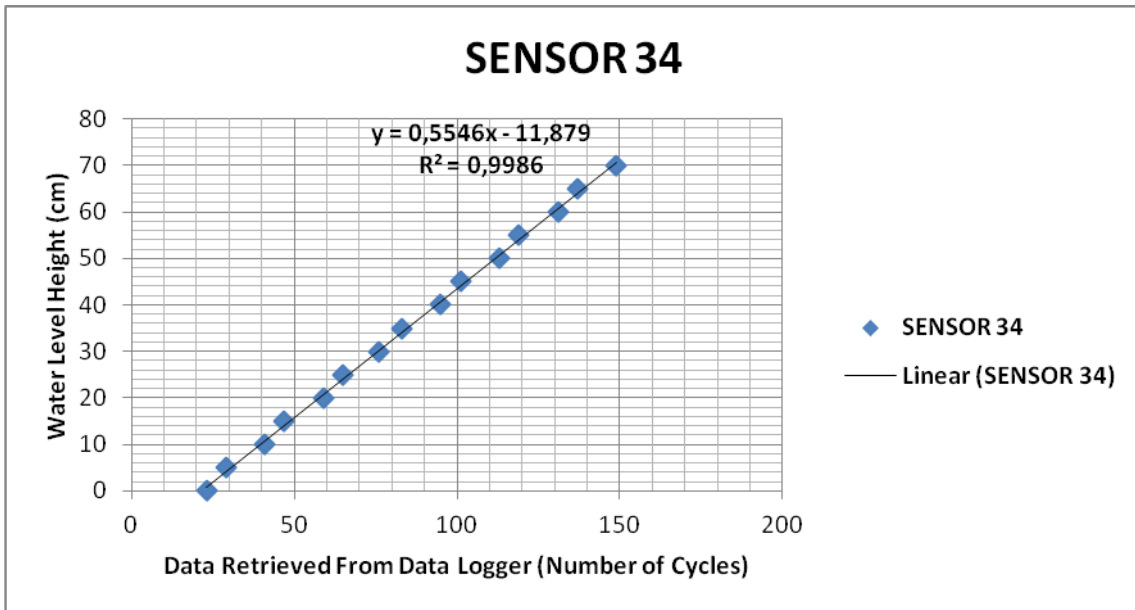


Figure i.1 – Calibration curve for several sensors.

Annex II - Calibration curves for water level and capacitance

Table II.1 - Linear regression results for the water level vs capacitance values for several sensors

Sensor	y	=	m	x	x	+	b
11	Level	=	0.5806	x	Readings	+	-11.601
12	Level	=	0.5335	x	Readings	+	-10.737
13	Level	=	0.6132	x	Readings	+	-11.932
14	Level	=	0.5540	x	Readings	+	-11.791
15	Level	=	0.6909	x	Readings	+	-18.980
16	Level	=	0.5758	x	Readings	+	-17.626
17	Level	=	0.5268	x	Readings	+	-10.653
18	Level	=	0.5299	x	Readings	+	-10.680
19	Level	=	0.5336	x	Readings	+	-10.996
20	Level	=	0.4914	x	Readings	+	-9.4522
21	Level	=	0.4786	x	Readings	+	-9.6368
22	Level	=	0.5299	x	Readings	+	-15.053
23	Level	=	0.5136	x	Readings	+	-10.435
24	Level	=	0.5648	x	Readings	+	-11.164
25	Level	=	0.5043	x	Readings	+	-11.123
26	Level	=	0.5491	x	Readings	+	-11.750
27	Level	=	0.5228	x	Readings	+	-11.844
28	Level	=	0.5278	x	Readings	+	-11.478
29	Level	=	0.5044	x	Readings	+	-10.061
30	Level	=	0.5109	x	Readings	+	-10.168
31	Level	=	0.5449	x	Readings	+	-12.876
32	Level	=	0.5923	x	Readings	+	-13.213
33	Level	=	0.5858	x	Readings	+	-11.588
34	Level	=	0.5546	x	Readings	+	-11.879

Annex III - Results of field work measurement

Table III.1 - Water level data for 11th February (17h30 - 00h00)

A1	B1	C1	D1	E1
103	65	76	71	77
95	65	71	65	77
89	59	65	65	77
83	59	64	65	77
83	59	59	65	77
77	58	59	59	76
77	53	59	59	72
71	53	53	59	71
71	53	53	57	71
71	49	53	53	71
67	47	53	53	71
65	47	53	53	71
65	47	47	53	71
65	47	47	47	71
59	41	47	47	71
59	41	47	47	70
59	41	101	59	71
113	59	101	65	77
113	65	101	70	77
113	65	101	71	77
113	65	89	65	77
113	59	77	59	71
101	53	65	53	71
95	53	53	53	71
77	47	53	53	71
71	47	47	47	71
65	47	47	47	71
65	41	47	47	71
59	41	41	47	65
59	41	41	41	65
59	41	41	41	65
53	35	41	41	65
53	35	41	41	65
53	35	36	41	59
53	35	35	41	59
53	35	35	35	59
47	35	35	35	59

47	33	35	35	59
47	29	35	35	59
47	31	95	41	59
83	41	101	53	71
113	53	101	53	76
113	59	101	59	77
113	59	101	59	76
113	59	95	59	76
113	59	95	59	73
108	59	85	53	71
101	53	71	47	71
89	47	53	47	71
71	47	47	47	71
65	41	41	41	65
59	41	41	41	65
58	35	41	41	65
53	35	35	41	65
53	35	35	41	65
53	35	35	35	59
47	35	35	35	59
47	35	35	35	59
47	29	35	35	59
47	29	35	35	59
47	29	34	35	59
47	35	101	48	71
112	53	101	59	77
113	59	101	65	77
115	65	101	65	77
117	65	95	65	77
119	65	95	65	77
117	65	95	65	77
113	65	89	59	77
107	59	77	53	76
95	53	59	53	72
83	47	53	47	71
71	47	47	47	71
65	41	47	47	71
59	41	41	41	67
59	41	41	41	65
53	41	89	53	76
89	47	101	59	77
113	59	101	60	77

Table III.2 - Water level data for the 12th of February 2012 (17h30 to 00h00).

<i>A1(cm)</i>	<i>B1(cm)</i>	<i>C1(cm)</i>	<i>D1(cm)</i>	<i>E1(cm)</i>
43,2	23,9	34,7	27,5	34,2
38,7	23,9	31,6	24,2	34,2
35,3	20,7	27,9	24,2	34,2
31,9	20,7	27,3	24,2	34,2
31,9	20,7	24,2	24,2	34,2
28,5	20,2	24,2	20,9	33,5
28,5	17,5	24,2	20,9	30,8
25,1	17,5	20,6	20,9	30,1
25,1	17,5	20,6	19,8	30,1
25,1	15,4	20,6	17,6	30,1
22,8	14,3	20,6	17,6	30,1
21,7	14,3	20,6	17,6	30,1
21,7	14,3	16,9	17,6	30,1
21,7	14,3	16,9	14,2	30,1
18,3	11,1	16,9	14,2	30,1
18,3	11,1	16,9	14,2	29,4
18,3	11,1	50,0	20,9	30,1
48,9	20,7	50,0	24,2	34,2
48,9	23,9	50,0	27,0	34,2
48,9	23,9	50,0	27,5	34,2
48,9	23,9	42,6	24,2	34,2
48,9	20,7	35,3	20,9	30,1
42,1	17,5	27,9	17,6	30,1
38,7	17,5	20,6	17,6	30,1
28,5	14,3	20,6	17,6	30,1
25,1	14,3	16,9	14,2	30,1
21,7	14,3	16,9	14,2	30,1
21,7	11,1	16,9	14,2	30,1
18,3	11,1	13,2	14,2	25,9
18,3	11,1	13,2	10,9	25,9
18,3	11,1	13,2	10,9	25,9
14,9	7,9	13,2	10,9	25,9
14,9	7,9	13,2	10,9	25,9
14,9	7,9	10,1	10,9	21,8
14,9	7,9	9,5	10,9	21,8
14,9	7,9	9,5	7,6	21,8
11,5	7,9	9,5	7,6	21,8
11,5	6,9	9,5	7,6	21,8

11,5	4,7	9,5	7,6	21,8
11,5	5,8	46,3	10,9	21,8
31,9	11,1	50,0	17,6	30,1
48,9	17,5	50,0	17,6	33,5
48,9	20,7	50,0	20,9	34,2
48,9	20,7	50,0	20,9	33,5
48,9	20,7	46,3	20,9	33,5
48,9	20,7	46,3	20,9	31,5
46,1	20,7	40,2	17,6	30,1
42,1	17,5	31,6	14,2	30,1
35,3	14,3	20,6	14,2	30,1
25,1	14,3	16,9	14,2	30,1
21,7	11,1	13,2	10,9	25,9
18,3	11,1	13,2	10,9	25,9
17,7	7,9	13,2	10,9	25,9
14,9	7,9	9,5	10,9	25,9
14,9	7,9	9,5	10,9	25,9
14,9	7,9	9,5	7,6	21,8
11,5	7,9	9,5	7,6	21,8
11,5	7,9	9,5	7,6	21,8
11,5	4,7	9,5	7,6	21,8
11,5	4,7	9,5	7,6	21,8
11,5	4,7	8,9	7,6	21,8
11,5	7,9	50,0	14,8	30,1
48,3	17,5	50,0	20,9	34,2
48,9	20,7	50,0	24,2	34,2
50,0	23,9	50,0	24,2	34,2
51,2	23,9	46,3	24,2	34,2
52,3	23,9	46,3	24,2	34,2
51,2	23,9	46,3	24,2	34,2
48,9	23,9	42,6	20,9	34,2
45,5	20,7	35,3	17,6	33,5
38,7	17,5	24,2	17,6	30,8
31,9	14,3	20,6	14,2	30,1
25,1	14,3	16,9	14,2	30,1
21,7	11,1	16,9	14,2	30,1
18,3	11,1	13,2	10,9	27,3
18,3	11,1	13,2	10,9	25,9
14,9	11,1	42,6	17,6	33,5
35,3	14,3	50,0	20,9	34,2
48,9	20,7	50,0	21,4	34,2

Table III.3 - Water level measurements for the first row.

A1(cm)	B1(cm)	C1(cm)	D1(cm)	E1(cm)
54,0	20,7	50,0	21,4	34,2
54,0	23,9	42,6	20,9	34,2
50,5	20,7	35,3	17,6	31,5
45,3	17,5	20,6	14,2	30,1
36,6	14,3	16,9	14,2	30,1
29,6	12,2	16,9	14,2	30,1
26,1	11,1	13,2	10,9	25,9
22,7	11,1	13,2	10,9	25,9
19,2	11,1	13,2	10,9	25,9
19,2	7,9	9,5	10,9	25,9
19,2	7,9	9,5	10,9	25,9
19,2	7,9	9,5	9,3	25,9
15,7	7,9	9,5	7,6	21,8
15,7	7,9	9,5	7,6	21,8
15,7	6,3	9,5	7,6	21,8
15,7	4,7	9,5	7,6	21,8
15,7	4,7	9,5	7,6	21,8
15,7	4,7	5,9	7,6	21,8
12,2	4,7	5,9	7,6	21,8
13,4	4,7	50,0	14,2	25,9
50,5	14,3	50,0	17,6	34,2
54,0	20,7	50,0	20,9	34,2
54,0	20,7	50,0	20,9	34,2
54,0	20,7	39,0	17,6	33,5
48,8	17,5	24,2	14,2	30,1
40,1	14,3	16,9	14,2	30,1
29,6	11,1	13,2	10,9	27,3
26,1	11,1	13,2	10,9	25,9
22,7	11,1	13,2	10,9	25,9
19,2	7,9	9,5	10,9	25,9
19,2	7,9	9,5	7,6	25,9
19,2	7,9	9,5	7,6	25,2
15,7	7,9	9,5	7,6	21,8
15,7	7,9	9,5	7,6	21,8
15,7	4,7	9,5	7,6	21,8
15,7	4,7	5,9	7,6	21,8
15,7	4,7	5,9	7,6	21,8
12,2	4,7	5,9	7,0	21,8

12,2	4,7	5,9	4,3	17,6
12,2	4,7	5,9	4,3	17,6
12,2	4,7	5,9	4,3	17,6
12,2	4,7	5,9	4,3	17,6
12,2	4,7	5,9	4,3	17,6
12,2	1,5	5,9	4,3	17,6
12,2	1,5	5,9	4,3	17,6
12,2	1,5	20,6	4,3	17,6
12,2	4,7	43,9	10,9	21,8
50,5	12,2	45,7	14,2	34,2
50,5	14,3	45,1	14,2	34,2
50,5	17,5	42,6	14,2	34,2
50,5	17,5	42,6	14,8	34,2
50,5	17,5	39,0	14,2	31,5
47,0	14,3	24,2	10,9	30,1
37,2	11,1	16,9	10,9	25,9
26,1	11,1	13,2	10,9	25,9
22,7	7,9	9,5	7,6	25,9
19,2	7,9	9,5	7,6	25,9
19,2	7,9	9,5	7,6	21,8
15,7	7,9	9,5	7,6	21,8
15,7	4,7	9,5	7,6	21,8
15,7	4,7	5,9	7,6	21,8
15,7	4,7	5,9	7,6	21,8
13,4	4,7	5,9	7,0	21,8
12,2	4,7	5,9	4,3	20,4
12,2	4,7	5,9	4,3	17,6
12,2	4,7	5,9	4,3	17,6
12,2	4,7	5,9	4,3	17,6
12,2	4,7	5,9	4,3	17,6
12,2	1,5	5,9	4,3	17,6
12,2	1,5	5,9	4,3	17,6
12,2	1,5	5,9	4,3	17,6
9,9	1,5	2,2	4,3	17,6
8,7	1,5	9,5	4,3	17,6
12,2	4,7	42,6	7,6	21,8
43,6	11,1	42,6	10,9	30,1
50,5	14,3	42,6	14,2	34,2
50,5	14,3	42,6	14,2	34,2
50,5	17,5	42,6	14,2	32,8
47,0	14,3	27,9	10,9	30,1
39,5	11,1	13,2	10,9	25,9

26,1	11,1	9,5	7,6	25,9
22,7	7,9	9,5	7,6	25,9
19,2	7,9	9,5	7,6	22,5
15,7	7,9	9,5	7,6	21,8
15,7	4,7	9,5	7,6	21,8
15,7	4,7	5,9	7,6	21,8
15,7	4,7	5,9	7,6	21,8
12,2	4,7	5,9	4,8	21,8
12,2	4,7	5,9	4,3	21,8
12,2	4,7	5,9	4,3	18,3
12,2	4,7	5,9	4,3	17,6
12,2	4,7	5,9	4,3	17,6
12,2	4,7	5,9	4,3	17,6
12,2	1,5	5,9	4,3	17,6
12,2	1,5	5,9	4,3	17,6
12,2	1,5	5,9	4,3	17,6
11,6	1,5	2,2	4,3	17,6
8,7	1,5	2,2	4,3	17,6
8,7	1,5	2,2	4,3	17,6
11,0	4,7	45,1	10,9	25,9
47,0	11,1	50,0	14,2	34,2
54,0	17,5	50,0	17,6	34,2
54,0	17,5	42,6	14,2	34,2
47,0	14,3	24,2	10,9	30,1
36,6	11,1	13,2	10,9	29,4
26,1	11,1	9,5	10,9	25,9
19,8	7,9	9,5	7,6	25,9
19,2	7,9	9,5	7,6	25,9
15,7	7,9	9,5	7,6	25,9
15,7	7,9	9,5	7,6	23,2
15,7	4,7	5,9	7,6	21,8
15,7	4,7	5,9	7,6	21,8
15,7	4,7	5,9	7,6	21,8
12,2	4,7	5,9	4,3	21,8
12,2	4,7	5,9	4,3	21,8
12,2	4,7	5,9	4,3	17,6
12,2	4,7	5,9	4,3	17,6
12,2	4,7	5,9	4,3	17,6
12,2	4,7	42,6	7,6	21,8
36,6	11,1	42,6	10,9	30,1
50,5	14,3	42,6	14,2	34,2
50,5	17,5	42,6	14,2	34,2

50,5	17,5	42,6	14,2	33,5
50,5	17,5	31,6	10,9	30,1
40,1	14,3	16,9	10,9	25,9
29,6	11,1	13,2	10,9	25,9
22,7	11,1	9,5	10,9	21,8
19,2	7,9	9,5	7,6	21,8
19,2	7,9	9,5	7,6	21,8
15,7	7,9	9,5	7,6	21,8
15,7	7,9	9,5	7,6	17,6
15,7	4,7	5,9	7,6	17,6
15,7	4,7	5,9	7,6	17,6
15,7	4,7	5,9	7,6	17,6
12,2	4,7	5,9	5,9	13,5
12,2	4,7	5,9	7,6	13,5
12,2	4,7	42,6	10,9	17,6
43,6	12,7	46,3	17,6	30,1
54,0	17,5	50,0	17,6	30,1
54,0	20,7	46,3	14,2	30,1
50,5	17,5	31,6	14,2	30,1
43,6	14,3	16,9	10,9	25,9
29,6	11,1	13,2	10,9	25,9
22,7	11,1	13,2	10,9	21,8
20,9	7,9	9,5	10,9	21,8
19,2	7,9	9,5	10,9	21,8
19,2	7,9	9,5	7,6	21,8
15,7	7,9	9,5	7,6	17,6
15,7	7,9	9,5	7,6	17,6
15,7	7,9	9,5	7,6	17,6
15,7	4,7	5,9	7,6	17,6
15,7	7,9	42,6	14,2	21,8
47,0	14,3	50,0	17,6	30,1
54,0	17,5	50,0	17,6	31,5
54,0	20,7	50,0	18,1	31,5
54,0	20,7	42,6	17,6	30,1
50,5	17,5	24,9	14,2	30,1
40,1	14,3	16,9	14,2	27,3
29,6	14,3	13,2	10,9	25,9
22,7	11,1	13,2	10,9	25,9
22,7	11,1	13,2	10,9	21,8
19,2	9,0	9,5	10,9	21,8
19,2	7,9	9,5	10,9	21,8
19,2	7,9	9,5	10,9	21,8

15,7	7,9	9,5	7,6	17,6
15,7	7,9	9,5	7,6	17,6
15,7	7,9	9,5	7,6	17,6
15,7	4,7	9,5	7,6	17,6
15,7	4,7	5,9	7,6	13,5
15,7	4,7	16,9	10,9	17,6
15,7	11,1	46,3	17,6	30,1
54,0	17,5	50,0	20,9	34,2
54,0	20,7	50,0	20,9	34,2
55,7	23,9	45,7	24,2	34,2
57,5	23,9	42,6	24,2	34,2
57,5	23,9	42,6	24,2	34,2
57,5	23,9	42,6	24,2	34,2
57,5	23,9	39,0	20,9	34,2
54,0	20,7	27,9	17,6	33,5
43,6	17,5	20,6	17,6	30,1
33,1	14,3	16,9	14,2	30,1
26,1	14,3	16,9	14,2	27,3
26,1	14,3	13,2	14,2	25,9
22,7	11,1	13,2	14,2	25,9
22,7	11,1	13,2	10,9	21,8
19,2	11,1	13,2	10,9	21,8
19,2	10,6	13,2	10,9	21,8
19,2	7,9	9,5	10,9	21,8
19,2	7,9	9,5	12,6	21,8
19,2	11,1	44,5	17,6	30,1
50,5	17,5	50,0	20,9	34,2
54,0	20,7	46,3	20,9	34,2
54,0	21,3	42,6	22,6	34,2
54,0	23,9	39,0	20,9	33,5
50,5	20,7	24,2	17,6	30,1
43,6	17,5	19,3	14,8	30,1
33,1	14,3	16,9	14,2	30,1
26,1	14,3	13,8	14,2	25,9
22,7	11,1	13,2	14,2	25,9
22,7	11,1	13,2	10,9	21,8
19,2	11,1	13,2	10,9	21,8
19,2	10,6	9,5	10,9	21,8
19,2	7,9	9,5	10,9	21,8
19,2	7,9	9,5	10,9	17,6
15,7	7,9	9,5	8,2	17,6
15,7	7,9	9,5	7,6	17,6

15,7	7,9	9,5	7,6	17,6
15,7	7,9	9,5	7,6	17,6
15,7	4,7	9,5	7,6	17,6
15,7	7,9	27,9	10,9	17,6
15,7	11,1	39,0	14,2	25,9
49,9	14,3	42,6	17,6	30,1
50,5	17,5	42,6	17,6	30,1
50,5	17,5	42,6	17,6	30,1
50,5	17,5	39,0	17,6	30,1
50,5	17,5	39,0	17,6	30,1
50,5	17,5	35,3	14,2	30,1
43,6	14,3	20,6	14,2	30,1
33,1	14,3	16,9	14,2	25,9
26,1	11,1	13,2	10,9	25,9
22,7	11,1	13,2	10,9	21,8
19,2	11,1	11,4	10,9	21,8
19,2	7,9	9,5	10,9	21,8
19,2	7,9	9,5	10,9	21,8
16,8	7,9	9,5	7,6	21,8
15,7	7,9	9,5	7,6	21,8
15,7	7,9	9,5	7,6	21,8
15,7	7,9	9,5	7,6	17,6
15,7	4,7	9,5	7,6	17,6
15,7	4,7	5,9	7,6	17,6
15,7	4,7	24,2	8,7	18,3
15,7	11,1	40,2	10,9	25,9
47,0	14,3	42,0	14,2	30,1
50,5	14,3	39,0	14,2	30,1
49,9	17,5	39,0	14,2	30,1
48,2	17,5	39,0	14,2	30,1
47,0	17,5	35,3	14,2	30,1
47,0	15,4	31,6	14,2	30,1
40,1	14,3	16,9	10,9	25,9
29,6	11,1	13,2	10,9	21,8
22,7	11,1	13,2	10,9	21,8
19,2	7,9	9,5	10,9	21,8
19,2	7,9	9,5	10,9	21,8
19,2	7,9	9,5	7,6	21,8
15,7	7,9	9,5	7,6	21,8
15,7	7,9	9,5	7,6	21,8
15,7	7,9	9,5	7,6	20,4
15,7	4,7	9,5	7,6	17,6

15,7	4,7	5,9	7,6	17,6
12,8	4,7	5,9	7,6	17,6
12,2	4,7	5,9	4,8	17,6
12,2	4,7	5,9	4,8	17,6
12,2	4,7	31,6	10,9	21,1
15,7	11,1	42,6	14,2	30,1
50,5	16,5	46,3	17,6	30,1
54,0	17,5	42,6	14,2	30,1
50,5	17,5	29,2	14,2	30,1
40,1	14,3	16,9	10,9	25,9
26,1	11,1	13,2	10,9	25,9
22,7	11,1	13,2	10,9	21,8
19,2	7,9	9,5	10,9	21,8
19,2	7,9	9,5	7,6	21,8
15,7	7,9	9,5	7,6	21,8
15,7	7,9	9,5	7,6	21,8
15,7	7,9	9,5	7,6	21,8
15,7	4,7	9,5	7,6	17,6
15,7	4,7	5,9	7,6	17,6
12,2	4,7	5,9	7,6	17,6
12,2	4,7	5,9	4,3	17,6
12,2	4,7	5,9	4,3	17,6
12,2	4,7	5,9	4,3	17,6
12,2	4,7	5,9	4,3	17,6
12,2	4,7	5,9	4,3	17,6
12,2	4,7	39,0	8,2	21,8
36,6	11,1	42,6	14,2	30,1
50,5	14,3	42,6	14,2	31,5
50,5	17,5	42,6	17,6	33,5
52,3	17,5	42,6	17,6	33,5
54,0	17,5	42,6	17,6	33,5
54,0	20,7	42,6	17,6	30,1
53,4	20,7	42,6	17,6	30,1
52,8	20,7	42,6	17,6	30,1
50,5	20,7	42,6	17,6	30,1
50,5	20,7	42,6	17,6	30,1
50,5	20,7	39,0	17,6	30,1
50,5	17,5	39,0	17,6	30,1
47,0	17,5	27,9	14,2	30,1
40,1	14,3	16,9	14,2	30,1
29,6	14,3	16,9	14,2	25,9

Table III.4 - Water level measurements for the second row

A2(cm)	B2(cm)	C2(cm)	D2(cm)	E2(cm)
18,1	14,1	14,2	13,5	0,0
19,8	14,1	17,4	14,1	0,0
21,0	14,1	14,2	16,2	0,0
19,8	14,1	14,2	14,1	0,0
19,8	14,1	14,2	14,1	0,0
16,3	10,9	11,0	10,9	0,0
16,3	10,9	11,0	10,9	0,0
16,3	10,9	11,0	10,9	0,0
12,9	10,9	11,0	10,9	0,0
12,9	7,8	11,0	10,9	0,0
12,9	7,8	7,9	7,7	0,0
12,9	7,8	7,9	7,7	0,0
12,9	7,8	7,9	7,7	0,0
9,4	7,8	7,9	7,7	0,0
9,4	7,8	7,9	7,7	0,0
9,4	7,8	7,9	7,7	0,0
9,4	4,6	7,9	7,7	0,0
9,4	4,6	7,9	7,7	0,0
9,4	4,6	6,3	7,7	0,0
9,4	4,6	7,9	4,5	0,0
9,4	7,8	11,0	7,7	0,0
16,3	10,9	11,0	7,7	0,0
19,8	14,1	14,2	10,9	0,0
19,8	14,1	14,2	14,1	0,0
19,8	14,1	14,2	14,1	0,0
16,3	10,9	11,0	10,9	0,0
16,3	10,9	11,0	10,9	0,0
15,2	10,9	11,0	10,9	0,0
12,9	7,8	11,0	10,9	0,0
12,9	7,8	7,9	7,7	0,0
12,9	7,8	7,9	7,7	0,0
9,4	7,8	7,9	7,7	0,0
9,4	7,8	7,9	7,7	0,0
9,4	7,8	7,9	7,7	0,0
9,4	4,6	7,9	7,7	0,0
9,4	4,6	7,9	7,7	0,0
9,4	4,6	4,7	7,7	0,0
9,4	4,6	4,7	4,5	0,0

6,0	4,6	4,7	4,5	0,0
6,0	4,6	4,7	4,5	0,0
6,0	4,6	4,7	4,5	0,0
6,0	4,6	4,7	4,5	0,0
6,0	4,6	4,7	4,5	0,0
6,0	4,6	4,7	4,5	0,0
6,0	4,6	4,7	4,5	0,0
6,0	4,6	4,7	4,5	0,0
6,0	4,6	4,7	4,5	0,0
6,0	4,6	7,9	4,5	0,0
12,9	7,8	7,9	4,5	0,0
12,9	10,9	11,0	7,7	0,0
16,3	10,9	11,0	9,3	0,0
16,3	10,9	11,0	10,9	0,0
16,3	10,9	11,0	10,9	0,0
16,3	10,9	11,0	10,9	0,0
12,9	7,8	8,4	7,7	0,0
12,9	7,8	7,9	7,7	0,0
12,9	7,8	7,9	7,7	0,0
9,4	7,8	7,9	7,7	0,0
9,4	7,8	7,9	7,7	0,0
9,4	4,6	7,9	7,7	0,0
9,4	4,6	7,9	7,7	0,0
9,4	4,6	4,7	4,5	0,0
9,4	4,6	4,7	4,5	0,0
6,0	4,6	4,7	4,5	0,0
6,0	4,6	4,7	4,5	0,0
6,0	4,6	4,7	4,5	0,0
6,0	4,6	4,7	4,5	0,0
6,0	4,6	4,7	4,5	0,0
6,0	4,6	4,7	4,5	0,0
6,0	4,6	4,7	4,5	0,0
6,0	4,6	4,7	4,5	0,0
6,0	1,5	4,7	4,5	0,0
6,0	1,5	4,7	4,5	0,0
6,0	1,5	4,7	4,5	0,0
6,0	4,6	4,7	4,5	0,0
6,0	4,6	4,7	4,5	0,0
9,4	7,8	7,9	4,5	0,0
12,9	7,8	7,9	7,7	0,0
12,9	10,9	11,0	7,7	0,0
15,2	10,9	11,0	9,3	0,0
12,9	8,3	7,9	7,7	0,0

12,9	7,8	7,9	7,7	0,0
12,9	7,8	7,9	7,7	0,0
9,4	7,8	7,9	7,7	0,0
9,4	7,3	7,9	7,7	0,0
9,4	4,6	7,9	7,7	0,0
9,4	4,6	4,7	4,5	0,0
9,4	4,6	4,7	4,5	0,0
6,0	4,6	4,7	4,5	0,0
6,0	4,6	4,7	4,5	0,0
6,0	4,6	4,7	4,5	0,0
6,0	4,6	4,7	4,5	0,0
6,0	4,6	4,7	4,5	0,0
6,0	4,6	4,7	4,5	0,0
6,0	4,6	4,7	4,5	0,0
6,0	4,6	4,7	4,5	0,0
6,0	1,5	4,7	4,5	0,0
6,0	1,5	4,7	4,5	0,0
6,0	1,5	1,5	4,5	0,0
6,0	1,5	1,5	3,4	0,0
6,0	1,5	4,7	2,3	0,0
6,0	4,6	7,9	4,5	0,0
9,4	7,8	7,9	4,5	0,0
14,0	10,9	11,0	7,7	0,0
16,3	10,9	11,0	10,9	0,0
12,9	9,9	7,9	10,9	0,0
12,9	7,8	7,9	7,7	0,0
12,9	7,8	7,9	7,7	0,0
9,4	7,8	7,9	7,7	0,0
9,4	7,3	7,9	7,7	0,0
9,4	4,6	7,9	7,7	0,0
9,4	4,6	4,7	7,7	0,0
9,4	4,6	4,7	4,5	0,0
9,4	4,6	4,7	4,5	0,0
6,0	4,6	4,7	4,5	0,0
6,0	4,6	4,7	4,5	0,0
6,0	4,6	4,7	4,5	0,0
6,0	4,6	4,7	4,5	0,0
6,0	4,6	4,7	4,5	0,0
6,0	4,6	4,7	4,5	0,0
6,0	4,6	7,9	4,5	0,0
9,4	7,8	7,9	4,5	0,0
12,9	10,9	11,0	7,7	0,0

16,3	10,9	11,0	7,7	0,0
16,3	10,9	11,0	10,9	0,0
16,3	10,9	11,0	10,9	0,0
12,9	10,9	7,9	10,3	0,0
12,9	7,8	7,9	7,7	0,0
12,9	7,8	7,9	7,7	0,0
9,4	7,8	7,9	7,7	0,0
9,4	7,8	7,9	7,7	0,0
9,4	7,8	7,9	7,7	0,0
9,4	7,3	4,7	7,7	0,0
9,4	4,6	4,7	7,7	0,0
9,4	4,6	4,7	4,5	0,0
9,4	4,6	4,7	4,5	0,0
7,1	4,6	4,7	4,5	0,0
6,0	4,6	4,7	4,5	0,0
9,4	7,8	7,9	4,5	0,0
12,9	10,9	11,0	7,7	0,0
16,3	14,1	11,0	10,9	0,0
19,8	14,1	11,0	10,9	0,0
16,3	10,9	11,0	10,9	0,0
16,3	10,9	10,5	10,9	0,0
12,9	10,9	7,9	10,9	0,0
12,9	7,8	7,9	7,7	0,0
12,9	7,8	7,9	7,7	0,0
12,9	7,8	7,9	7,7	0,0
9,4	7,8	7,9	7,7	0,0
9,4	7,8	4,7	7,7	0,0
9,4	7,8	4,7	7,7	0,0
9,4	4,6	4,7	7,7	0,0
9,4	7,8	7,9	7,7	0,0
9,4	7,8	7,9	7,7	0,0
16,3	10,9	11,0	7,7	0,0
19,8	14,1	14,2	10,9	0,0
19,8	14,1	14,2	13,5	0,0
19,8	14,1	14,2	14,1	0,0
19,8	14,1	11,0	10,9	0,0
16,3	10,9	11,0	10,9	0,0
16,3	10,9	11,0	10,9	0,0
12,9	10,9	7,9	10,9	0,0
12,9	8,8	7,9	10,9	0,0
12,9	7,8	7,9	7,7	0,0
12,9	7,8	7,9	7,7	0,0

12,9	7,8	7,9	7,7	0,0
9,4	7,8	7,9	7,7	0,0
9,4	7,8	7,9	7,7	0,0
9,4	7,8	4,7	7,7	0,0
9,4	7,3	4,7	7,7	0,0
9,4	4,6	4,7	7,7	0,0
9,4	7,8	7,9	7,7	0,0
12,9	10,9	11,0	7,7	0,0
16,3	14,1	12,6	10,9	0,0
19,8	14,1	14,2	10,9	0,0
23,3	14,1	14,2	14,1	0,0
23,3	17,3	16,3	17,3	0,0
23,3	17,3	17,4	17,3	0,0
26,1	17,3	17,4	17,3	0,0
23,8	17,3	17,4	17,3	0,0
23,3	17,3	14,2	17,3	0,0
19,8	14,1	14,2	14,1	0,0
19,8	14,1	14,2	14,1	0,0
19,2	14,1	11,0	14,1	0,0
16,3	10,9	11,0	10,9	0,0
16,3	10,9	11,0	10,9	0,0
16,3	10,9	11,0	10,9	0,0
12,9	10,9	10,5	10,9	0,0
12,9	10,9	7,9	10,9	0,0
12,9	7,8	7,9	10,9	0,0
12,9	10,9	11,0	7,7	0,0
15,2	10,9	11,0	10,9	0,0
19,8	14,1	14,2	10,9	0,0
23,3	14,1	14,2	14,1	0,0
23,3	17,3	14,2	14,1	0,0
23,3	15,2	14,2	14,1	0,0
21,0	14,1	14,2	14,1	0,0
19,8	14,1	13,7	14,1	0,0
19,8	14,1	11,0	14,1	0,0
16,3	10,9	11,0	10,9	0,0
16,3	10,9	11,0	10,9	0,0
16,3	10,9	11,0	10,9	0,0
12,9	10,9	7,9	10,9	0,0
12,9	7,8	7,9	10,9	0,0
12,9	7,8	7,9	9,8	0,0
12,9	7,8	7,9	7,7	0,0
12,9	7,8	7,9	7,7	0,0

12,9	7,8	7,9	7,7	0,0
9,4	7,8	7,9	7,7	0,0
9,4	7,8	7,9	7,7	0,0
9,4	7,8	7,9	7,7	0,0
9,4	7,8	7,9	7,7	0,0
12,9	10,9	7,9	7,7	0,0
16,3	10,9	11,0	10,9	0,0
19,2	14,1	11,0	10,9	0,0
19,8	14,1	11,0	10,9	0,0
19,8	14,1	14,2	13,5	0,0
19,8	14,1	14,2	14,1	0,0
19,8	14,1	11,0	14,1	0,0
16,3	10,9	11,0	10,9	0,0
16,3	10,9	11,0	10,9	0,0
16,3	10,9	11,0	10,9	0,0
12,9	10,9	7,9	10,9	0,0
12,9	7,8	7,9	10,9	0,0
12,9	7,8	7,9	7,7	0,0
12,9	7,8	7,9	7,7	0,0
12,9	7,8	7,9	7,7	0,0
9,4	7,8	7,9	7,7	0,0
9,4	7,8	7,9	7,7	0,0
9,4	7,8	7,3	7,7	0,0
9,4	4,6	4,7	7,7	0,0
9,4	4,6	7,9	7,7	0,0
9,4	7,8	7,9	7,7	0,0
9,4	7,8	7,9	7,7	0,0
12,9	10,9	11,0	7,7	0,0
16,3	10,9	11,0	10,9	0,0
16,3	10,9	11,0	10,9	0,0
16,3	10,9	11,0	10,9	0,0
16,3	10,9	11,0	10,9	0,0
16,3	10,9	11,0	10,9	0,0
16,3	10,9	11,0	10,9	0,0
12,9	7,8	7,9	10,9	0,0
12,9	7,8	7,9	7,7	0,0
12,9	7,8	7,9	7,7	0,0
12,9	7,8	7,9	7,7	0,0
9,4	7,8	7,9	7,7	0,0
9,4	7,8	7,9	7,7	0,0
9,4	7,8	7,9	7,7	0,0
9,4	4,6	4,7	7,7	0,0

9,4	4,6	4,7	7,7	0,0
9,4	4,6	4,7	4,5	0,0
9,4	4,6	4,7	4,5	0,0
9,4	4,6	4,7	4,5	0,0
9,4	4,6	4,7	4,5	0,0
9,4	4,6	7,9	4,5	0,0
12,9	7,8	7,9	7,7	0,0
16,3	10,9	11,0	7,7	0,0
16,3	10,9	11,0	10,9	0,0
16,3	10,9	11,0	10,9	0,0
13,5	10,9	7,9	10,9	0,0
12,9	7,8	7,9	7,7	0,0
12,9	7,8	7,9	7,7	0,0
12,9	7,8	7,9	7,7	0,0
9,4	7,8	7,9	7,7	0,0
9,4	7,8	7,9	7,7	0,0
9,4	4,6	7,9	7,7	0,0
9,4	4,6	4,7	7,7	0,0
9,4	4,6	4,7	4,5	0,0
9,4	4,6	4,7	4,5	0,0
9,4	4,6	4,7	4,5	0,0
9,4	4,6	4,7	4,5	0,0
6,0	4,6	4,7	4,5	0,0
6,0	4,6	4,7	4,5	0,0
6,0	4,6	4,7	4,5	0,0
6,0	4,6	4,7	4,5	0,0
9,4	4,6	7,9	4,5	0,0
9,4	7,8	7,9	4,5	0,0
12,9	10,9	11,0	7,7	0,0
16,3	10,9	11,0	10,9	0,0
16,3	14,1	13,7	10,9	0,0
19,8	14,1	14,2	10,9	0,0
19,8	14,1	14,2	14,1	0,0
19,8	14,1	14,2	14,1	0,0
19,8	14,1	14,2	14,1	0,0
19,8	14,1	14,2	14,1	0,0
19,8	14,1	14,2	14,1	0,0
19,8	14,1	14,2	14,1	0,0
19,8	14,1	14,2	14,1	0,0
19,8	14,1	14,2	14,1	0,0
19,8	14,1	14,2	14,1	0,0
19,8	14,1	14,2	14,1	0,0
16,3	10,9	11,0	10,9	0,0

Table III.5 - Water level measurements for the third row

<i>A3(cm)</i>	<i>B3(cm)</i>	<i>C3(cm)</i>	<i>D3(cm)</i>	<i>E3(cm)</i>
0,0	0,0	0,0	0,0	12,6
0,0	0,0	0,0	0,0	15,6
0,0	0,0	0,0	0,0	15,6
0,0	0,0	0,0	0,0	15,6
0,0	0,0	0,0	0,0	15,6
0,0	0,0	0,0	0,0	15,6
0,0	0,0	0,0	0,0	12,6
0,0	0,0	0,0	0,0	12,6
0,0	0,0	0,0	0,0	12,6
0,0	0,0	0,0	0,0	12,6
0,0	0,0	0,0	0,0	12,6
0,0	0,0	0,0	0,0	10,6
0,0	0,0	0,0	0,0	9,6
0,0	0,0	0,0	0,0	9,6
0,0	0,0	0,0	0,0	9,6
0,0	0,0	0,0	0,0	9,6
0,0	0,0	0,0	0,0	9,6
0,0	0,0	0,0	0,0	9,6
0,0	0,0	0,0	0,0	9,6
0,0	0,0	0,0	0,0	9,6
0,0	0,0	0,0	0,0	9,6
0,0	0,0	0,0	0,0	12,6
0,0	0,0	0,0	0,0	12,6
0,0	0,0	0,0	0,0	15,6
0,0	0,0	0,0	0,0	15,6
0,0	0,0	0,0	0,0	12,6
0,0	0,0	0,0	0,0	12,6
0,0	0,0	0,0	0,0	12,6
0,0	0,0	0,0	0,0	12,6
0,0	0,0	0,0	0,0	12,6
0,0	0,0	0,0	0,0	12,1
0,0	0,0	0,0	0,0	9,6
0,0	0,0	0,0	0,0	9,6
0,0	0,0	0,0	0,0	9,6
0,0	0,0	0,0	0,0	9,6
0,0	0,0	0,0	0,0	9,6
0,0	0,0	0,0	0,0	9,6
0,0	0,0	0,0	0,0	9,6
0,0	0,0	0,0	0,0	8,0

0,0	0,0	0,0	0,0	6,5
0,0	0,0	0,0	0,0	6,5
0,0	0,0	0,0	0,0	6,5
0,0	0,0	0,0	0,0	6,5
0,0	0,0	0,0	0,0	6,5
0,0	0,0	0,0	0,0	6,5
0,0	0,0	0,0	0,0	6,5
0,0	0,0	0,0	0,0	6,5
0,0	0,0	0,0	0,0	6,5
0,0	0,0	0,0	0,0	6,5
0,0	0,0	0,0	0,0	6,5
0,0	0,0	0,0	0,0	9,6
0,0	0,0	0,0	0,0	9,6
0,0	0,0	0,0	0,0	12,6
0,0	0,0	0,0	0,0	12,6
0,0	0,0	0,0	0,0	12,6
0,0	0,0	0,0	0,0	12,6
0,0	0,0	0,0	0,0	9,6
0,0	0,0	0,0	0,0	9,6
0,0	0,0	0,0	0,0	9,6
0,0	0,0	0,0	0,0	9,6
0,0	0,0	0,0	0,0	9,6
0,0	0,0	0,0	0,0	9,6
0,0	0,0	0,0	0,0	9,6
0,0	0,0	0,0	0,0	7,5
0,0	0,0	0,0	0,0	6,5
0,0	0,0	0,0	0,0	6,5
0,0	0,0	0,0	0,0	6,5
0,0	0,0	0,0	0,0	6,5
0,0	0,0	0,0	0,0	6,5
0,0	0,0	0,0	0,0	6,5
0,0	0,0	0,0	0,0	6,5
0,0	0,0	0,0	0,0	6,5
0,0	0,0	0,0	0,0	6,5
0,0	0,0	0,0	0,0	6,5
0,0	0,0	0,0	0,0	3,5
0,0	0,0	0,0	0,0	3,5
0,0	0,0	0,0	0,0	6,5
0,0	0,0	0,0	0,0	6,5
0,0	0,0	0,0	0,0	6,5
0,0	0,0	0,0	0,0	9,6
0,0	0,0	0,0	0,0	9,6
0,0	0,0	0,0	0,0	9,6

0,0	0,0	0,0	0,0	9,6
0,0	0,0	0,0	0,0	9,6
0,0	0,0	0,0	0,0	9,6
0,0	0,0	0,0	0,0	9,6
0,0	0,0	0,0	0,0	9,6
0,0	0,0	0,0	0,0	8,0
0,0	0,0	0,0	0,0	6,5
0,0	0,0	0,0	0,0	6,5
0,0	0,0	0,0	0,0	6,5
0,0	0,0	0,0	0,0	6,5
0,0	0,0	0,0	0,0	6,5
0,0	0,0	0,0	0,0	6,5
0,0	0,0	0,0	0,0	6,5
0,0	0,0	0,0	0,0	6,5
0,0	0,0	0,0	0,0	6,5
0,0	0,0	0,0	0,0	6,5
0,0	0,0	0,0	0,0	6,5
0,0	0,0	0,0	0,0	3,5
0,0	0,0	0,0	0,0	3,5
0,0	0,0	0,0	0,0	3,5
0,0	0,0	0,0	0,0	3,5
0,0	0,0	0,0	0,0	6,5
0,0	0,0	0,0	0,0	9,6
0,0	0,0	0,0	0,0	9,6
0,0	0,0	0,0	0,0	12,6
0,0	0,0	0,0	0,0	11,1
0,0	0,0	0,0	0,0	9,6
0,0	0,0	0,0	0,0	9,6
0,0	0,0	0,0	0,0	9,6
0,0	0,0	0,0	0,0	9,6
0,0	0,0	0,0	0,0	6,5
0,0	0,0	0,0	0,0	6,5
0,0	0,0	0,0	0,0	6,5
0,0	0,0	0,0	0,0	6,5
0,0	0,0	0,0	0,0	6,5
0,0	0,0	0,0	0,0	6,5
0,0	0,0	0,0	0,0	6,5
0,0	0,0	0,0	0,0	6,5
0,0	0,0	0,0	0,0	6,5
0,0	0,0	0,0	0,0	6,5
0,0	0,0	0,0	0,0	9,6

0,0	0,0	0,0	0,0	9,6
0,0	0,0	0,0	0,0	12,6
0,0	0,0	0,0	0,0	12,6
0,0	0,0	0,0	0,0	12,6
0,0	0,0	0,0	0,0	12,6
0,0	0,0	0,0	0,0	9,6
0,0	0,0	0,0	0,0	9,6
0,0	0,0	0,0	0,0	9,6
0,0	0,0	0,0	0,0	9,6
0,0	0,0	0,0	0,0	6,5
0,0	0,0	0,0	0,0	6,5
0,0	0,0	0,0	0,0	6,5
0,0	0,0	0,0	0,0	6,5
0,0	0,0	0,0	0,0	6,5
0,0	0,0	0,0	0,0	9,6
0,0	0,0	0,0	0,0	12,6
0,0	0,0	0,0	0,0	12,6
0,0	0,0	0,0	0,0	12,6
0,0	0,0	0,0	0,0	12,6
0,0	0,0	0,0	0,0	12,6
0,0	0,0	0,0	0,0	9,6
0,0	0,0	0,0	0,0	9,6
0,0	0,0	0,0	0,0	9,6
0,0	0,0	0,0	0,0	9,6
0,0	0,0	0,0	0,0	9,6
0,0	0,0	0,0	0,0	6,5
0,0	0,0	0,0	0,0	6,5
0,0	0,0	0,0	0,0	6,5
0,0	0,0	0,0	0,0	6,5
0,0	0,0	0,0	0,0	9,6
0,0	0,0	0,0	0,0	12,6
0,0	0,0	0,0	0,0	12,6
0,0	0,0	0,0	0,0	12,6
0,0	0,0	0,0	0,0	12,6
0,0	0,0	0,0	0,0	12,6
0,0	0,0	0,0	0,0	9,6
0,0	0,0	0,0	0,0	9,6
0,0	0,0	0,0	0,0	9,6
0,0	0,0	0,0	0,0	9,6

0,0	0,0	0,0	0,0	9,6
0,0	0,0	0,0	0,0	9,0
0,0	0,0	0,0	0,0	6,5
0,0	0,0	0,0	0,0	6,5
0,0	0,0	0,0	0,0	6,5
0,0	0,0	0,0	0,0	6,5
0,0	0,0	0,0	0,0	6,5
0,0	0,0	0,0	0,0	6,5
0,0	0,0	0,0	0,0	9,6
0,0	0,0	0,0	0,0	12,6
0,0	0,0	0,0	0,0	12,6
0,0	0,0	0,0	0,0	15,6
0,0	0,0	0,0	0,0	15,6
0,0	0,0	0,0	0,0	15,6
0,0	0,0	0,0	0,0	15,6
0,0	0,0	0,0	0,0	15,6
0,0	0,0	0,0	0,0	15,6
0,0	0,0	0,0	0,0	12,6
0,0	0,0	0,0	0,0	12,6
0,0	0,0	0,0	0,0	12,6
0,0	0,0	0,0	0,0	12,6
0,0	0,0	0,0	0,0	12,6
0,0	0,0	0,0	0,0	9,6
0,0	0,0	0,0	0,0	9,6
0,0	0,0	0,0	0,0	9,6
0,0	0,0	0,0	0,0	9,6
0,0	0,0	0,0	0,0	9,6
0,0	0,0	0,0	0,0	9,6
0,0	0,0	0,0	0,0	9,6
0,0	0,0	0,0	0,0	12,6
0,0	0,0	0,0	0,0	12,6
0,0	0,0	0,0	0,0	15,6
0,0	0,0	0,0	0,0	12,6
0,0	0,0	0,0	0,0	12,6
0,0	0,0	0,0	0,0	12,6
0,0	0,0	0,0	0,0	12,6
0,0	0,0	0,0	0,0	9,6
0,0	0,0	0,0	0,0	9,6
0,0	0,0	0,0	0,0	9,6
0,0	0,0	0,0	0,0	9,6
0,0	0,0	0,0	0,0	9,6
0,0	0,0	0,0	0,0	9,6
0,0	0,0	0,0	0,0	9,6
0,0	0,0	0,0	0,0	9,6
0,0	0,0	0,0	0,0	7,5
0,0	0,0	0,0	0,0	6,5

Table III.6 - Water level measurements for the fourth row

<i>A4(cm)</i>	<i>B4(cm)</i>	<i>C4(cm)</i>	<i>D4(cm)</i>	<i>E4(cm)</i>
0,0	0,0	9,6	0,0	22,8
0,0	0,0	12,7	0,0	26,0
0,0	0,0	12,7	0,0	26,0
0,0	0,0	12,7	0,0	26,0
0,0	0,0	12,7	0,0	26,0
0,0	0,0	12,7	0,0	26,0
0,0	0,0	12,7	0,0	26,0
0,0	0,0	9,6	0,0	26,0
0,0	0,0	9,6	0,0	25,5
0,0	0,0	9,6	0,0	22,8
0,0	0,0	9,6	0,0	22,8
0,0	0,0	9,6	0,0	22,8
0,0	0,0	9,6	0,0	22,8
0,0	0,0	9,6	0,0	22,8
0,0	0,0	8,5	0,0	22,8
0,0	0,0	6,5	0,0	21,2
0,0	0,0	6,5	0,0	19,7
0,0	0,0	6,5	0,0	19,7
0,0	0,0	6,5	0,0	19,7
0,0	0,0	6,5	0,0	19,7
0,0	0,0	6,5	0,0	19,7
0,0	0,0	6,5	0,0	19,7
0,0	0,0	9,6	0,0	22,3
0,0	0,0	9,6	0,0	22,8
0,0	0,0	9,6	0,0	23,9
0,0	0,0	9,6	0,0	25,5
0,0	0,0	9,6	0,0	25,5
0,0	0,0	9,6	0,0	23,4
0,0	0,0	9,6	0,0	22,8
0,0	0,0	9,6	0,0	22,8
0,0	0,0	9,6	0,0	22,8
0,0	0,0	6,5	0,0	22,8
0,0	0,0	6,5	0,0	22,3
0,0	0,0	6,5	0,0	19,7
0,0	0,0	6,5	0,0	19,7
0,0	0,0	6,5	0,0	19,7
0,0	0,0	6,5	0,0	19,7

0,0	0,0	6,5	0,0	19,7
0,0	0,0	6,5	0,0	19,7
0,0	0,0	6,5	0,0	19,7
0,0	0,0	6,5	0,0	17,0
0,0	0,0	6,5	0,0	16,5
0,0	0,0	6,5	0,0	16,5
0,0	0,0	6,5	0,0	16,5
0,0	0,0	6,5	0,0	16,5
0,0	0,0	6,5	0,0	16,5
0,0	0,0	6,5	0,0	16,5
0,0	0,0	6,5	0,0	19,7
0,0	0,0	6,5	0,0	19,7
0,0	0,0	6,5	0,0	19,7
0,0	0,0	9,6	0,0	22,8
0,0	0,0	9,6	0,0	22,8
0,0	0,0	9,6	0,0	22,8
0,0	0,0	9,6	0,0	22,8
0,0	0,0	9,6	0,0	22,8
0,0	0,0	6,5	0,0	20,7
0,0	0,0	6,5	0,0	19,7
0,0	0,0	6,5	0,0	19,7
0,0	0,0	6,5	0,0	19,7
0,0	0,0	6,5	0,0	19,7
0,0	0,0	6,5	0,0	19,7
0,0	0,0	6,5	0,0	19,7
0,0	0,0	6,5	0,0	19,7
0,0	0,0	6,5	0,0	18,6
0,0	0,0	6,5	0,0	16,5
0,0	0,0	6,5	0,0	16,5
0,0	0,0	6,5	0,0	16,5
0,0	0,0	6,5	0,0	16,5
0,0	0,0	6,5	0,0	16,5
0,0	0,0	3,8	0,0	16,5
0,0	0,0	3,3	0,0	16,5
0,0	0,0	3,3	0,0	16,5
0,0	0,0	3,3	0,0	16,5
0,0	0,0	6,5	0,0	16,5
0,0	0,0	6,5	0,0	16,5
0,0	0,0	6,5	0,0	19,7
0,0	0,0	6,5	0,0	19,7
0,0	0,0	6,5	0,0	19,7

0,0	0,0	6,5	0,0	29,2
0,0	0,0	9,6	0,0	32,3
0,0	0,0	9,6	0,0	32,3
0,0	0,0	9,6	0,0	32,3
0,0	0,0	9,6	0,0	32,3
0,0	0,0	9,6	0,0	32,3
0,0	0,0	9,6	0,0	32,3
0,0	0,0	9,6	0,0	32,3
0,0	0,0	6,5	0,0	32,3
0,0	0,0	6,5	0,0	31,3
0,0	0,0	6,5	0,0	29,2
0,0	0,0	6,5	0,0	29,2
0,0	0,0	6,5	0,0	29,2
0,0	0,0	6,5	0,0	29,2
0,0	0,0	6,5	0,0	28,6
0,0	0,0	6,5	0,0	29,2
0,0	0,0	9,6	0,0	32,3
0,0	0,0	9,6	0,0	32,3
0,0	0,0	9,6	0,0	32,3
0,0	0,0	9,6	0,0	32,3
0,0	0,0	9,6	0,0	32,3
0,0	0,0	9,6	0,0	32,3
0,0	0,0	9,6	0,0	32,3
0,0	0,0	9,6	0,0	32,3
0,0	0,0	8,0	0,0	29,2
0,0	0,0	6,5	0,0	29,2
0,0	0,0	6,5	0,0	29,2
0,0	0,0	6,5	0,0	29,2
0,0	0,0	6,5	0,0	26,0
0,0	0,0	6,5	0,0	26,0
0,0	0,0	6,5	0,0	29,2
0,0	0,0	9,6	0,0	32,3
0,0	0,0	9,6	0,0	32,3
0,0	0,0	12,7	0,0	32,3
0,0	0,0	12,7	0,0	32,3
0,0	0,0	12,7	0,0	32,3
0,0	0,0	9,6	0,0	32,3
0,0	0,0	9,6	0,0	32,3
0,0	0,0	9,6	0,0	32,3
0,0	0,0	9,6	0,0	32,3
0,0	0,0	9,6	0,0	29,2

0,0	0,0	6,5	0,0	22,8
0,0	0,0	6,5	0,0	22,8
0,0	0,0	6,5	0,0	22,8
0,0	0,0	6,5	0,0	22,8
0,0	0,0	6,5	0,0	22,8
0,0	0,0	6,5	0,0	22,3
0,0	0,0	6,5	0,0	22,8
0,0	0,0	6,5	0,0	22,8
0,0	0,0	6,5	0,0	22,8
0,0	0,0	9,6	0,0	25,5
0,0	0,0	9,6	0,0	26,0
0,0	0,0	9,6	0,0	26,0
0,0	0,0	9,6	0,0	23,9
0,0	0,0	6,5	0,0	22,8
0,0	0,0	6,5	0,0	22,8
0,0	0,0	6,5	0,0	22,8
0,0	0,0	6,5	0,0	22,8
0,0	0,0	6,5	0,0	22,8
0,0	0,0	6,5	0,0	22,3
0,0	0,0	6,5	0,0	19,7
0,0	0,0	6,5	0,0	19,7
0,0	0,0	6,5	0,0	19,7
0,0	0,0	6,5	0,0	19,7
0,0	0,0	6,5	0,0	20,2
0,0	0,0	6,5	0,0	21,2
0,0	0,0	6,5	0,0	22,3
0,0	0,0	6,5	0,0	22,8
0,0	0,0	6,5	0,0	22,8
0,0	0,0	6,5	0,0	22,8
0,0	0,0	6,5	0,0	26,0
0,0	0,0	7,5	0,0	26,0
0,0	0,0	9,6	0,0	29,2
0,0	0,0	9,6	0,0	29,2
0,0	0,0	9,6	0,0	29,2
0,0	0,0	11,2	0,0	32,3
0,0	0,0	12,7	0,0	32,3
0,0	0,0	12,7	0,0	32,3
0,0	0,0	12,7	0,0	32,3
0,0	0,0	12,7	0,0	32,3
0,0	0,0	12,7	0,0	32,3
0,0	0,0	12,7	0,0	32,3

Table III.7 - Water level measurements for the sixth row

A6(cm)	B6(cm)	C6(cm)	D6(cm)	E6(cm)
22,7	0,0	23,0	0,0	0,0
22,7	0,0	23,0	0,0	0,0
22,7	0,0	23,0	0,0	0,0
22,7	0,0	24,1	0,0	0,0
25,8	0,0	26,1	0,0	0,0
25,8	0,0	26,1	0,0	0,0
25,8	0,0	26,1	0,0	0,0
22,7	0,0	23,0	0,0	0,0
22,7	0,0	23,0	0,0	0,0
22,7	0,0	23,0	0,0	0,0
22,7	0,0	23,0	0,0	0,0
22,7	0,0	23,0	0,0	0,0
22,7	0,0	23,0	0,0	0,0
22,7	0,0	23,0	0,0	0,0
22,7	0,0	23,0	0,0	0,0
22,7	0,0	23,0	0,0	0,0
22,7	0,0	23,0	0,0	0,0
22,7	0,0	23,0	0,0	0,0
19,7	0,0	20,0	0,0	0,0
19,7	0,0	20,0	0,0	0,0
19,7	0,0	20,0	0,0	0,0
19,7	0,0	20,0	0,0	0,0
19,7	0,0	20,0	0,0	0,0
19,7	0,0	20,0	0,0	0,0
19,7	0,0	20,0	0,0	0,0
19,7	0,0	20,0	0,0	0,0
19,7	0,0	20,0	0,0	0,0
19,7	0,0	20,0	0,0	0,0
22,7	0,0	23,0	0,0	0,0
22,7	0,0	23,0	0,0	0,0
22,7	0,0	23,0	0,0	0,0
22,7	0,0	23,0	0,0	0,0
22,7	0,0	23,0	0,0	0,0
22,7	0,0	23,0	0,0	0,0
22,7	0,0	23,0	0,0	0,0
22,7	0,0	23,0	0,0	0,0
22,2	0,0	22,5	0,0	0,0
19,7	0,0	20,0	0,0	0,0
19,7	0,0	20,0	0,0	0,0
19,7	0,0	20,0	0,0	0,0
19,7	0,0	20,0	0,0	0,0
19,7	0,0	20,0	0,0	0,0

19,7	0,0	20,0	0,0	0,0
19,7	0,0	20,0	0,0	0,0
19,7	0,0	20,0	0,0	0,0
19,7	0,0	20,0	0,0	0,0
19,7	0,0	20,0	0,0	0,0
19,7	0,0	20,0	0,0	0,0
19,7	0,0	20,0	0,0	0,0
19,7	0,0	20,0	0,0	0,0
19,7	0,0	20,0	0,0	0,0
19,7	0,0	20,0	0,0	0,0
19,7	0,0	20,0	0,0	0,0
19,7	0,0	20,0	0,0	0,0
19,7	0,0	20,0	0,0	0,0
19,7	0,0	20,0	0,0	0,0
19,7	0,0	20,0	0,0	0,0
19,7	0,0	20,0	0,0	0,0
19,7	0,0	20,0	0,0	0,0
19,7	0,0	19,5	0,0	0,0
19,7	0,0	19,0	0,0	0,0
19,7	0,0	17,4	0,0	0,0
19,7	0,0	16,9	0,0	0,0
19,7	0,0	16,9	0,0	0,0
19,7	0,0	16,9	0,0	0,0
19,7	0,0	20,0	0,0	0,0
19,7	0,0	20,0	0,0	0,0
19,7	0,0	20,0	0,0	0,0
20,2	0,0	20,0	0,0	0,0
22,7	0,0	20,0	0,0	0,0
22,7	0,0	20,0	0,0	0,0
22,7	0,0	20,0	0,0	0,0
22,7	0,0	20,0	0,0	0,0
22,7	0,0	20,0	0,0	0,0
22,7	0,0	20,0	0,0	0,0
22,7	0,0	20,0	0,0	0,0
22,7	0,0	20,0	0,0	0,0
22,7	0,0	20,0	0,0	0,0
20,7	0,0	20,0	0,0	0,0
19,7	0,0	20,0	0,0	0,0
19,7	0,0	20,0	0,0	0,0
19,7	0,0	20,0	0,0	0,0
19,7	0,0	20,0	0,0	0,0
19,7	0,0	20,0	0,0	0,0

22,7	0,0	23,0	0,0	0,0
22,7	0,0	23,0	0,0	0,0
22,7	0,0	23,0	0,0	0,0
22,7	0,0	22,5	0,0	0,0
22,2	0,0	20,0	0,0	0,0
19,7	0,0	20,0	0,0	0,0
19,7	0,0	20,0	0,0	0,0
19,7	0,0	20,0	0,0	0,0
19,7	0,0	20,0	0,0	0,0
19,7	0,0	20,0	0,0	0,0
22,7	0,0	21,0	0,0	0,0
22,7	0,0	23,0	0,0	0,0
22,7	0,0	23,0	0,0	0,0
23,7	0,0	24,1	0,0	0,0
25,8	0,0	26,1	0,0	0,0
25,8	0,0	26,1	0,0	0,0
25,8	0,0	26,1	0,0	0,0
25,8	0,0	26,1	0,0	0,0
25,8	0,0	26,1	0,0	0,0
25,8	0,0	26,1	0,0	0,0
25,8	0,0	26,1	0,0	0,0
25,8	0,0	24,1	0,0	0,0
23,7	0,0	23,0	0,0	0,0
22,7	0,0	23,0	0,0	0,0
22,7	0,0	23,0	0,0	0,0
22,7	0,0	23,0	0,0	0,0
22,7	0,0	23,0	0,0	0,0
22,7	0,0	23,0	0,0	0,0
22,7	0,0	23,0	0,0	0,0
22,7	0,0	23,0	0,0	0,0
22,7	0,0	23,0	0,0	0,0
22,7	0,0	23,0	0,0	0,0
22,7	0,0	23,0	0,0	0,0
23,2	0,0	23,0	0,0	0,0
25,8	0,0	26,1	0,0	0,0
25,8	0,0	26,1	0,0	0,0
25,8	0,0	26,1	0,0	0,0
25,8	0,0	23,0	0,0	0,0
22,7	0,0	23,0	0,0	0,0
22,7	0,0	23,0	0,0	0,0
22,7	0,0	23,0	0,0	0,0
22,7	0,0	23,0	0,0	0,0
22,7	0,0	23,0	0,0	0,0

19,7	0,0	20,0	0,0	0,0
19,7	0,0	20,0	0,0	0,0
19,7	0,0	20,0	0,0	0,0
19,7	0,0	20,0	0,0	0,0
19,7	0,0	20,0	0,0	0,0
19,7	0,0	20,0	0,0	0,0
19,7	0,0	17,4	0,0	0,0
19,7	0,0	16,9	0,0	0,0
19,7	0,0	20,0	0,0	0,0
19,7	0,0	20,0	0,0	0,0
19,7	0,0	20,0	0,0	0,0
19,7	0,0	20,0	0,0	0,0
19,7	0,0	20,0	0,0	0,0
19,7	0,0	20,0	0,0	0,0
19,7	0,0	20,0	0,0	0,0
19,7	0,0	20,0	0,0	0,0
19,7	0,0	20,0	0,0	0,0
19,7	0,0	20,0	0,0	0,0
19,7	0,0	20,0	0,0	0,0
19,7	0,0	20,0	0,0	0,0
19,7	0,0	20,0	0,0	0,0
19,7	0,0	19,5	0,0	0,0
19,7	0,0	17,4	0,0	0,0
19,7	0,0	16,9	0,0	0,0
19,7	0,0	16,9	0,0	0,0
19,7	0,0	16,9	0,0	0,0
19,7	0,0	16,9	0,0	0,0
19,7	0,0	16,9	0,0	0,0
19,7	0,0	16,9	0,0	0,0
19,7	0,0	20,0	0,0	0,0
19,7	0,0	20,0	0,0	0,0
19,7	0,0	20,0	0,0	0,0
19,7	0,0	20,0	0,0	0,0
22,2	0,0	20,0	0,0	0,0
22,7	0,0	23,0	0,0	0,0
22,7	0,0	23,0	0,0	0,0
22,7	0,0	23,0	0,0	0,0
22,7	0,0	23,0	0,0	0,0
22,7	0,0	23,0	0,0	0,0
22,7	0,0	23,0	0,0	0,0
22,7	0,0	23,0	0,0	0,0

0,0	0,0	26,5	27,5	0,0
0,0	0,0	26,5	27,5	0,0
0,0	0,0	27,1	27,5	0,0
0,0	0,0	27,7	27,5	0,0
0,0	0,0	27,1	27,5	0,0
0,0	0,0	26,5	27,5	0,0
0,0	0,0	26,5	26,9	0,0
0,0	0,0	26,5	25,3	0,0
0,0	0,0	26,5	24,7	0,0
0,0	0,0	26,5	24,2	0,0
0,0	0,0	26,5	24,2	0,0
0,0	0,0	26,5	24,2	0,0
0,0	0,0	26,5	24,2	0,0
0,0	0,0	26,5	24,2	0,0
0,0	0,0	26,5	24,2	0,0
0,0	0,0	26,5	24,2	0,0
0,0	0,0	27,7	24,2	0,0
0,0	0,0	30,0	24,2	0,0
0,0	0,0	30,0	24,2	0,0
0,0	0,0	30,0	24,2	0,0
0,0	0,0	30,0	24,2	0,0
0,0	0,0	30,0	24,2	0,0
0,0	0,0	30,0	24,2	0,0
0,0	0,0	30,0	24,2	0,0
0,0	0,0	30,0	25,3	0,0
0,0	0,0	30,0	27,5	0,0
0,0	0,0	30,0	27,5	0,0
0,0	0,0	30,0	27,5	0,0
0,0	0,0	30,0	27,5	0,0
0,0	0,0	30,0	27,5	0,0
0,0	0,0	30,0	27,5	0,0
0,0	0,0	30,0	27,5	0,0
0,0	0,0	30,0	27,5	0,0
0,0	0,0	30,0	27,5	0,0
0,0	0,0	30,0	27,5	0,0
0,0	0,0	29,4	27,5	0,0
0,0	0,0	27,7	27,5	0,0
0,0	0,0	27,7	27,5	0,0
0,0	0,0	30,0	27,5	0,0

0,0	0,0	30,0	27,5	0,0
0,0	0,0	30,0	27,5	0,0
0,0	0,0	30,0	26,9	0,0
0,0	0,0	30,0	25,3	0,0
0,0	0,0	30,0	24,2	0,0
0,0	0,0	30,0	24,2	0,0
0,0	0,0	30,0	24,2	0,0
0,0	0,0	30,0	24,2	0,0
0,0	0,0	30,0	24,2	0,0
0,0	0,0	30,0	26,9	0,0
0,0	0,0	31,2	27,5	0,0
0,0	0,0	33,5	27,5	0,0
0,0	0,0	33,5	27,5	0,0
0,0	0,0	33,5	27,5	0,0
0,0	0,0	33,5	30,3	0,0
0,0	0,0	33,5	30,8	0,0
0,0	0,0	33,5	30,8	0,0
0,0	0,0	33,5	30,3	0,0
0,0	0,0	33,5	30,3	0,0
0,0	0,0	33,5	29,7	0,0
0,0	0,0	33,5	27,5	0,0
0,0	0,0	33,5	27,5	0,0
0,0	0,0	33,5	27,5	0,0
0,0	0,0	33,5	27,5	0,0
0,0	0,0	32,9	27,5	0,0
0,0	0,0	32,3	27,5	0,0
0,0	0,0	32,9	27,5	0,0
0,0	0,0	33,5	27,5	0,0
0,0	0,0	33,5	27,5	0,0
0,0	0,0	33,5	27,5	0,0
0,0	0,0	33,5	27,5	0,0
0,0	0,0	33,5	27,5	0,0
0,0	0,0	33,5	27,5	0,0
0,0	0,0	33,5	27,5	0,0
0,0	0,0	33,5	27,5	0,0
0,0	0,0	33,5	27,5	0,0
0,0	0,0	31,2	27,5	0,0
0,0	0,0	30,0	27,5	0,0

0,0	0,0	30,0	27,5	0,0
0,0	0,0	30,0	27,5	0,0
0,0	0,0	30,0	27,5	0,0
0,0	0,0	30,0	27,5	0,0
0,0	0,0	30,0	27,5	0,0
0,0	0,0	30,0	27,5	0,0
0,0	0,0	30,0	27,5	0,0
0,0	0,0	30,0	27,5	0,0
0,0	0,0	30,0	27,5	0,0
0,0	0,0	30,0	27,5	0,0
0,0	0,0	30,0	27,5	0,0
0,0	0,0	30,0	27,5	0,0
0,0	0,0	30,0	27,5	0,0
0,0	0,0	30,0	27,5	0,0
0,0	0,0	30,0	27,5	0,0
0,0	0,0	30,0	27,5	0,0
0,0	0,0	30,0	27,5	0,0
0,0	0,0	30,0	27,5	0,0
0,0	0,0	30,0	27,5	0,0
0,0	0,0	30,0	27,5	0,0
0,0	0,0	30,0	27,5	0,0
0,0	0,0	30,0	27,5	0,0
0,0	0,0	30,0	26,9	0,0
0,0	0,0	30,0	24,7	0,0
0,0	0,0	30,0	24,2	0,0
0,0	0,0	30,0	24,2	0,0
0,0	0,0	30,0	24,7	0,0
0,0	0,0	30,0	26,4	0,0
0,0	0,0	30,0	27,5	0,0
0,0	0,0	30,0	27,5	0,0
0,0	0,0	30,0	27,5	0,0
0,0	0,0	30,0	27,5	0,0
0,0	0,0	30,0	27,5	0,0
0,0	0,0	30,0	27,5	0,0
0,0	0,0	30,0	27,5	0,0
0,0	0,0	30,0	27,5	0,0
0,0	0,0	30,0	27,5	0,0
0,0	0,0	30,0	27,5	0,0
0,0	0,0	29,4	27,5	0,0

